

Walking in the Shadow: A New Perspective on Descent Directions for Constrained Minimization

Hassan Mortagy¹, Swati Gupta¹, and Sebastian Pokutta²

¹Georgia Institute of Technology
¹{hmortagy, swatig}@gatech.edu

²Zuse Institute Berlin and Technische Universität Berlin
²pokutta@zib.de

Abstract

Descent directions such as movement towards Frank-Wolfe vertices, away steps, in-face away steps and pairwise directions have been an important design consideration in conditional gradient descent (CGD) variants. In this work, we attempt to demystify the impact of movement in these directions towards attaining constrained minimizers. The best local direction of descent is the directional derivative of the projection of the gradient, which we refer to as the *shadow* of the gradient. We show that the continuous-time dynamics of moving in the shadow are equivalent to those of PGD however non-trivial to discretize. By projecting gradients in PGD, one not only ensures feasibility but is also able to “wrap” around the convex region. We show that Frank-Wolfe (FW) vertices in fact recover the maximal wrap one can obtain by projecting gradients, thus providing a new perspective on these steps. We also claim that the shadow steps give the best direction of descent emanating from the convex hull of all possible away-steps. Viewing PGD movements in terms of shadow steps gives linear convergence, dependent on the number of faces. We combine these insights into a novel SHADOW-CG method that uses FW steps and shadow steps, while enjoying linear convergence. Our analysis develops properties of the curve formed by projecting a line on a polytope, which may be of independent interest.

1 Introduction

We consider the problem $\min_{\mathbf{x} \in P} f(\mathbf{x})$, where $P \subseteq \mathbb{R}^n$ is a polytope with vertex set $\text{vert}(P)$, and $f : P \rightarrow \mathbb{R}$ is a smooth and strongly convex function. Smooth convex optimization problems over polytopes are an important class of problems that appear in many settings, such as low-rank matrix completion [1], structured supervised learning [2, 3], electrical flows over graphs [4], video co-localization in computer vision [5], traffic assignment problems [6], and submodular function minimization [7]. First-order methods in convex optimization rely on movement in the best local direction for descent (e.g., negative gradient), and this is enough to obtain linear convergence for

unconstrained optimization. In constrained settings however, the gradient may no longer be a feasible direction of descent, and traditionally there are two broad classes of methods traditionally: projection-based methods (i.e., move in the direction of the negative gradient, but project to ensure feasibility), and conditional gradient methods (i.e., move in feasible directions that approximate the gradient). Projection-based methods such as projected gradient descent or mirror descent [8] enjoy dimension independent linear rates of convergence (assuming no acceleration), e.g., $(1 - \frac{\mu}{L})$ contraction in the objective per iteration (so that the number of iterations to get an ϵ -accurate solution is $O(\frac{L}{\mu} \log \frac{1}{\epsilon})$), for μ -strongly convex and L -smooth functions, but need to compute an expensive projection step (another constrained convex optimization) in (almost) every iteration. On the other hand, conditional gradient methods (such as the Frank-Wolfe algorithm [9]) solely rely on solving linear optimization (LO) problems in every iteration and the rates of convergence become dimension-dependent, e.g., the away-step Frank-Wolfe algorithm has a linear rate of $(1 - \frac{\mu\delta^2}{LD^2})$, where δ is a polytope dependent geometric constant and D is the diameter of the polytope [10].

The vanilla Conditional Gradient method (CG) or the Frank-Wolfe algorithm (FW) [9, 11] has received a lot of interest from the ML community mainly because of its iteration complexity, tractability and sparsity of iterates. In each iteration, the CG algorithm computes the *Frank-Wolfe vertex* \mathbf{v}_t with respect to the current iterate and moves towards that vertex:

$$\mathbf{v}_t = \arg \min_{\mathbf{v} \in \text{vert}(P)} \langle \nabla f(\mathbf{x}_t), \mathbf{v} \rangle, \quad \mathbf{x}_{t+1} = \mathbf{x}_t + \gamma_t(\mathbf{v}_t - \mathbf{x}_t), \quad \gamma_t \in [0, 1]. \quad (1)$$

CG's primary direction of descent is $\mathbf{v}_t - \mathbf{x}_t$ (\mathbf{d}_t^{FW} in Figure 1) and its step-size γ_t can be selected, e.g., using line-search; this ensures feasibility of \mathbf{x}_{t+1} . The FW algorithm however, can only guarantee a sub-linear rate of convergence $O(1/t)$ for smooth and strongly convex optimization on a polytope [9, 2]. Moreover, this convergence rate is tight [12, 13]. An active area of research, therefore, has been to find other descent directions that can enable linear convergence. One reason for vanilla CG's $O(1/t)$ rate is the fact that the algorithm might zig-zag as it approaches the optimal face, slowing down progress [10, 12]. The key idea for obtaining linear convergence was to use the so-called *away steps* that help push iterates to the optimal face:

$$\mathbf{a}_t = \arg \max_{\mathbf{v} \in \text{vert}(F)} \langle \nabla f(\mathbf{x}_t), \mathbf{v} \rangle, \quad \text{for } F \subseteq P, \quad (2)$$

$$\mathbf{x}_{t+1} = \mathbf{x}_t + \gamma_t(\mathbf{x}_t - \mathbf{a}_t), \quad \text{where } \gamma_t \in \mathbb{R}_+ \text{ such that } \mathbf{x}_{t+1} \in P, \quad (3)$$

thus, augmenting the potential directions of descent using directions of the form $\mathbf{x}_t - \mathbf{a}_t$, for some $\mathbf{a}_t \in F$, where the precise choice of F in (2) has evolved in CG variants.

As early as 1986, Guélat and Marcotte showed that by adding away steps (with $F =$ minimal face of the current iterate*) to vanilla CG, their algorithm has an asymptotic linear convergence rate [14]. In 2015, Lacoste-Julien and Jaggi [10] showed linear convergence results for CG with away

*The minimal face F with respect to \mathbf{x}_t is a face of the polytope that contains \mathbf{x}_t in its relative interior, i.e., all active constraints at \mathbf{x}_t are tight.

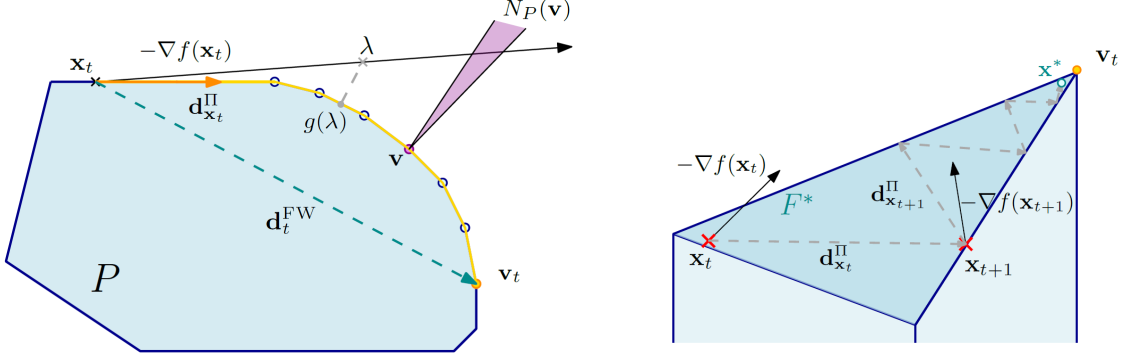


Figure 1: **Left:** Piecewise linearity of the parametric projections curve $g(\lambda) = \Pi_P(\mathbf{x}_t - \lambda \nabla f(\mathbf{x}_t))$ (yellow line). The end point is the FW vertex \mathbf{v}_t and \mathbf{d}_t^{FW} is the FW direction. Note that $g(\lambda)$ does not change at the same speed as λ , e.g., $g(\lambda) = \mathbf{v}$ for each λ such that $\mathbf{x}_t - \lambda \nabla f(\mathbf{x}_t) - \mathbf{v} \in N_P(\mathbf{v})$ (purple normal cone). **Right:** Moving along the shadow might lead to arbitrarily small progress even once we reach the optimal face $F^* \ni \mathbf{x}^*$. On the contrary, the away-step FW does not leave F^* after a polytope-dependent iteration [14].

steps[†] (over $F = \text{convex hull of the current active set}$, i.e., a specific convex decomposition of the current iterate). They also showed a linear rate of convergence for CG with pairwise-steps (of the form $\mathbf{v}_t - \mathbf{a}_t$), another direction of descent. In 2015, Freund et. al [1] showed a $O(1/t)$ convergence for convex functions, with F as the minimal face of the current iterate. In 2016, Garber and Meshi [16] showed that pairwise-steps (over 0/1 polytopes) with respect to non-zero components of the gradient are enough for linear convergence, i.e., they also set F to be the minimal face with respect to \mathbf{x}_t . In 2017, Bashiri and Zhang [3] generalized this result to show linear convergence for the same F for general polytopes (however at the cost of two expensive oracles).

Other related work includes linear convergence for the conditional gradient method over strongly-convex domains with a lower bound on the norm of the optimum gradient [11], or when the FW-vertex is constrained to a ball around the iterate [13, 16], bringing in regularization-like ideas of mirror-descent variants to CG. There has also been extensive work on mixing Frank-Wolfe and gradient descent steps [17, 18] or solving projections approximately using Frank-Wolfe steps [19] (with the aim of better computational performance) while enjoying linear convergence [20, 17]. Our goal in this work is to put these CG variants in perspective and understand desired properties of feasible directions of descent. We summarize related work in Table 1.

Although all these variants obtain linear convergence, their rates depend on polytope-dependent geometric, affine-invariant constants (that can be arbitrarily small for non-polyhedral sets like the ℓ_2 -ball) such as the pyramidal width [10], vertex-facet distance [21], eccentricity of the polytope [10] or sparsity-dependent constants [3], which have been shown to be essentially equivalent[‡] [22]. The iterates in CG algorithms are (basically) affine-invariant, which is the reason why a dimension-dependent factor is unavoidable in the current arguments. Following our work, there have been recent results on extensions using procedures similar to our TRACE-OPT procedure to avoid “bad” steps in

[†]To the best of our knowledge, Garber and Hazan [15] were the first to present a CG variant with global linear convergence for polytopes.

[‡]Eccentricity = D/δ , where D and δ are the diameter and pyramidal width of the domain respectively [10].

Paper	Algorithm	Steps to get ϵ -error
Frank and Wolfe (1956) [25]	Vanilla FW with the uniform step-size rule $\gamma_t = \frac{2}{t+2}$.	$O\left(\frac{LD^2}{\epsilon}\right)$
Dunn (1979) [26]	Geometric analysis for vanilla CG.	$O\left(\frac{LD^2}{\epsilon}\right)$
Guélat and Marcotte (1986) [14]	Vanilla FW with \mathbf{x}^* having distance $\Delta > 0$ from the boundary.	$O\left(\kappa\left(\frac{D}{\Delta}\right)^2 \log \frac{1}{\epsilon}\right)$
Lan (2013) [13]	Constraining FW vertex to a ball around the current iterate.	$O\left(\kappa \log \frac{D\mu}{\epsilon}\right)$
Freund et. al (2015) [1]	FW with in-face directions (promoting sparsity) as a generalization to away steps.	$O\left(\frac{LD^2}{\epsilon}\right)$
Lacoste-Julien and Jaggi (2015) [10]	FW & away steps (over current active set) for general polytopes (AFW & PFW).	$O\left(\kappa\left(\frac{D}{\delta}\right)^2 \log \frac{1}{\epsilon}\right)$
Garber and Hazan (2016) [15]	Constraining FW vertex to a ball around the current iterate with a focus on polytopes.	$O\left(\kappa n \rho \log \frac{1}{\epsilon}\right)$
Garber and Meshi (2016) [16]	Pairwise steps for structured 0/1 polytopes [§] using best away vertex in minimal face of iterate (DICG).	$O\left(\kappa \ \mathbf{x}^*\ _0 D^2 \log \frac{1}{\epsilon}\right)$
Beck and Shtern (2017) [3]	FW & away steps using best away vertex in current active set for specific non-strongly convex objective functions [¶] .	$O\left(Ln\left(\frac{D}{\Phi}\right)^2 \log \frac{1}{\epsilon}\right)$
Bashiri and Zhang (2017) [3]	FW & Away steps using best away vertex in the minimal face of iterate.	$O\left(n\kappa D^2 H_s \log \frac{1}{\epsilon}\right)$
Braun et. al (2018) [17]	Lazy FW & gradient descent steps over simplex formed by current active set.	$O\left(K\kappa\left(\frac{D}{\delta}\right)^2 \log \frac{1}{\epsilon}\right)$
Combettes and Pokutta (2020) [18]	FW with descent directions better aligned with the negative gradients.	$O\left(\frac{\kappa}{\alpha^2 \omega} \log \frac{1}{\epsilon}\right)$
Rinaldi and Zeffiro (2020) [23, 24]	Use procedure called SSC that chains consecutive FW like descent steps .	$O\left(\gamma \log^{-1} \frac{\tau^2 \kappa}{(1+\tau)^2} \log \frac{1}{\epsilon}\right)$
This paper	Moving along the ‘shadow’ of the negative gradient (SHADOW-WALK).	$O\left(\kappa \beta \log \frac{1}{\epsilon}\right)$
This paper	Moving in the ‘shadow’ of the negative gradient with FW steps. (SHADOW-CG)	$O\left(\kappa(D^2 + \beta) \log \frac{1}{\epsilon}\right)$

Table 1: Summary of different descent techniques used in CG variants and their convergence rates. The factor $\kappa := L/\mu$ is the condition number of the function and D is the diameter of the domain. Also, δ is the pyramidal width, ρ and Φ are notions of vertex-facet distance and H_s is a sparsity-dependent geometric constant. Moreover, K is a parameter for finding approximate FW vertices. The constants α and ω arise from the gradient alignment procedure. Further, τ is a directional slope constant and γ is the number of iterations performed within SSC. Finally, β is the number of breakpoints visited when walking along the shadow of the gradient (within TRACE-OPT), which depends on the number of facets of the polytope.

CG variants and accordingly obtain linear convergence rates that depend on a slope condition rather than geometric constants [23, 24].

[§]These include: the path polytope of a graph (aka the unit flow polytope), the perfect matching polytope of a bipartite graph, and the base polyhedron of a matroid, for which we have efficient algorithms for linear optimization.

[¶]They consider objective functions of the form $f(\mathbf{x}) := g(\mathbf{Ex}) + \langle \mathbf{b}, \mathbf{x} \rangle$, where g is strongly convex and \mathbf{E} is a general matrix, so that f is not necessarily strongly convex, but is gradient dominated via the Hoffman bound.

^{||}Following our work, Rinaldi and Zeffiro [23, 24] proposed the SSC procedure, which every iteration chains short first-order feasible descent steps (e.g. AFW steps as opposed to shadow steps) within a ball around the current iterate until sufficient progress is achieved. This could be viewed as an approximation of our TRACE-OPT procedure.

A natural question at this point is why are these different descent directions useful and which of these are necessary for linear convergence. If one had oracle access to the “best” local direction of descent for constrained minimization, what would it be and is it enough to obtain linear convergence (as in unconstrained optimization)? Moreover, can we avoid rates of convergence that are dependent on the geometry of the polytope? We partially answer these questions below.

Contributions. We show that the “best” local feasible direction of descent, that gives the maximum function value decrease in the diminishing neighborhood of the current iterate \mathbf{x}_t , is the *directional derivative* $\mathbf{d}_{\mathbf{x}_t}^{\Pi}$ of the projection of the gradient, which we refer to as the *shadow* of the gradient:

$$\mathbf{d}_{\mathbf{x}_t}^{\Pi} := \lim_{\epsilon \downarrow 0} \frac{\Pi_P(\mathbf{x}_t - \epsilon \nabla f(\mathbf{x}_t)) - \mathbf{x}_t}{\epsilon},$$

where $\Pi_P(\mathbf{y}) = \arg \min_{\mathbf{x} \in P} \|\mathbf{x} - \mathbf{y}\|^2$ is the Euclidean projection operator. Further, a continuous time dynamical system can be defined using infinitesimal movement in the shadow direction at the current point: $\dot{X}(t) = \mathbf{d}_{X(t)}^{\Pi}$, with $X(0) = \mathbf{x}_0 \in P$. We show that this ODE is equivalent to that of projected gradient descent (Theorem 5), and that it is non-trivial to discretize due to non-differentiability of the curve.

Second, we explore structural properties of shadow steps. For any $\mathbf{x} \in P$, we characterize the curve $g(\lambda) = \Pi_P(\mathbf{x} - \lambda \nabla f(\mathbf{x}))$ as a piecewise linear curve, where the breakpoints of the curve typically occur at points where there is a change in the normal cone (Theorem 1) and show how to compute this curve for all $\lambda \geq 0$ (Theorem 2). Moreover, we show the following properties for descent directions:

(i) Shadow Steps ($\mathbf{d}_{\mathbf{x}_t}^{\Pi}$): These are the *best normalized feasible directions* of descent (Lemma 6), so that $\|\mathbf{d}_{\mathbf{x}_t}^{\Pi}\| = 0$ if and only if $\mathbf{x}_t = \arg \min_{\mathbf{x} \in P} f(\mathbf{x})$ (Lemma 7). Hence, $\|\mathbf{d}_{\mathbf{x}_t}^{\Pi}\|$ is a natural quantity to use for bounding primal gaps without any dependence on geometric constants like those used in other CG variants. We show that multiple shadow steps approximate a single projected gradient descent step (Theorem 2). The rate of linear convergence using shadow steps is dependent on the number of facets (independent of geometric constants but dimension dependent due to number of facets), and *interpolate smoothly* between projected gradient and conditional gradient methods (Theorem 7).

(ii) FW Steps ($\mathbf{v}_t - \mathbf{x}_t$): Projected gradient steps provide a contraction in the objective independent of the geometric constants or facets of the polytope; they are also able to “wrap” around the polytope by taking unconstrained gradient steps and then projecting. Under mild technical conditions (uniqueness of \mathbf{v}_t), the Frank-Wolfe vertices are in fact the projection of an infinite descent in the negative gradient direction (Theorem 4). This allows the CG methods to wrap around the polytope maximally, compared to PGD methods, thereby giving FW steps a new perspective.

(iii) Away Steps ($\mathbf{x}_t - \mathbf{a}_t$): Shadow steps are the *best normalized away-direction* with steepest local descent (Lemma 6). Shadow steps are in general convex combinations of potential active vertices minus the current iterate (Lemma 8) and therefore loose combinatorial properties such as dimension

drop in active sets [3]. Shadow steps can bounce off faces (i.e. visit the same face multiple times - (see Figure 1 (right) for an example) unlike away steps that use vertices and have a monotone decrease in dimension when they are consecutive.

(vi) Pairwise Steps ($\mathbf{v}_t - \mathbf{a}_t$): The progress in CG variants is bounded crucially using the inner product of the descent direction with the negative gradient. In this sense, pairwise steps are simply the *sum of the FW step and away directions*, and a simple algorithm, the pairwise FW algorithm, that only uses these steps does converge linearly (with geometric constants) [10, 3]. Moreover, for feasibility of the descent direction, one requires \mathbf{a}_t to be in the active set of the current iterate (shown in [3], and Lemma 10, Appendix C.3).

Armed with these structural properties, we consider a descent algorithm SHADOW-WALK: trace the projections curve by moving in the shadow or an in-face directional derivative with respect to a fixed iterate, until sufficient progress, then update the shadow based on the current iterate. Using properties of normal cones, we can show that once the projections curve at a fixed iterate leaves a face, it can never visit the face again (Theorem 3). We are thus able to break a single PGD step into multiple descent steps, and show linear convergence with rate dependent on the number of facets, but independent of geometric constants like the pyramidal width.

We combine these insights into a novel SHADOW-CG method which uses FW steps and shadow steps (both over the tangent cone and minimal face), while enjoying linear convergence. This method prioritizes FW steps that achieve maximal “coarse” progress in earlier iterations and shadow steps avoid zig-zagging in the latter iterations. Garber and Meshi [16] and Bashiri and Zhang [3] both compute the best away vertex in the minimal face containing the current iterate, whereas the shadow step recovers the best convex combination of such vertices aligned with the negative gradient. Therefore, these previously mentioned CG methods can *both* be viewed as approximations of SHADOW-CG. Moreover, Garber and Hazan [15] emulate a shadow computation by constraining the FW vertex to a ball around the current iterate. Therefore, their algorithm can be interpreted as an approximation of SHADOW-WALK. Finally, we propose a practical variant of SHADOW-CG, called SHADOW-CG², which reduces the number of shadow computations.

Outline. We next review preliminaries in Section 2. In Section 3, we derive theoretical properties of the piecewise-linear projections curve. Next, we derive properties of descent directions in Section 4 and present the continuous time dynamics for movement along the shadow and its discretization SHADOW-WALK in Section 5. Finally, we propose SHADOW-CG and SHADOW-CG² in Section 6 and provide computational experiments in Section 7.

2 Preliminaries

Let $\|\cdot\|$ denote the Euclidean norm. Denote $[m] = \{1, \dots, m\}$ and let P be defined in the form

$$P = \{\mathbf{x} \in \mathbb{R}^n : \langle \mathbf{a}_i, \mathbf{x} \rangle \leq b_i \forall i \in [m]\}. \quad (4)$$

We use $\text{vert}(P)$ to denote the *vertices of P* . A function $f : \mathcal{D} \rightarrow \mathbb{R}$ (for $\mathcal{D} \subseteq \mathbb{R}^n$ and $P \subseteq \mathcal{D}$) is said to be *L -smooth* if $f(\mathbf{y}) \leq f(\mathbf{x}) + \langle \nabla f(\mathbf{x}), \mathbf{y} - \mathbf{x} \rangle + \frac{L}{2} \|\mathbf{y} - \mathbf{x}\|^2$ for all $\mathbf{x}, \mathbf{y} \in \mathcal{D}$. Furthermore, $f : \mathcal{D} \rightarrow \mathbb{R}$ is said to be *μ -strongly-convex* if $f(\mathbf{y}) \geq f(\mathbf{x}) + \langle \nabla f(\mathbf{x}), \mathbf{y} - \mathbf{x} \rangle + \frac{\mu}{2} \|\mathbf{y} - \mathbf{x}\|^2$ for all $\mathbf{x}, \mathbf{y} \in \mathcal{D}$. Let $D := \sup_{\mathbf{x}, \mathbf{y} \in P} \|\mathbf{x} - \mathbf{y}\|$ be the *diameter of P* and $\mathbf{x}^* = \arg \min_{\mathbf{x} \in P} f(\mathbf{x})$, where uniqueness follows from the strong convexity of the f . For any $\mathbf{x} \in P$, let $I(\mathbf{x}) = \{i \in [m] : \langle \mathbf{a}_i, \mathbf{x} \rangle = b_i\}$ be the index set of active constraints at \mathbf{x} . Similarly, let $J(\mathbf{x})$ be the index set of inactive constraints at \mathbf{x} . Denote by $\mathbf{A}_{I(\mathbf{x})} = [\mathbf{a}_i]_{i \in I(\mathbf{x})}$ the sub-matrix of active constraints at \mathbf{x} and $\mathbf{b}_{I(\mathbf{x})} = [b_i]_{i \in I(\mathbf{x})}$ the corresponding right-hand side.

The *normal cone at a point $\mathbf{x} \in P$* is defined as

$$\begin{aligned} N_P(\mathbf{x}) &:= \{\mathbf{y} \in \mathbb{R}^n : \langle \mathbf{y}, \mathbf{z} - \mathbf{x} \rangle \leq 0 \ \forall \mathbf{z} \in P\} \\ &= \{\mathbf{y} \in \mathbb{R}^n : \exists \boldsymbol{\mu} : \mathbf{y} = (A_{I(\mathbf{x})})^\top \boldsymbol{\mu}, \boldsymbol{\mu} \geq 0\}, \end{aligned} \quad (5)$$

which is essentially the cone of the normals of constraints tight at \mathbf{x} . Let $\Pi_P(\mathbf{y}) = \arg \min_{\mathbf{x} \in P} \frac{1}{2} \|\mathbf{x} - \mathbf{y}\|^2$ be the *Euclidean projection operator*. Using first-order optimality,

$$\langle \mathbf{y} - \mathbf{x}, \mathbf{z} - \mathbf{x} \rangle \leq 0 \quad \forall \mathbf{z} \in P \iff (\mathbf{y} - \mathbf{x}) \in N_P(\mathbf{x}), \quad (6)$$

which implies that $\mathbf{x} = \Pi_P(\mathbf{y})$ if and only if $(\mathbf{y} - \mathbf{x}) \in N_P(\mathbf{x})$, i.e., moving any closer to \mathbf{y} from \mathbf{x} will violate feasibility in P . It is well known that the Euclidean projection operator over convex sets is non-expansive (see e.g., [27]): $\|\Pi_P(\mathbf{y}) - \Pi_P(\mathbf{x})\| \leq \|\mathbf{y} - \mathbf{x}\|$ for all $\mathbf{x}, \mathbf{y} \in \mathbb{R}^n$.

Given any point $\mathbf{x} \in P$ and $\mathbf{w} \in \mathbb{R}^n$, let the *directional derivative* of \mathbf{w} at \mathbf{x} be defined as:

$$\mathbf{d}_\mathbf{x}^\Pi(\mathbf{w}) := \lim_{\epsilon \downarrow 0} \frac{\Pi_P(\mathbf{x} - \epsilon \mathbf{w}) - \mathbf{x}}{\epsilon}. \quad (7)$$

When $\mathbf{w} = \nabla f(\mathbf{x})$, then we call $\mathbf{d}_\mathbf{x}^\Pi(\nabla f(\mathbf{x}))$ the *shadow of the negative gradient* at \mathbf{x} , and use notation $\mathbf{d}_\mathbf{x}^\Pi$ for brevity. In [28], Tapia et. al show that $\mathbf{d}_\mathbf{x}^\Pi$ is the projection of $-\nabla f(\mathbf{x})$ onto the *tangent cone* at \mathbf{x} , which we denote by $T_P(\mathbf{x}) := \{\mathbf{d} \in \mathbb{R}^n : \mathbf{A}_{I(\mathbf{x})}\mathbf{d} \leq \mathbf{0}\}$ (i.e., $T_P(\mathbf{x}) = \text{Cone}(P - \mathbf{x})$ is the set of feasible directions at \mathbf{x}). That is $\mathbf{d}_\mathbf{x}^\Pi = \arg \min_{\mathbf{d} \in T_P(\mathbf{x})} \{\|-\nabla f(\mathbf{x}) - \mathbf{d}\|^2\} = \arg \min_{\mathbf{d}} \{\|-\nabla f(\mathbf{x}) - \mathbf{d}\|^2 : \mathbf{A}_{I(\mathbf{x})}\mathbf{d} \leq \mathbf{0}\}$, where the uniqueness of the solution follows from strong convexity of the objective. Further, let $\hat{\mathbf{d}}_\mathbf{x}^\Pi(\nabla f(\mathbf{x}))$ be the projection of $-\nabla f(\mathbf{x})$ onto $\text{Cone}(F - \mathbf{x}) = \{\mathbf{d} \in \mathbb{R}^n : \mathbf{A}_{I(\mathbf{x})}\mathbf{d} = \mathbf{0}\}$, where F is the minimal face of P containing \mathbf{x}^{**} . That is, $\hat{\mathbf{d}}_\mathbf{x}^\Pi(\nabla f(\mathbf{x}))$ is the projection of $-\nabla f(\mathbf{x})$ onto the set of in-face feasible directions and can be computed in closed-form using: $\hat{\mathbf{d}}_\mathbf{x}^\Pi(\nabla f(\mathbf{x})) = \arg \min_{\mathbf{d}} \{\|-\nabla f(\mathbf{x}) - \mathbf{d}\|^2 : \mathbf{A}_{I(\mathbf{x})}\mathbf{d} = \mathbf{0}\} = (\mathbf{I} - \mathbf{A}_{I(\mathbf{x})}^\dagger \mathbf{A}_{I(\mathbf{x})})(-\nabla f(\mathbf{x}))$, where $\mathbf{I} \in \mathbb{R}^{n \times n}$ is the identity matrix, and $\mathbf{A}_{I(\mathbf{x})}^\dagger$ is the Moore-Penrose inverse of $\mathbf{A}_{I(\mathbf{x})}$ (see Section 5.13 in [29] for more details). We refer to $\hat{\mathbf{d}}_\mathbf{x}^\Pi(\nabla f(\mathbf{x}))$ as the *in-face shadow* or *in-face directional derivative*.

We assume access to (i) a *linear optimization* (LO) oracle to compute $\mathbf{v} = \arg \min_{\mathbf{x} \in P} \langle \mathbf{c}, \mathbf{x} \rangle$ for $\mathbf{c} \in \mathbb{R}^n$, (ii) a *shadow oracle*: given any $\mathbf{x} \in P$, compute $\mathbf{d}_\mathbf{x}^\Pi$, and (iii) *line-search oracle*: given any

**Note that $-(\mathbf{z} - \mathbf{x})$ is also a feasible direction at \mathbf{x} for any $\mathbf{z} \in F$, since \mathbf{x} is in the relative interior of F by definition. This implies that $\text{Cone}(F - \mathbf{x}) = -\text{Cone}(F - \mathbf{x})$, and therefore $\text{Cone}(F - \mathbf{x})$ is in fact a subspace.

$\mathbf{x} \in P$ and direction $\mathbf{d} \in \mathbb{R}^n$, we can evaluate $\gamma^{\max} = \max\{\delta : \mathbf{x} + \delta\mathbf{d} \in P\}$. We use these oracles to study descent directions and their necessity for linear convergence.

3 Structure of the Parametric Projections Curve

In this section, we characterize properties of the directional derivative at any $\mathbf{x} \in P$ and the structure of the parametric projections curve $g_{\mathbf{x}, \mathbf{w}}(\lambda) = \Pi_P(\mathbf{x} - \lambda\mathbf{w})$, for $\lambda \geq 0$, under Euclidean projections. For brevity, we use $g(\cdot)$ when \mathbf{x} and \mathbf{w} are clear from context. The following theorem summarizes our results and it is crucial to our analysis of descent directions:

Theorem 1 (Structure of Parametric Projections Curve). *Let $P \subseteq \mathbb{R}^n$ be a polytope, with m facet inequalities (e.g., as in (4)). For any $\mathbf{x}_0 \in P, \mathbf{w} \in \mathbb{R}^n$, let $g(\lambda) = \Pi_P(\mathbf{x}_0 - \lambda\mathbf{w})$ be the projections curve at \mathbf{x}_0 with respect to \mathbf{w} parametrized by $\lambda \in \mathbb{R}_+$. Then, this curve is piecewise linear starting at \mathbf{x}_0 : there exist k breakpoints $\mathbf{x}_1, \mathbf{x}_2, \dots, \mathbf{x}_k \in P$, corresponding to projections with λ equal to $0 = \lambda_0^- \leq \lambda_0^+ < \lambda_1^- \leq \lambda_1^+ < \lambda_2^- \leq \lambda_2^+ \dots < \lambda_k^- \leq \lambda_k^+$, where*

- (a) $\lambda_i^- := \min\{\lambda \geq 0 \mid g(\lambda) = \mathbf{x}_i\}$, $\lambda_i^+ := \max\{\lambda \geq 0 \mid g(\lambda) = \mathbf{x}_i\}$, for $i \geq 0$,
- (b) $g(\lambda) = \mathbf{x}_{i-1} + \frac{\mathbf{x}_i - \mathbf{x}_{i-1}}{\lambda_i^- - \lambda_{i-1}^+}(\lambda - \lambda_{i-1}^+)$, for $\lambda \in [\lambda_{i-1}^+, \lambda_i^-]$ for all $i \geq 1$.

Moreover, for each $1 \leq i \leq k$ and all $\lambda, \lambda' \in (\lambda_{i-1}^+, \lambda_i^-)$, the following hold:

- (i) **Potentially drop tight constraints on leaving breakpoints:** $N_P(\mathbf{x}_{i-1}) = N_P(g(\lambda_{i-1}^+)) \supseteq N_P(g(\lambda))$. Moreover, if $\lambda_{i-1}^- < \lambda_{i-1}^+$, then the containment is strict.
- (ii) **Constant normal cone between breakpoints:** $N_P(g(\lambda)) = N_P(g(\lambda'))$,
- (iii) **Potentially add tight constraints on reaching breakpoints:** $N_P(g(\lambda)) \subseteq N_P(g(\lambda_i^-)) = N_P(\mathbf{x}_i)$.

Further, the following properties also hold:

- (iv) **Equivalence of constant normal cones with linearity:** If $N_P(g(\lambda)) = N_P(g(\lambda'))$ for some $\lambda < \lambda'$, then the curve between $g(\lambda)$ and $g(\lambda')$ is linear (Lemma 2).
- (v) **Bound on breakpoints:** The number of breakpoints of $g(\cdot)$ is at most the number of faces of the polytope (Theorem 3).
- (vi) **Limit of $g(\cdot)$:** The end point of the curve $g(\lambda)$ is $\lim_{\lambda \rightarrow \infty} g(\lambda) = \mathbf{x}_k \in \arg \min_{\mathbf{x} \in P} \langle \mathbf{x}, \mathbf{w} \rangle$. In fact, \mathbf{x}_k minimizes $\|\mathbf{y} - \mathbf{x}_0\|$ over $\mathbf{y} \in \arg \min_{\mathbf{x} \in P} \langle \mathbf{x}, \mathbf{w} \rangle$ (Theorem 4, Section 4).

To see an example of the projections curve, we refer the reader to Figure 2. Even though our results hold for any $\mathbf{w} \in \mathbb{R}^n$, we will prove the statements for $\mathbf{w} = \nabla f(\mathbf{x}_0)$ for readability in the context of the paper. Before we present the proof of Theorem 1, we first show that if $-\nabla f(\mathbf{x}_0) \in N_P(\mathbf{x}_0)$, then $g(\lambda)$ reduces down to a single point \mathbf{x}_0 .

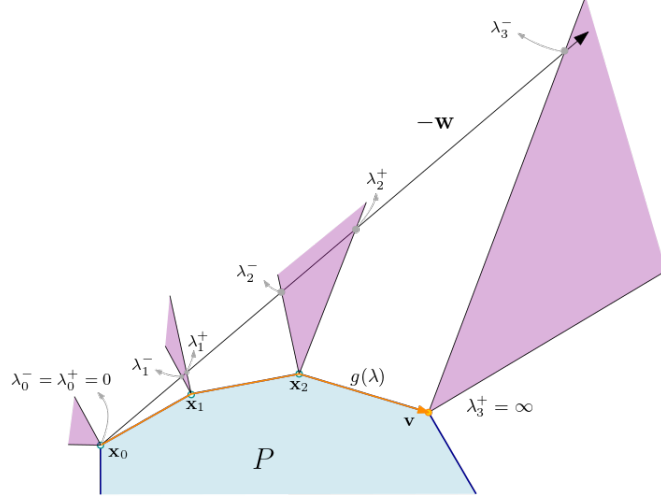


Figure 2: Figure showing the structure of the projections curve $g(\lambda) = \Pi_P(\mathbf{x}_0 - \lambda \mathbf{w})$ for $\lambda \geq 0$, which is depicted by the orange line. Breakpoints in the curve correspond to \mathbf{x}_i with $g(\lambda_i^-) = g(\lambda_i^+) = \mathbf{x}_i$, and $\lambda_3^+ = \infty$ since $\lim_{\lambda \rightarrow \infty} g(\lambda) = \mathbf{v} = \arg \min_{\mathbf{y} \in P} \langle \mathbf{y}, \mathbf{w} \rangle$. Consider the first linear segment from \mathbf{x}_0 to \mathbf{x}_1 . We have $N_P(g(\lambda)) = N_P(g(\lambda')) \subset N_P(\mathbf{x}_0)$ for all $\lambda, \lambda' \in (0, \lambda_1^-)$. Then, another constraint becomes tight at the end point of the first segment \mathbf{x}_1 , and thus we have $N_P(g(\lambda)) \subset N_P(\mathbf{x}_1)$ for all $\lambda \in (0, \lambda_1^-)$. This process of dropping and adding constraints (given by Theorem 1(i) – (iii)) continues until we reach the endpoint \mathbf{v} .

Lemma 1. *We have $g(\lambda) = \Pi_P(\mathbf{x}_0 - \lambda \nabla f(\mathbf{x}_0)) = \mathbf{x}_0$ for all $\lambda \in \mathbb{R}_+$ if and only if $-\nabla f(\mathbf{x}_0) \in N_P(\mathbf{x}_0)$.*

Proof. Note that $g(\lambda) = \mathbf{x}_0$ if and only if \mathbf{x}_0 satisfies the first order optimality condition for $g(\lambda)$: $\langle \mathbf{x}_0 - \lambda \nabla f(\mathbf{x}_0) - \mathbf{x}_0, \mathbf{z} - \mathbf{x}_0 \rangle = \lambda \langle -\nabla f(\mathbf{x}_0), \mathbf{z} - \mathbf{x}_0 \rangle \leq 0$ for all $\mathbf{z} \in P$. Since $\lambda \geq 0$, we can conclude that $g(\lambda) = \mathbf{x}_0$ if and only if $\langle -\nabla f(\mathbf{x}_0), \mathbf{z} - \mathbf{x}_0 \rangle \leq 0$ for all $\mathbf{z} \in P$. Note that $\langle -\nabla f(\mathbf{x}_0), \mathbf{z} - \mathbf{x}_0 \rangle \leq 0$ for all $\mathbf{z} \in P$ is equivalent to saying that $-\nabla f(\mathbf{x}_0) \in N_P(\mathbf{x}_0)$. \square

Thus, in the notation of Theorem 1, λ_0^+ is either infinity (when $-\nabla f(\mathbf{x}_0) \in N_P(\mathbf{x}_0)$) or it is zero. In the former case, Theorem 1 holds trivially with $g(\lambda) = \mathbf{x}_0$ for all $\lambda \in \mathbb{R}$. We will therefore assume that $\lambda_0^+ = 0$, without loss of generality.

The rest of this section is organized as follows. In Section 3.1, we show that the projections curve is piecewise linear as characterized in Theorem 1(a)-(b). In Section 3.2, we prove the normal cone properties of the projections curve from Theorem 1(i) – (iii). Finally in Section 3.3 we prove the bound on the number of breakpoints of the projections curve Theorem 1(v) and present our TRACE procedure, which traces the projections curve and computes its linear segments.

3.1 The Projections Curve is Piecewise Linear

We first show that the segment of the projections curve between two projected points with the same normal cones has to be linear (Theorem 1(iv)). This result will be crucial to prove that the projections curve is piecewise linear and the bound on the number of breakpoints of the curve.

Lemma 2. Let $P \subseteq \mathbb{R}^n$ be a polytope. Let $\mathbf{x}_0 \in P$ and we are given $\nabla f(\mathbf{x}_0) \in \mathbb{R}^n$. Let $g(\lambda) = \Pi_P(\mathbf{x}_0 - \lambda \nabla f(\mathbf{x}_0))$ be the parametric projections curve. Then, if $N_P(g(\lambda)) = N_P(g(\lambda'))$ for some $\lambda < \lambda'$, then the curve between $g(\lambda)$ and $g(\lambda')$ is linear, i.e., $g(\delta\lambda + (1 - \delta)\lambda') = \delta g(\lambda) + (1 - \delta)g(\lambda')$, where $\delta \in [0, 1]$.

The idea of the proof is to show that $\delta g(\lambda) + (1 - \delta)g(\lambda')$ satisfies the first-order optimality condition of Euclidean projections given in (6) for $g(\delta\lambda + (1 - \delta)\lambda')$ when $N_P(g(\lambda)) = N_P(g(\lambda'))$. The complete proof of this lemma can be found in found in Appendix B.1. Note that as an immediate corollary of this lemma we know that the projections curve does not intersect itself. That is, if the projections curve leaves the point $\mathbf{x} := g(\lambda)$ for an arbitrary $\lambda > 0$ (i.e. $g(\lambda + \epsilon) \neq \mathbf{x}$ for some $\epsilon > 0$), then $g(\lambda') \neq \mathbf{x}$ for all $\lambda' > \lambda + \epsilon$.

We next show that the projections curve is in fact piecewise linear and continuous. The proof uses non-expansivity of the Euclidean projection operator to show continuity of the curve, and the previous lemma combined with the fact that the number of distinct normal cones over a polytope is finite (the proof is included in Appendix B.1).

Lemma 3. Let $P \subseteq \mathbb{R}^n$ be a polytope. Let $\mathbf{x}_0 \in P$ and $\nabla f(\mathbf{x}_0) \in \mathbb{R}^n$ be given. Further, let $g(\lambda) = \Pi_P(\mathbf{x}_0 - \lambda \nabla f(\mathbf{x}_0))$ denote the projections curve. Fix an arbitrary $\lambda > 0$. Then, $\lim_{\lambda' \downarrow \lambda} g(\lambda') = \lim_{\lambda' \uparrow \lambda} g(\lambda') = g(\lambda)$. Moreover, there exists $\delta' > 0$ and directions $\underline{\mathbf{d}}, \bar{\mathbf{d}} \in \mathbb{R}^n$ such that $g(\lambda - \epsilon) = g(\lambda) - \epsilon \underline{\mathbf{d}}$ and $g(\lambda + \epsilon) = g(\lambda) + \epsilon \bar{\mathbf{d}}$, for all $\epsilon \in (0, \delta']$.

Since the projections curve is piecewise linear, we naturally obtain a set of breakpoints k breakpoints $\mathbf{x}_1, \mathbf{x}_2, \dots, \mathbf{x}_k \in P$, corresponding to projections with λ equal to $0 = \lambda_0^- \leq \lambda_0^+ < \lambda_1^- \leq \lambda_1^+ < \lambda_2^- \leq \lambda_2^+ \dots < \lambda_k^- \leq \lambda_k^+$, satisfying properties in (a) and (b) in Theorem 1:

- (a) $\lambda_i^- := \min\{\lambda \geq 0 \mid g(\lambda) = \mathbf{x}_i\}$, $\lambda_i^+ := \max\{\lambda \geq 0 \mid g(\lambda) = \mathbf{x}_i\}$, for $i \geq 0$,
- (b) $g(\lambda) = \mathbf{x}_{i-1} + \frac{\mathbf{x}_i - \mathbf{x}_{i-1}}{\lambda_i^- - \lambda_{i-1}^+}(\lambda - \lambda_{i-1}^+)$, for $\lambda \in [\lambda_{i-1}^+, \lambda_i^-]$ for all $i \geq 1$.

Note that we can now establish the existence of the shadow as a corollary of the previous result about the piecewise linearity of $g(\lambda)$. Indeed, since $g(\lambda) = \mathbf{x}_0 + \frac{\mathbf{x}_1 - \mathbf{x}_0}{\lambda_1^-} \lambda$, for $\lambda \in [0, \lambda_1^-]$, using the definition of $\mathbf{d}_{\mathbf{x}_0}^\Pi$ we have

$$\mathbf{d}_{\mathbf{x}_0}^\Pi := \lim_{\epsilon \downarrow 0} \frac{\Pi_P(\mathbf{x}_0 - \epsilon \nabla f(\mathbf{x}_0)) - \mathbf{x}_0}{\epsilon} = \lim_{\epsilon \downarrow 0} \frac{g(\epsilon) - \mathbf{x}_0}{\epsilon} = \frac{\mathbf{x}_1 - \mathbf{x}_0}{\lambda_1^-}, \quad (8)$$

which shows existence and equivalence of the first segment of the projections curve to the shadow, i.e., $g(\lambda) = \mathbf{x}_0 + \lambda \mathbf{d}_{\mathbf{x}_0}^\Pi$ for all $\lambda \in [0, \lambda_1^-]$. This will be useful in justifying our continuous-time dynamics later Section 5. This also gives a different proof for existence of $\mathbf{d}_{\mathbf{x}_0}^\Pi$ for polytopes, compared to Tapia et. al [28].

3.2 Normal Cone Properties of the Projections Curve

We now show the growth and subset properties of normal cones when tracing the projections curve. We first show that (a) movement away from a point along a linear segment can only drop constraints

in its neighborhood, and (b) maximum movement along a linear segment must add a tight constraint at the endpoint. The idea of the proof is to simply track the effect of movement along linear directions on the activity and inactivity of the constraints defining the polytope.

Lemma 4. *Let $P \subseteq \mathbb{R}^n$ be a polytope and consider any $\mathbf{x} \in P$. Let $\mathbf{d} \in \mathbb{R}^n$ be any direction that is feasible at \mathbf{x} , and let $\delta = \max\{\lambda \mid \mathbf{x} + \lambda\mathbf{d} \in P\}$. Then,*

- (a) $N_P(\mathbf{x} + \lambda\mathbf{d}) = N_P(\mathbf{x} + \lambda'\mathbf{d}) \subseteq N_P(\mathbf{x})$, for all $0 < \lambda < \lambda' < \delta$;
- (b) $N_P(\mathbf{x} + \lambda\mathbf{d}) \subset N_P(\mathbf{x} + \delta\mathbf{d})$, for all $0 < \lambda < \delta$.

Proof. First note that $\delta > 0$ since \mathbf{d} is feasible at \mathbf{x} , and $\delta < \infty$ since P is a polytope and movements along any direction are bounded. For brevity, we let I and J denote the index-set of active and inactive constraints at \mathbf{x} respectively. Fix $\lambda, \lambda' \in (0, \delta)$ arbitrarily such that $\lambda < \lambda'$. We prove the lemma in the next two claims.

(a) *We first show that $N_P(\mathbf{x} + \lambda\mathbf{d}) = N_P(\mathbf{x} + \lambda'\mathbf{d}) \subseteq N_P(\mathbf{x})$.* We prove Claim (a) in the next two sub-claims:

(a.i) *Inactive constraints remain inactive:* $N_P(\mathbf{x} + \lambda\mathbf{d}) \subseteq N_P(\mathbf{x})$. Since $\mathbf{x} + \delta\mathbf{d} \in P$, we have $\mathbf{A}_J(\mathbf{x} + \delta\mathbf{d}) \leq \mathbf{b}_J$, which implies that $\mathbf{A}_J\mathbf{d} \leq \frac{\mathbf{b}_J - \mathbf{A}_J\mathbf{x}}{\delta}$. Moreover, for any $\lambda < \delta$, we have

$$\mathbf{A}_J(\mathbf{x} + \lambda\mathbf{d}) \leq \mathbf{A}_J\mathbf{x} + \lambda \frac{\mathbf{b}_J - \mathbf{A}_J\mathbf{x}}{\delta} = \left(1 - \frac{\lambda}{\delta}\right) \mathbf{A}_J\mathbf{x} + \mathbf{b}_J \frac{\lambda}{\delta} < \mathbf{b}_J,$$

where the last (strict) inequality follows from the fact that we are taking a convex combination. This shows $\mathbf{A}_J(\mathbf{x} + \lambda\mathbf{d}) < \mathbf{b}_J$ (component-wise) for all $\lambda \in (0, \delta)$, i.e., $N_P(\mathbf{x} + \lambda\mathbf{d}) \subseteq N_P(\mathbf{x})$.

(a.ii) *Active constraints are maintained:* $N_P(\mathbf{x} + \lambda\mathbf{d}) = N_P(\mathbf{x} + \lambda'\mathbf{d})$. Since the inactive constraints remain inactive, we just need to check the constraints in the index set I . Consider any $i \in I$. Since $\langle \mathbf{a}_i, \mathbf{x}_0 \rangle = b_i$ and $\mathbf{x}_0 + \delta\mathbf{d} \in P$ ($\delta > 0$), we know that $\langle \mathbf{a}_i, \mathbf{d} \rangle \leq 0$. If $\langle \mathbf{a}_i, \mathbf{d} \rangle = 0$, then $\langle \mathbf{a}_i, \mathbf{x} + \lambda\mathbf{d} \rangle = b_i$ for all $\lambda \in [0, \delta]$. So the constraint corresponding to \mathbf{a}_i is active at both $\mathbf{x} + \lambda\mathbf{d}$ and $\mathbf{x} + \lambda'\mathbf{d}$. On the other hand, if $\langle \mathbf{a}_i, \mathbf{d} \rangle < 0$, then $\langle \mathbf{a}_i, \mathbf{x} + \lambda\mathbf{d} \rangle < b_i$ for all $\lambda \in [0, \delta]$. Thus, the constraint corresponding to \mathbf{a}_i is inactive at both $\mathbf{x} + \lambda\mathbf{d}$ and $\mathbf{x} + \lambda'\mathbf{d}$.

(b) *We next show that $N_P(\mathbf{x} + \lambda\mathbf{d}) \subset N_P(\mathbf{x} + \delta\mathbf{d})$.* Let \tilde{I} denote the index set of active constraints at $\mathbf{x} + \lambda\mathbf{d}$. Using Claim (a.i), we know that $\tilde{I} \subseteq I$. Therefore, for any $i \in \tilde{I}$, we have

$$\langle \mathbf{a}_i, \mathbf{x} + \lambda\mathbf{d} \rangle = b_i \implies \langle \mathbf{a}_i, \mathbf{d} \rangle = 0 \implies \langle \mathbf{a}_i, \mathbf{x} + \delta\mathbf{d} \rangle = b_i,$$

and so the constraint corresponding to \mathbf{a}_i (which is active at $\mathbf{x} + \lambda\mathbf{d}$) is also active at $\mathbf{x} + \delta\mathbf{d}$. We have thus shown that $N_P(\mathbf{x} + \lambda\mathbf{d}) \subseteq N_P(\mathbf{x} + \delta\mathbf{d})$. It remains to show that this containment

is strict. Since \mathbf{d} is a feasible direction at \mathbf{x} , we have $\langle \mathbf{a}_i, \mathbf{d} \rangle \leq 0$ for all $i \in I$. Thus

$$\delta = \min_{\substack{j \in J: \\ \langle \mathbf{a}_j, \mathbf{d} \rangle > 0}} \frac{b_j - \langle \mathbf{a}_j, \mathbf{x} \rangle}{\langle \mathbf{a}_j, \mathbf{d} \rangle}, \quad (9)$$

where the feasible set of the above problem is non-empty, since otherwise this would imply that \mathbf{d} is a recessive direction (i.e., direction of unboundedness), contradicting the fact that P is a polytope. Let j^* be any optimal index to the optimization problem in (9), where by definition $\langle \mathbf{a}_{j^*}, \mathbf{x} + \delta \mathbf{d} \rangle = b_{j^*}$. Now, since $\langle \mathbf{a}_{j^*}, \mathbf{d} \rangle > 0$ and $\lambda < \delta$, we have $\langle \mathbf{a}_{j^*}, \mathbf{x} + \lambda \mathbf{d} \rangle < \langle \mathbf{a}_{j^*}, \mathbf{x} + \delta \mathbf{d} \rangle$, implying that the constraint \mathbf{a}_{j^*} is not active at $\mathbf{x} + \lambda \mathbf{d}$. Thus, $N_P(\mathbf{x} + \lambda \mathbf{d}) \subset N_P(\mathbf{x} + \delta \mathbf{d})$.

This completes the proof since λ, λ' were chosen arbitrarily. \square

We show next that the projections curve is piecewise linear. Note that Lemma 4 and Lemma 5 together prove the normal cone properties in Theorem 1(i) - (iii).

Lemma 5. *Let $P \subseteq \mathbb{R}^n$ be a polytope. Let $\mathbf{x}_0 \in P$ and $\nabla f(\mathbf{x}_0) \in \mathbb{R}^n$ be given. Further, let $\mathbf{x}_{i-1} \in P$ be the i th breakpoint in the projections curve $g(\lambda) = \Pi_P(\mathbf{x}_0 - \lambda \nabla f(\mathbf{x}_0))$, with $\mathbf{x}_{i-1} = \mathbf{x}_0$ for $i = 1$. Define $\lambda_{i-1}^- := \min\{\lambda \mid g(\lambda) = \mathbf{x}_{i-1}\}$, $\lambda_{i-1}^+ := \max\{\lambda \mid g(\lambda) = \mathbf{x}_{i-1}\}$, and let k be the number of breakpoints of $g(\lambda)$. Then, the following properties hold for all $1 \leq i \leq k$ and $\lambda, \lambda' \in (\lambda_{i-1}^+, \lambda_i^-)$:*

- (i) $N_P(\mathbf{x}_{i-1}) = N_P(g(\lambda_{i-1}^+)) \supseteq N_P(g(\lambda))$. Moreover, if $\lambda_{i-1}^- < \lambda_{i-1}^+$, then the containment is strict,
- (ii) $N_P(g(\lambda)) = N_P(g(\lambda'))$, and
- (iii) $N_P(g(\lambda)) \subseteq N_P(g(\lambda_i^-)) = N_P(\mathbf{x}_i)$.

Proof. Consider a breakpoint \mathbf{x}_{i-1} of $g(\lambda)$, where $1 \leq i \leq k$. Using Theorem 1(a)-(b), we know that $g(\lambda) = \mathbf{x}_{i-1} + (\lambda - \lambda_{i-1}^+) \mathbf{d}$ for $\lambda \in [\lambda_{i-1}^+, \lambda_i^-]$ and some direction $\mathbf{d} \in \mathbb{R}^n$. Using the normal cone properties given in Lemma 4 applied with $\mathbf{x} := \mathbf{x}_{i-1}$ and parameter $(\lambda - \lambda_{i-1}^+)$ in place of λ , we immediately have that the first part of property (i) ($N_P(\mathbf{x}_{i-1}) = N_P(g(\lambda_{i-1}^+)) \supseteq N_P(g(\lambda))$ for all $\lambda \in (\lambda_{i-1}^+, \lambda_i^-)$), (ii) and (iii) hold. It remains to show that if $\lambda_{i-1}^- < \lambda_{i-1}^+$, then the containment in (i) is strict. Suppose for a contradiction that $\lambda_{i-1}^- < \lambda_{i-1}^+$ but $N_P(g(\tilde{\lambda})) = N_P(\mathbf{x}_{i-1})$ for some $\lambda_{i-1}^+ < \tilde{\lambda} < \lambda_i^-$. Since $\lambda_{i-1}^+ < \infty$ (as $i-1 < k$), it follows that $g(\tilde{\lambda}) \neq \mathbf{x}_{i-1}$. Using Lemma 2 (linearity of projections), we know that $g(\lambda_{i-1}^+) = \theta g(\lambda_{i-1}^-) + (1-\theta)g(\tilde{\lambda})$ for $\theta = \frac{\lambda_{i-1}^+ - \lambda_{i-1}^-}{\tilde{\lambda} - \lambda_{i-1}^-} \in (0, 1)$. This is a contradiction since $g(\lambda_{i-1}^+) = g(\lambda_{i-1}^-) = \mathbf{x}_{i-1}$ but $g(\tilde{\lambda}) \neq \mathbf{x}_{i-1}$. \square

3.3 Tracing the Projections Curve

We next show how to iteratively trace the projections curve $g(\lambda)$ and construct all of its linear segments for all $\lambda \geq 0$. Consider a breakpoint \mathbf{x}_{i-1} of $g(\lambda)$ where $i \geq 1$. Then, depending on the structure current breakpoint (see Theorem 2 below and also Figure 3), the next linear segment and breakpoint \mathbf{x}_i of the curve can be obtained by either (a) projecting $\nabla f(\mathbf{x}_0)$ onto the tangent cone

at \mathbf{x}_{i-1} (i.e. computing the shadow $\mathbf{d}_{\mathbf{x}_{i-1}}^{\Pi}(\nabla f(\mathbf{x}_0))$ at \mathbf{x}_{i-1} with respect to $\nabla f(\mathbf{x}_0)$), and moving maximally along that direction using line search; or (b) by projecting $\nabla f(\mathbf{x}_0)$ onto the minimal face of \mathbf{x}_{i-1} (i.e. computing the in-face shadow $\hat{\mathbf{d}}_{\mathbf{x}_{i-1}}^{\Pi}(\nabla f(\mathbf{x}_0))$ at \mathbf{x}_{i-1} with respect to $\nabla f(\mathbf{x}_0)$), and moving along that direction until the curve $g(\lambda)$ leaves the minimal face:

Theorem 2 (Tracing the projections curve). *Let $P \subseteq \mathbb{R}^n$ be a polytope. Let $\mathbf{x}_{i-1} \in P$ be the i th breakpoint in the projections curve $g(\lambda) = \Pi_P(\mathbf{x}_0 - \lambda \nabla f(\mathbf{x}_0))$, with $\mathbf{x}_{i-1} = \mathbf{x}_0$ for $i = 1$. Suppose we are given $\lambda_{i-1}^-, \lambda_{i-1}^+ \in \mathbb{R}$ so that they are respectively the minimum and the maximum step-sizes λ such that $g(\lambda) = \mathbf{x}_{i-1}$. If $\mathbf{d}_{\mathbf{x}_{i-1}}^{\Pi}(\nabla f(\mathbf{x}_0)) = \mathbf{0}$, then $\lim_{\lambda \rightarrow \infty} g(\lambda) = \mathbf{x}_{i-1}$ is the end point of $g(\lambda)$. Otherwise, $\mathbf{d}_{\mathbf{x}_{i-1}}^{\Pi}(\nabla f(\mathbf{x}_0)) \neq \mathbf{0}$, in which case we claim that:*

- (a) **Shadow steps:** *If $\langle \mathbf{x}_0 - \lambda_{i-1}^+ \nabla f(\mathbf{x}_0) - \mathbf{x}_{i-1}, \mathbf{d}_{\mathbf{x}_{i-1}}^{\Pi}(\nabla f(\mathbf{x}_0)) \rangle = 0$, then the projections curve moves maximally in the shadow direction, i.e., $\mathbf{x}_i := g(\lambda_i^-) = \mathbf{x}_{i-1} + (\lambda_i^- - \lambda_{i-1}^+) \mathbf{d}_{\mathbf{x}_{i-1}}^{\Pi}(\nabla f(\mathbf{x}_0))$ where $\lambda_i^- := \lambda_{i-1}^+ + \max\{\delta : \mathbf{x}_{i-1} + \delta \mathbf{d}_{\mathbf{x}_{i-1}}^{\Pi}(\nabla f(\mathbf{x}_0)) \in P\}$.*
- (b) **In-face steps:** *Otherwise, $\langle \mathbf{x}_0 - \lambda_{i-1}^+ \nabla f(\mathbf{x}_0) - \mathbf{x}_{i-1}, \mathbf{d}_{\mathbf{x}_{i-1}}^{\Pi}(\nabla f(\mathbf{x}_0)) \rangle \neq 0$. Let $\hat{\lambda}_{i-1} := \sup\{\lambda \mid N_P(g(\lambda')) = N_P(\mathbf{x}_{i-1}) \forall \lambda' \in [\lambda_{i-1}^-, \lambda]\}$. Then, $\hat{\mathbf{d}}_{\mathbf{x}_{i-1}}^{\Pi}(\nabla f(\mathbf{x}_0)) \neq \mathbf{d}_{\mathbf{x}_{i-1}}^{\Pi}(\nabla f(\mathbf{x}_0))$, $\lambda_{i-1}^+ < \hat{\lambda}_{i-1} < \infty$, and the next breakpoint in the curve occurs by walking in-face up to $\hat{\lambda}_{i-1}$, i.e., $\mathbf{x}_i := g(\hat{\lambda}_{i-1}) = \mathbf{x}_{i-1} + (\hat{\lambda}_{i-1} - \lambda_{i-1}^+) \hat{\mathbf{d}}_{\mathbf{x}_{i-1}}^{\Pi}(\nabla f(\mathbf{x}_0))$ and $\lambda_i^- := \hat{\lambda}_{i-1}$.*

The idea of the proof is as follows. Consider a breakpoint $\mathbf{x}_{i-1} := g(\lambda_{i-1}^+)$ that is not the endpoint of the projections curve. For brevity, let $\mathbf{p}_{i-1} := \mathbf{x}_0 - \lambda_{i-1}^+ \nabla f(\mathbf{x}_0) - \mathbf{x}_{i-1}$ denote the normal vector of the projection at \mathbf{x}_{i-1} . Since the projections curve is piecewise linear (Theorem 1), we know that $g(\lambda) = \mathbf{x}_{i-1} + (\lambda_i^- - \lambda_{i-1}^+) \mathbf{d}$ for $\lambda \in [\lambda_{i-1}^+, \lambda_i^-]$ and some direction $\mathbf{d} \in \mathbb{R}^n$. We also know that $N_P(g(\lambda)) \subseteq N_P(\mathbf{x}_{i-1})$ for $\lambda \in (\lambda_{i-1}^+, \lambda_i^-)$, so that the direction \mathbf{d} either (i) relaxes some of the active constraints at \mathbf{x}_{i-1} , or (ii) is an in-face direction. Using first-order optimality of conditions at $g(\lambda_{i+1}^+)$ and $g(\lambda_{i+1}^+ + \epsilon)$, for any $\epsilon \in (0, \lambda_i^- - \lambda_{i-1}^+)$, and Moreau's decomposition theorem^{††} [30], we show that: in case (i) we have $\mathbf{d} = \mathbf{d}_{\mathbf{x}_{i-1}}^{\Pi}(\nabla f(\mathbf{x}_0))$ and the next breakpoint \mathbf{x}_i is obtained by walking maximally along the shadow; in case (ii) we have $\mathbf{d} = \hat{\mathbf{d}}_{\mathbf{x}_{i-1}}^{\Pi}(\nabla f(\mathbf{x}_0))$ and the next \mathbf{x}_i is obtained by walking along the in-face shadow until the projections curve leaves the minimal face at \mathbf{x}_{i-1} . Moreover, as a byproduct of our constructive proof we show that we take a shadow step if and only if $\langle \mathbf{p}_{i-1}, \mathbf{d}_{\mathbf{x}_{i-1}}^{\Pi}(\nabla f(\mathbf{x}_0)) \rangle = 0$. For example, in Figure 3-right at the first breakpoint \mathbf{x}_1 we have $\langle \mathbf{p}_1, \mathbf{d}_{\mathbf{x}_1}^{\Pi}(\nabla f(\mathbf{x}_0)) \rangle \neq 0$ in which case we take an in-face step, whereas at \mathbf{x}_2 we have $\langle \mathbf{p}_2, \mathbf{d}_{\mathbf{x}_2}^{\Pi}(\nabla f(\mathbf{x}_0)) \rangle = 0$, in which case we take a shadow step. The complete proof is in Appendix B.2.

Remark 1. We now add a few remarks about the previous theorem:

^{††}**Moreau's decomposition theorem** [30]: Let \mathcal{K} be a closed convex cone and let \mathcal{K}° be its polar cone, that is, the closed convex cone defined by $\mathcal{K}^\circ = \{\mathbf{y} \in \mathbb{R}^n \mid \langle \mathbf{x}, \mathbf{y} \rangle \leq 0, \forall \mathbf{x} \in \mathcal{K}\}$. Then, for $\mathbf{x}, \mathbf{y}, \mathbf{z} \in \mathbb{R}^n$, the following statements are equivalent: (i) $\mathbf{z} = \mathbf{x} + \mathbf{y}$, $\mathbf{x} \in \mathcal{K}$, $\mathbf{y} \in \mathcal{K}^\circ$, and $\langle \mathbf{x}, \mathbf{y} \rangle = 0$; (ii) $\mathbf{x} = \Pi_{\mathcal{K}}(\mathbf{z})$ and $\mathbf{y} = \Pi_{\mathcal{K}^\circ}(\mathbf{z})$.

Algorithm 1 Tracing Parametric Projections Curve: $\text{TRACE}(\mathbf{x}_0, \mathbf{x}, \mathbf{w}, \lambda_{\mathbf{x}})$

Input: Polytope $P \subseteq \mathbb{R}^n$, starting point of the projections curve $\mathbf{x}_0 \in P$, $\mathbf{w} \in \mathbb{R}^n$, and a point on the projections curve $\mathbf{x} \in P$ such that $g(\lambda_{\mathbf{x}}) = \Pi_P(\mathbf{x}_0 - \lambda_{\mathbf{x}}\mathbf{w}) = \mathbf{x}$, for a given $\lambda_{\mathbf{x}}$.

Output: Next breakpoint \mathbf{y} (if any) and step-size $\lambda_{\mathbf{y}}$ such that $g(\lambda_{\mathbf{y}}) = \mathbf{y}$.

```

1: Compute  $\mathbf{d}_{\mathbf{x}}^{\Pi} := \lim_{\epsilon \downarrow 0} \frac{\Pi_P(\mathbf{x} - \epsilon\mathbf{w}) - \mathbf{x}}{\epsilon}$ .
2: if  $\mathbf{d}_{\mathbf{x}}^{\Pi} \neq \mathbf{0}$  then
3:   if  $\langle \mathbf{x}_0 - \lambda_{\mathbf{x}}\mathbf{w} - \mathbf{x}, \mathbf{d}_{\mathbf{x}}^{\Pi} \rangle = 0$  then
4:     Compute  $\gamma^{\max} = \max\{\delta \mid \mathbf{x} + \delta\mathbf{d}_{\mathbf{x}}^{\Pi} \in P\}$ 
5:     Set  $\mathbf{d} = \mathbf{d}_{\mathbf{x}}^{\Pi}$ .
6:   else
7:      $\hat{\mathbf{d}}_{\mathbf{x}}^{\Pi}, \gamma^{\max} = \text{TRACE-IN-FACE}(\mathbf{x}_0, \mathbf{x}, \mathbf{w}, \lambda_{\mathbf{x}})$ .
8:     Set  $\mathbf{d} = \hat{\mathbf{d}}_{\mathbf{x}}^{\Pi}$ .
9:   end if
10:  Compute next break point  $\mathbf{y} = \mathbf{x} + (\gamma^{\max})\mathbf{d}$ 
11:  Update  $\lambda_{\mathbf{y}}^- = \lambda_{\mathbf{x}} + \gamma^{\max}$ .
12: else
13:   Set  $\mathbf{y} = \mathbf{x}$  and  $\lambda_{\mathbf{y}} = \lambda_{\mathbf{x}}$ 
14: end if
Return:  $\mathbf{y}, \lambda_{\mathbf{y}}$ 

```

Algorithm 2 Tracing in-face movement: $\text{TRACE-IN-FACE}(\mathbf{x}_0, \mathbf{x}, \mathbf{w}, \lambda_{\mathbf{x}})$

Input: Polytope $P \subseteq \mathbb{R}^n$, starting point of projections curve $\mathbf{x}_0 \in P$, current breakpoint $\mathbf{x} \in P$, direction $\mathbf{w} \in \mathbb{R}^n$, and $\lambda_{\mathbf{x}}$ satisfying $g(\lambda_{\mathbf{x}}) = \Pi_P(\mathbf{x}_0 - \lambda_{\mathbf{x}}\mathbf{w}) = \mathbf{x}$.

```

1: Compute  $\hat{\mathbf{d}}_{\mathbf{x}}^{\Pi} = (\mathbf{I} - \mathbf{A}_{I(\mathbf{x})}^{\dagger} \mathbf{A}_{I(\mathbf{x})})(-\mathbf{w})$                                 ▷ in-face directional derivative at  $\mathbf{x}$ 
2: Evaluate  $\hat{\lambda} = \sup\{\lambda \mid N_P(g(\lambda')) = N_P(\mathbf{x}_{i-1}) \forall \lambda' \in [\lambda_{\mathbf{x}}, \lambda]\}$           ▷ see remark 3
Return:  $\hat{\mathbf{d}}_{\mathbf{x}}^{\Pi}, \hat{\lambda}$ 

```

- (a) Theorem 2 applied at \mathbf{x}_0 implies that the first segment of the projections curve is given by walking maximally along the shadow. This generalizes our earlier discussion about the first segment of the projections curve.
- (b) Whenever we take a shadow step in case (a), we are guaranteed to add a tight constraint at the subsequent breakpoint. This follows by Lemma 4 since the next breakpoint is obtained by taking the maximum movement along the directional derivative $\mathbf{d}_{\mathbf{x}_{i-1}}^{\Pi}(\nabla f(\mathbf{x}_0))$. However this need not be true in case (b), unless the maximum movement along the in-face shadow takes place, i.e., $\hat{\lambda}_{i-1} = \lambda_{i-1}^+ + \max\{\delta : \mathbf{x}_{i-1} + \delta\hat{\mathbf{d}}_{\mathbf{x}_{i-1}}^{\Pi}(\nabla f(\mathbf{x}_0)) \in P\}$.

Assuming oracle access to compute $\mathbf{d}_{\mathbf{x}}^{\Pi}(\mathbf{w})$ and $\hat{\lambda}_{i-1}$ for any $\mathbf{x} \in P$, Theorem 2 gives a constructive method for tracing the whole piecewise linear curve of $g_{\mathbf{x}, \mathbf{w}}(\cdot)$. We include this as an algorithm, $\text{TRACE}(\mathbf{x}_0, \mathbf{x}, \mathbf{w}, \lambda_{\mathbf{x}})$, which traces the projections curve until a target step-size λ , and give its complete description in Algorithm 1. The following remarks about the TRACE algorithm (Algorithm 1) will be useful to understand its implementation and correctness. We first remark that the TRACE algorithm correctly keeps track of the total step-sizes accrued. This is important since given a breakpoint \mathbf{x} , the TRACE-IN-FACE procedure requires $\lambda_{\mathbf{x}}$ satisfying $g(\lambda_{\mathbf{x}}) = \Pi_P(\mathbf{x}_0 - \lambda_{\mathbf{x}}\mathbf{w}) = \mathbf{x}$ (\mathbf{w} is the direction we are computing the projections curve with respect to).

Remark 2. The TRACE algorithm identifies when the projections curve does not change with the same speed as the step-size λ . Suppose that TRACE starts with a point on the projections curve $\mathbf{x} \in P$ such that $g(\lambda_{\mathbf{x}}) = \Pi_P(\mathbf{x}_0 - \lambda_{\mathbf{x}}\mathbf{w}) = \mathbf{x}$, for a given $\lambda_{\mathbf{x}}$. Similar to before, let $\lambda_{\mathbf{x}}^-, \lambda_{\mathbf{x}}^+ \in \mathbb{R}$ respectively be the minimum and maximum step-sizes λ such that $g(\lambda) = \mathbf{x}$. Now suppose that \mathbf{x} is not the endpoint of $g(\lambda)$ (i.e. $\hat{\mathbf{d}}_{\mathbf{x}}^{\Pi} \neq \mathbf{0}$) and that we have $\lambda_{\mathbf{x}} < \lambda_{\mathbf{x}}^+ < \infty$, so that the projections curve moves in-face trivially in the interval $[\lambda_{\mathbf{x}}, \lambda_{\mathbf{x}}^+]$. Then, in a such a case, we take an in-face step with an in-face direction $\hat{\mathbf{d}}_{\mathbf{x}}^{\Pi} = \mathbf{0}$, where we still have $\mathbf{y} = \mathbf{x}$ but correctly update $\lambda_{\mathbf{y}}$ to $\lambda_{\mathbf{x}}^+$. At this point we can run another iteration of TRACE initialized with \mathbf{y} and $\lambda_{\mathbf{y}}$ to obtain the next breakpoint of the curve.

Remark 3. Computing maximum in-face movement. Suppose that we are at a breakpoint \mathbf{x} and we have that $\langle \mathbf{x}_0 - \lambda_{\mathbf{x}}\nabla f(\mathbf{x}_0) - \mathbf{x}, \hat{\mathbf{d}}_{\mathbf{x}}^{\Pi} \rangle \neq 0$. First, compute the maximum feasible movement along $\hat{\mathbf{d}}_{\mathbf{x}}^{\Pi}$, i.e., $\hat{\gamma}^{\max} = \max\{\delta \mid \mathbf{x} + \delta\hat{\mathbf{d}}_{\mathbf{x}}^{\Pi} \in P\}$. We know that $\hat{\lambda} \in [\lambda_{\mathbf{x}}, \hat{\gamma}^{\max}]$. We first check if $\hat{\lambda} = \hat{\gamma}^{\max}$ by checking the first-order optimality:

$$\langle \mathbf{x}_0 - (\lambda_{\mathbf{x}} + \hat{\gamma}^{\max})\mathbf{w} - (\mathbf{x} + \hat{\gamma}^{\max}\hat{\mathbf{d}}_{\mathbf{x}}^{\Pi}), \mathbf{z} - (\mathbf{x} + \hat{\gamma}^{\max}\hat{\mathbf{d}}_{\mathbf{x}}^{\Pi}) \rangle \leq 0 \quad \forall \mathbf{z} \in P, \quad (10)$$

which could be checked using a linear program. If first order-optimality holds, then $\hat{\lambda} = \hat{\gamma}^{\max}$. Otherwise, we know that $\hat{\lambda} < \hat{\gamma}^{\max}$ and thus $\hat{\lambda} = \max\{\lambda \mid N_P(g(\lambda')) = N_P(\mathbf{x}) \ \forall \lambda' \in [\lambda_{\mathbf{x}}, \lambda]\}$. Computing $\hat{\lambda}$ amounts to finding the maximum λ such that $\mathbf{x}_0 - \lambda\mathbf{w} - (\mathbf{x} + (\lambda - \lambda_{\mathbf{x}})\hat{\mathbf{d}}_{\mathbf{x}}^{\Pi}) \in N_P(\mathbf{x} + (\lambda - \lambda_{\mathbf{x}})\hat{\mathbf{d}}_{\mathbf{x}}^{\Pi})$, which can again be computed by the solving the following linear program:

$$\begin{aligned} & \max \quad \lambda \\ & \text{s.t. } \mathbf{x}_0 - \lambda\mathbf{w} - \mathbf{x} - (\lambda - \lambda_{\mathbf{x}})\hat{\mathbf{d}}_{\mathbf{x}}^{\Pi} = \mathbf{A}_{I(\mathbf{x})}^{\top} \boldsymbol{\mu} \\ & \quad \boldsymbol{\mu} \geq 0. \end{aligned} \quad (11)$$

Note that $\lambda = \lambda_{\mathbf{x}}$ is a feasible solution to (11), which is also the optimal solution when the projections curve is moving to another facet and not moving in-face (case (b) in Theorem 2). Furthermore, we know that optimal solution λ^* to the above LP satisfies $\lambda^* < \hat{\gamma}^{\max}$. Hence, (11) is always feasible and bounded, and thus always has an optimal solution.

We now establish the correctness of TRACE and prove the bound on the number of breakpoints of projections curve:

Theorem 3 (Bound on breakpoints in parametric projections curve). *Let $P \subseteq \mathbb{R}^n$ be a polytope, with m facet inequalities (e.g., as in (4)) and fix $\mathbf{x}_0 \in P$. Consider any point $\mathbf{x} \in P$ on the projections curve $g(\lambda) = \Pi_P(\mathbf{x}_0 - \lambda\mathbf{w})$ with an accompanying step-size $\lambda_{\mathbf{x}}$ satisfying $g(\lambda_{\mathbf{x}}) = \Pi_P(\mathbf{x}_0 - \lambda_{\mathbf{x}}\mathbf{w}) = \mathbf{x}$. Then, the procedure TRACE($\mathbf{x}_0, \mathbf{x}, \nabla f(\mathbf{x}), \lambda_{\mathbf{x}}$) is correct and traces the projections piecewise linear curve until the subsequent breakpoint. Moreover, the total number of breakpoints of the projections curve is at most $O(2^m)$ steps.*

^{§§}This example is inspired by Damiano Zeffiro.

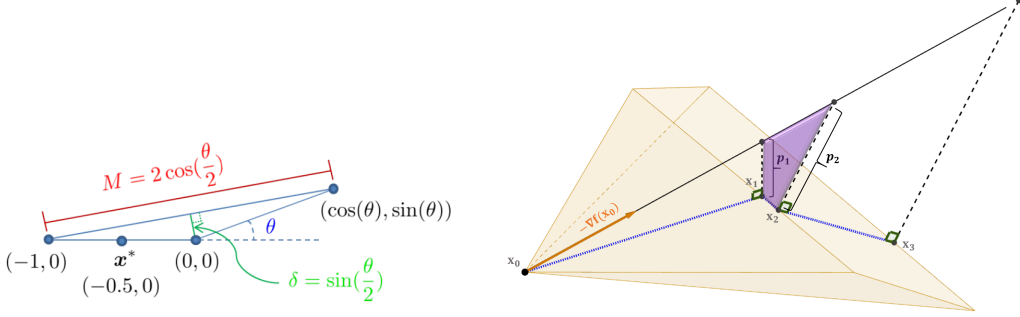


Figure 3: **Left:** Figure from Lacoste-Julien and Jaggi’s work [10] showing the pyramidal width δ of a simple triangle domain as a function of the angle θ . **Right:** An example of the projections curve, showing how the structure of the normal vectors $\mathbf{p}_i := \mathbf{x}_0 - \lambda_i^+ \nabla f(\mathbf{x}_0) - \mathbf{x}_i$ determine whether we take an in-face step or shadow step^{§§}.

Proof. $\text{TRACE}(\mathbf{x}_0, \mathbf{x}, \nabla f(\mathbf{x}_0), \lambda_{\mathbf{x}})$ correctly traces the curve $g(\lambda) = \Pi_P(\mathbf{x}_0 - \lambda \nabla f(\mathbf{x}))$, due to the constructive proof given for Theorem 2. Once the curve leaves the interior of a face, it can no longer visit the face again, since the equivalence of normal cones at two projections implies the projections curve is linear between the two points (which must necessarily lie on the same face) (Lemma 2). Therefore, the number of breakpoints can be at most the number of faces, i.e., $O(2^m)$. \square

4 Descent Directions

Having characterized the properties of the parametric projections curve, we highlight connections with descent directions in conditional gradient and projected gradient methods. We first highlight a connection between the shadow and the *gradient mapping*. Given any scalar $\eta > 0$, the gradient mapping is defined as $G_\eta(\mathbf{x}) := \eta(\mathbf{x} - \Pi_P(\mathbf{x} - \nabla f(\mathbf{x})/\eta)) = \eta(\mathbf{x} - g(1/\eta))$ ^{¶¶}. Observe that if $\eta \leq \lambda_1^-$, then we have that $G_\eta(\mathbf{x}) = -\eta^2 \mathbf{d}_{\mathbf{x}}^\Pi$ using the fact $g(\lambda) = \mathbf{x} + \lambda \mathbf{d}_{\mathbf{x}}^\Pi$, for all $\lambda \in [0, \lambda_1^-]$ (8).

We next claim that the shadow is the best local feasible direction of descent in the following sense: it has the highest inner product with the negative gradient at \mathbf{x} compared to any other normalized feasible direction.

Lemma 6 (Steepest feasible descent of Shadow Steps). *Let P be a polytope defined as in (4) and let $\mathbf{x} \in P$ with gradient $\nabla f(\mathbf{x})$. Let \mathbf{y} be any feasible direction at \mathbf{x} , i.e., $\exists \gamma > 0$ s.t. $\mathbf{x} + \gamma \mathbf{y} \in P$. Then*

$$\left\langle -\nabla f(\mathbf{x}), \frac{\mathbf{d}_{\mathbf{x}}^\Pi}{\|\mathbf{d}_{\mathbf{x}}^\Pi\|} \right\rangle^2 = \|\mathbf{d}_{\mathbf{x}}^\Pi\|^2 \geq \left\langle \mathbf{d}_{\mathbf{x}}^\Pi, \frac{\mathbf{y}}{\|\mathbf{y}\|} \right\rangle^2 \geq \left\langle -\nabla f(\mathbf{x}), \frac{\mathbf{y}}{\|\mathbf{y}\|} \right\rangle^2. \quad (12)$$

This result is intuitive as $\mathbf{d}_{\mathbf{x}}^\Pi$ is projection of $-\nabla f(\mathbf{x})$ onto the set of feasible directions at \mathbf{x} ; this is the fact crucially used to prove this result (proof in Appendix C.1). The above lemma will be useful in the convergence proof for our novel SHADOW-CG (Theorem 8) and SHADOW-CG² (Theorem 9) algorithms. We also show that the shadow gives a true estimate of convergence to

^{¶¶}Note that $g(1/\eta)$ can be obtained using $\text{TRACE}(\mathbf{x}, \nabla f(\mathbf{x}), 1/\eta)$.

optimal***, in the sense that $\|\mathbf{d}_{\mathbf{x}_t}^{\Pi}\| = 0$ if and only if $\mathbf{x}_t = \arg \min_{\mathbf{x} \in P} f(\mathbf{x})$ (Lemma 7). On the other hand, note that $\|\nabla f(\mathbf{x}_t)\|$ does not satisfy this property and can be strictly positive at the constrained optimal solution. Hence, $\|\mathbf{d}_{\mathbf{x}_t}^{\Pi}\|$ is a natural quantity for estimating primal gaps without any dependence on geometric constants like those used in other CG variants such as away steps FW and pairwise FW.

Lemma 7 (Primal gap estimate). *Let P be a polytope defined as in (4) and fix $\mathbf{x} \in P$. Then, $\|\mathbf{d}_{\mathbf{x}}^{\Pi}\| = 0$ if and only if $\mathbf{x} = \mathbf{x}^*$, where $\mathbf{x}^* = \arg \min_{\mathbf{x} \in P} f(\mathbf{x})$.*

The proof follows from first-order optimality and can be found in Appendix C.2. We next show that the end point of the projections curve is in fact the FW vertex under mild technical conditions. In other words, FW vertices are the projection of an infinite descent in the direction of the negative gradient (Theorem 4). Thus, FW vertices are able to obtain the maximum movement in the negative gradient direction while remaining feasible compared to PGD, thereby giving FW steps a new perspective.

Theorem 4 (Optimism of FW vertex). *Let $P \subseteq \mathbb{R}^n$ be a polytope and let $\mathbf{x} \in P$. Let $g(\lambda) = \Pi_P(\mathbf{x} - \lambda \nabla f(\mathbf{x}))$ for $\lambda \geq 0$. Then, the end point of this curve is: $\lim_{\lambda \rightarrow \infty} g(\lambda) = \mathbf{v}^* = \arg \min_{\mathbf{v} \in F} \|\mathbf{x} - \mathbf{v}\|^2$, where $F = \arg \min_{\mathbf{v} \in P} \langle \nabla f(\mathbf{x}), \mathbf{v} \rangle$ is the face of P that minimizes the gradient $\nabla f(\mathbf{x})$. In particular, if F is a vertex, then $\lim_{\lambda \rightarrow \infty} g(\lambda) = \mathbf{v}^*$ is the FW vertex.*

Proof. If $\nabla f(\mathbf{x}) = 0$, then $g(\lambda) = \mathbf{x}$ for all $\lambda \in \mathbb{R}^n$, and the theorem holds trivially. We therefore assume that $\nabla f(\mathbf{x}) \neq 0$. Let $\mathbf{x}_i \in P$ be the i th breakpoint in the projections curve $g(\lambda) = \Pi_P(\mathbf{x}_0 - \lambda \nabla f(\mathbf{x}_0))$, with $\mathbf{x}_i = \mathbf{x}$ for $i = 0$. Using Theorem 3, we know that the number of breakpoints curve $k \leq 2^m$. Consider the last breakpoint \mathbf{x}_k in the curve and let $\lambda_k^- = \min\{\lambda \geq 0 \mid g(\lambda) = \mathbf{x}_k\}$. We will now show that $\mathbf{x}_k = \mathbf{v}^*$.

- (i) We first show that $\mathbf{x}_k \in F$, i.e. $-\nabla f(\mathbf{x}) \in N_P(\mathbf{x}_k)$. Suppose for a contradiction that this not true. Then there exists some $\mathbf{z} \in P$ such that $\langle -\nabla f(\mathbf{x}), \mathbf{z} - \mathbf{x}_k \rangle > 0$. Consider any scalar $\bar{\lambda}$ satisfying $\bar{\lambda} > \max\{-\frac{\langle \mathbf{x} - \mathbf{x}_k, \mathbf{z} - \mathbf{x}_k \rangle}{\langle -\nabla f(\mathbf{x}), \mathbf{z} - \mathbf{x}_k \rangle}, \lambda_k^- \}$. Then, using the choice of $\bar{\lambda}$ we have

$$\begin{aligned} \langle \mathbf{x} - \mathbf{x}_k, \mathbf{z} - \mathbf{x}_k \rangle + \bar{\lambda} \langle -\nabla f(\mathbf{x}), \mathbf{z} - \mathbf{x}_k \rangle &> 0 \\ \implies \langle \mathbf{x} - \mathbf{x}_k - \bar{\lambda} \nabla f(\mathbf{x}), \mathbf{z} - \mathbf{x}_k \rangle &> 0. \end{aligned}$$

Now, since $g(\lambda) = \mathbf{x}_k$ for $\lambda \geq \lambda_k^-$, we know that $g(\bar{\lambda}) = \mathbf{x}_k$. Thus, the above equation could be written as

$$\langle \mathbf{x} - \bar{\lambda} \nabla f(\mathbf{x}) - g(\bar{\lambda}), \mathbf{z} - g(\bar{\lambda}) \rangle > 0,$$

which contradicts the first-order optimality for $g(\bar{\lambda})$.

- (ii) We will now show that \mathbf{x}_k is additionally the closest point to \mathbf{x} in ℓ_2 norm. Again, suppose for contradiction that this not true. Let $\epsilon := \|\mathbf{x}_k - \mathbf{v}^*\| > 0$. First, note that by definition,

***Lemma 6 with $\mathbf{y} = \mathbf{x}^* - \mathbf{x}$ can be used to estimate the primal gap: $\|\mathbf{d}_{\mathbf{x}}^{\Pi}\|^2 \geq 2\mu(f(\mathbf{x}) - f(\mathbf{x}^*))$ (see (23)).

$g(\lambda) = \arg \min_{\mathbf{y} \in P} \left\{ \frac{\|\mathbf{x} - \mathbf{y}\|^2}{2\lambda} + \langle \nabla f(\mathbf{x}), \mathbf{y} \rangle \right\}$ for any $\lambda > 0$. Then, since $g(\lambda_k^-) = \mathbf{x}_k$ we have

$$\frac{\|\mathbf{x} - \mathbf{x}_k\|^2}{2\lambda_k^-} + \langle \nabla f(\mathbf{x}), \mathbf{x}_k \rangle \leq \frac{\|\mathbf{x} - \mathbf{z}\|^2}{2\lambda_k^-} + \langle \nabla f(\mathbf{x}), \mathbf{z} \rangle, \quad \forall \mathbf{z} \in P. \quad (13)$$

Moreover, the first-order optimality condition for \mathbf{v}^* (for minimizing $\|\mathbf{x} - \mathbf{y}\|^2$ over $\mathbf{y} \in F$) implies $\langle \mathbf{v}^* - \mathbf{x}, \mathbf{z} - \mathbf{v}^* \rangle \geq 0$ for all $\mathbf{z} \in F$. In particular, $(\mathbf{v}^* - \mathbf{x})^T(\mathbf{x}_k - \mathbf{v}^*) \geq 0$ since $\mathbf{x}_k \in F$. Therefore,

$$\|\mathbf{x} - \mathbf{v}^*\|^2 + \|\mathbf{x}_k - \mathbf{v}^*\|^2 = \|\mathbf{x}\|^2 + 2\|\mathbf{v}^*\|^2 - 2\mathbf{x}^T \mathbf{v}^* + \|\mathbf{x}_k\|^2 - 2\mathbf{x}_k^T \mathbf{v}^* \quad (14)$$

$$= \|\mathbf{x}_k - \mathbf{x}\|^2 - 2(\mathbf{v}^* - \mathbf{x})^T(\mathbf{x}_k - \mathbf{v}^*) \quad (15)$$

$$\leq \|\mathbf{x}_k - \mathbf{x}\|^2. \quad (16)$$

But then, since $\mathbf{x}_k \in F$, we know that $\langle \nabla f(\mathbf{x}), \mathbf{x}_k \rangle = \langle \nabla f(\mathbf{x}), \mathbf{v}^* \rangle$, which implies

$$\begin{aligned} \frac{\|\mathbf{x} - \mathbf{v}^*\|^2}{2\lambda_k^-} + \langle \nabla f(\mathbf{x}), \mathbf{v}^* \rangle &\leq \frac{\|\mathbf{x}_k - \mathbf{x}\|^2 - \|\mathbf{x}_k - \mathbf{v}^*\|^2}{2\lambda_k^-} + \langle \nabla f(\mathbf{x}), \mathbf{v}^* \rangle \quad (\text{using (16)}) \\ &= \frac{\|\mathbf{x}_k - \mathbf{x}\|^2 - \epsilon}{2\lambda_k^-} + \langle \nabla f(\mathbf{x}), \mathbf{v}^* \rangle \quad (\|\mathbf{x}_k - \mathbf{v}^*\| = \epsilon) \\ &< \frac{\|\mathbf{x}_k - \mathbf{x}\|^2}{2\lambda_k^-} + \langle \nabla f(\mathbf{x}), \mathbf{x}_k \rangle, \quad (\epsilon > 0) \end{aligned}$$

contradicting optimality of \mathbf{x}_k (13). □

Next, we show that the shadow steps also give the best away direction emanating from away-vertices in the minimal face at any $\mathbf{x} \in P$ (which is precisely the set of *possible* away vertices (see Appendix C.3), using Lemma 6 and the following result:

Lemma 8 (Away steps). *Let P be a polytope defined as in (4) and fix $\mathbf{x} \in P$. Let $F = \{\mathbf{z} \in P : \mathbf{A}_{I(\mathbf{x})}\mathbf{z} = \mathbf{b}_{I(\mathbf{x})}\}$ be the minimal face containing \mathbf{x} . Further, choose $\delta_{\max} = \max\{\delta : \mathbf{x} - \delta \mathbf{d}_{\mathbf{x}}^{\Pi} \in P\}$ and consider the away point $\mathbf{a}_{\mathbf{x}} = \mathbf{x} - \delta_{\max} \mathbf{d}_{\mathbf{x}}^{\Pi}$ obtained by moving maximally along the the direction of the negative shadow. Then, $\mathbf{a}_{\mathbf{x}}$ lies in F and the corresponding away-direction is simply $\mathbf{x} - \mathbf{a}_{\mathbf{x}} = \delta_{\max} \mathbf{d}_{\mathbf{x}}^{\Pi}$.*

Lemma 8 states that the away point obtained by the maximal movement along the negative shadow from \mathbf{x} , $\mathbf{a}_{\mathbf{x}}$, lies in the convex hull of $A := \{\mathbf{v} \in \text{vert}(P) \cap F\}$. The set A is precisely the set of all possible away vertices (see Appendix C.3). Thus, the shadow gives the best direction of descent emanating from the convex hull of all possible away-vertices. We include a proof of this lemma in Appendix C.3.

5 Continuous-time Dynamics and SHADOW-WALK Algorithm

We established in the last section that the shadow of the negative gradient $\mathbf{d}_{\mathbf{x}_t}^{\Pi}$ is indeed the best “local” direction of descent (Lemma 6), and a true measure of the primal gap since convergence in $\|\mathbf{d}_{\mathbf{x}_t}^{\Pi}\|$ implies optimality (Lemma 7). Having characterized the parametric projections curve, the natural question is if a shadow-descent algorithm that walks along the directional derivative with respect to negative gradient at iterate \mathbf{x}_t , converge linearly? We start by answering that question positively for continuous-time dynamics.

We now present the continuous-time dynamics for moving along the shadow of the gradient in the polytope. In this section we let \mathcal{D}^* be the dual space of \mathcal{D} (in our case since $\mathcal{D} \subseteq \mathbb{R}^n$, \mathcal{D}^* can also be identified with \mathbb{R}^n). Let $\phi : \mathcal{D} \rightarrow \mathbb{R}$ be a strongly convex and differentiable function. This function will be used as the *mirror-map* in a generalization of the projected gradient descent algorithm, known as *mirror descent* [8]. We now briefly discuss the mirror descent algorithm and review simple preliminaries needed for what follows. Let ϕ^* be the Fenchel-conjugate of ϕ with effective domain P , that is $\phi^*(\mathbf{y}) = \max_{\mathbf{x} \in P} \{\langle \mathbf{y}, \mathbf{x} \rangle - \phi(\mathbf{x})\}$. From Danskin’s theorem (see e.g., [31]), we know that $\nabla \phi^*(\mathbf{y}) = \arg \max_{\mathbf{x} \in P} \{\langle \mathbf{y}, \mathbf{x} \rangle - \phi(\mathbf{x})\}$, so that $\nabla \phi^* : \mathcal{D}^* \rightarrow P$ is the mirror-map operator mapping from \mathcal{D}^* to \mathcal{D} . We use $\nabla^2 \phi^*(\cdot)$ to denote the Hessian of ϕ^* . The mirror descent algorithm is iterative and starts with any point $\mathbf{x}_0 \in P$. Then for any $t \geq 1$, the algorithm first performs *unconstrained* gradient descent steps in the dual space:

$$\mathbf{z}_t = \nabla \phi(\mathbf{x}_t) - \gamma_t \nabla f(\mathbf{x}_t) \text{ for some step size } \gamma_t \geq 0,$$

and then maps back these descent steps to the primal space by computing a so-called *Bregman projection*: $\mathbf{x}_{t+1} = \nabla \phi^*(\mathbf{z}_t)$.

5.1 ODE for Moving in the Shadow of the Gradient

Let $X(t)$ denote the continuous-time trajectory of our dynamics and \dot{X} denote the time-derivative of $X(t)$, i.e., $\dot{X}(t) = \frac{d}{dt} X(t)$. In [32], Krichene et. al propose the following coupled dynamics $(X(t), Z(t))$ for mirror descent, where $X(t)$ evolves in the primal space \mathcal{D} , and $Z(t)$ evolves in the dual space \mathcal{D}^* , as follows, initialized with $Z(0) = \mathbf{z}_0$ with $\nabla \phi^*(\mathbf{z}_0) = \mathbf{x}_0 \in P$:

$$\dot{Z}(t) = -\nabla f(X(t)), \quad X(t) = \nabla \phi^*(Z(t)). \quad (17)$$

Let $\mathbf{d}_{X(t)}^\phi$ be the directional derivative with respect to the Bregman projections in the mirror descent algorithm, i.e., $\mathbf{d}_{X(t)}^\phi = \lim_{\epsilon \downarrow 0} \frac{\nabla \phi^*(\nabla \phi(X(t)) - \epsilon \nabla f(X(t))) - X(t)}{\epsilon}$. The continuous time dynamics of tracing this directional derivative are simply

$$\dot{X}(t) = \mathbf{d}_{X(t)}^\phi. \quad (18)$$

These dynamics in (18) solely operate in the primal space and one can initialize them with $X(0) = \mathbf{x}_0 \in P$ and show that they are equivalent to (17) under mild technical conditions as specified below

(the proof is in Appendix E.1):

Theorem 5. *Let $\phi : \mathcal{D} \rightarrow \mathbb{R}$ be a mirror map that is strongly convex and differentiable, and assume that the directional derivative $\mathbf{d}_{X(t)}^\phi$ exists for all $t \geq 0$. Then, the dynamics for mirror descent (17) are equivalent to the shadow dynamics $\dot{X}(t) = \mathbf{d}_{X(t)}^\phi$ with the same initial conditions $X(0) = \mathbf{x}_0 \in P$.*

Although the results of Theorem 5 hold for general mirror-maps, in this work we focus on the case when $\phi = \frac{1}{2}\|\cdot\|^2$ to exploit the piecewise linear structure of the projections curve (with respect to the gradient) proved in Theorem 1. Note that when the mirror map $\phi = \frac{1}{2}\|\cdot\|^2$, we have

$$\nabla\phi^*(\mathbf{y}) = \arg\max_{\mathbf{x} \in P}\{\langle \mathbf{y}, \mathbf{x} \rangle - \phi(\mathbf{x})\} = \arg\min_{\mathbf{x} \in P}\left\{\frac{1}{2}\|\mathbf{x}\| - \langle \mathbf{y}, \mathbf{x} \rangle\right\} = \arg\min_{\mathbf{x} \in P}\frac{1}{2}\|\mathbf{y} - \mathbf{x}\|^2,$$

so that we recover a Euclidean projection onto P . This implies

$$\begin{aligned} \mathbf{d}_{X(t)}^\phi &= \lim_{\epsilon \downarrow 0} \frac{\nabla\phi^*(X(t) - \epsilon \nabla f(X(t))) - X(t)}{\epsilon} && (\nabla\phi(X(t)) = X(t)) \\ &= \lim_{\epsilon \downarrow 0} \frac{\arg\min_{\mathbf{x} \in P} \frac{1}{2}\|X(t) - \epsilon \nabla f(X(t)) - \mathbf{x}\|^2 - X(t)}{\epsilon} && (\text{by definition of } \nabla\phi^*) \\ &= \mathbf{d}_{X(t)}^\Pi. \end{aligned}$$

Therefore, Theorem 5 shows that the continuous-time dynamics of moving in the (Euclidean) shadow of the gradient are equivalent to those of PGD. Moreover, we also show the following convergence result of those dynamics (proof in Appendix E.2):

Theorem 6. *Let $P \subseteq \mathbb{R}^n$ be a polytope and suppose that $f : P \rightarrow \mathbb{R}$ is differentiable and μ -strongly convex over P . Consider the shadow dynamics $\dot{X}(t) = \mathbf{d}_{X(t)}^\Pi$ with initial conditions $X(0) = \mathbf{x}_0 \in P$. Then for each $t \geq 0$, we have $X(t) \in P$. Moreover, the primal gap $h(X(t)) := f(X(t)) - f(\mathbf{x}^*)$ associated with the shadow dynamics decreases as: $h(X(t)) \leq e^{-2\mu t}h(\mathbf{x}_0)$.*

5.2 Shadow-Walk Method

Although the continuous-dynamics of moving along the shadow are the same as those of PGD and achieve linear convergence, it is unclear how to discretize this continuous-time process and obtain a linearly convergent algorithm. To ensure feasibility we may have arbitrarily small step-sizes, and therefore, cannot show sufficient progress in such cases. This is a phenomenon similar to that in the Away-Step and Pairwise CG variants, where the maximum step-size that one can take might not be big enough to show sufficient progress. In [10], the authors overcome this problem by bounding the number of such ‘bad’ steps using dimension reduction arguments crucially relying on the fact that these algorithms maintain their iterates as a convex combination of vertices. However, unlike away-steps in CG variants, we consider shadow directions $(\mathbf{d}_x^\Pi, \hat{\mathbf{d}}_x^\Pi)$ for descent, which are independent from the vertices of P and thus eliminating the need to maintain active sets for the iterates of the algorithm. In general, the shadow ODE might revisit a fixed facet a large number

Algorithm 3 SHADOW-WALK Algorithm

Input: Polytope $P \subseteq \mathbb{R}^n$, function $f : P \rightarrow \mathbb{R}$ and initialization $\mathbf{x}_0 \in P$.

```
1: for  $t = 0, \dots, T$  do
2:   Update  $\mathbf{x}_{t+1} := \text{TRACE-OPT}(\mathbf{x}_t, \nabla f(\mathbf{x}_t))$ . ▷ trace projections curve
3: end for
```

Return: \mathbf{x}_{T+1}

times (see Figure 1) with decreasing step-sizes. This problem does not occur when discretizing PGD’s continuous time dynamics since we can take *unconstrained* gradient steps and then the projections ensure feasibility.

Inspired by PGD’s discretization and the structure of the parametric projections curve, we propose a SHADOW-WALK algorithm (Algorithm 3) with a slight twist: trace the projections curve by walking along the shadow at an iterate \mathbf{x}_t until enough progress is ensured. To do this, we use the TRACE-OPT procedure, which chains together consecutive short descent steps and uses line-search until it minimizes the function f over the linear segments of projections curve. The complete description of the algorithm is given in Algorithm 6 in Appendix A. One important property of TRACE-OPT is that it only requires one gradient oracle call. Also, if we know the smoothness constant L , then TRACE-OPT can be terminated early once we have traced the projections curve until we reach the PGD step with a fixed $1/L$ step size. This results in linear convergence, as long as the number of steps taken by the TRACE-OPT procedure are bounded, i.e., the number of “bad” boundary cases. Using fundamental properties of normal cones attained in the projections curve, we are able bound these steps to be at most the number of faces of the polytope (Theorem 3). We thus establish the following result (proof in Appendix E.3):

Theorem 7. *Let $P \subseteq \mathbb{R}^n$ be a polytope and suppose that $f : P \rightarrow \mathbb{R}$ is L -smooth and μ -strongly convex over P . Then the primal gap $h(\mathbf{x}_t) := f(\mathbf{x}_t) - f(\mathbf{x}^*)$ of the SHADOW WALK algorithm decreases geometrically:*

$$h(\mathbf{x}_{t+1}) \leq \left(1 - \frac{\mu}{L}\right) h(\mathbf{x}_t)$$

with each iteration of the SHADOW WALK algorithm (assuming TRACE-OPT is a single step). Moreover, the number of oracle calls to shadow, in-face shadow and line-search oracles to obtain an ϵ -accurate solution is $O\left(\beta \frac{L}{\mu} \log\left(\frac{1}{\epsilon}\right)\right)$, where β is the maximum number of breakpoints of the parametric projections curve that the TRACE-OPT method visits.

This result is the key interpolation between PGD and CGD methods, attaining geometric constant independent rates. Comparing this convergence rate with the one in Theorem 6, we see that we pay for discretization of the ODE with the constants L and β . Although the constant β depends on the number of facets m and in fact the combinatorial structure of the face-lattice of the polytope, it is invariant under any deformations of the actual geometry of the polytope preserving the face-lattice (in contrast to vertex-facet distance and pyramidal width) as we discuss next. Although we show $\beta \leq O(2^m)$, we conjecture that it can be much smaller (i.e., $O(nm)$) for structured polytopes. Moreover, computationally we see much fewer calls to the oracle than $O(2^m)$.

Algorithm 4 Shadow Conditional Gradient (SHADOW-CG)

Input: Polytope $P \subseteq \mathbb{R}^n$, function $f : P \rightarrow \mathbb{R}$, $\mathbf{x}_0 \in P$ and accuracy parameter ε .

```

1: for  $t = 0, \dots, T$  do
2:   Let  $\mathbf{v}_t := \arg \min_{\mathbf{v} \in P} \langle \nabla f(\mathbf{x}_t), \mathbf{v} \rangle$  and  $\mathbf{d}_t^{\text{FW}} := \mathbf{v}_t - \mathbf{x}_t$ .            $\triangleright$  FW direction
3:   if  $\langle -\nabla f(\mathbf{x}_t), \mathbf{d}_t^{\text{FW}} \rangle \leq \varepsilon$  then return  $\mathbf{x}_t$                                  $\triangleright$  primal gap is small enough
4:   Compute the derivative of projection of the gradient  $\mathbf{d}_{\mathbf{x}_t}^{\Pi}$ 
5:   if  $\langle -\nabla f(\mathbf{x}_t), \mathbf{d}_{\mathbf{x}_t}^{\Pi} / \|\mathbf{d}_{\mathbf{x}_t}^{\Pi}\| \rangle \leq \langle -\nabla f(\mathbf{x}_t), \mathbf{d}_t^{\text{FW}} \rangle$ 
6:      $\mathbf{d}_t := \mathbf{d}_t^{\text{FW}}$  and  $\mathbf{x}_{t+1} := \mathbf{x}_t + \gamma_t \mathbf{d}_t$  ( $\gamma_t \in [0, 1]$ ).            $\triangleright$  use line-search
7:   else  $\mathbf{x}_{t+1} := \text{TRACE-OPT}(\mathbf{x}_t, \nabla f(\mathbf{x}_t))$ .            $\triangleright$  trace projections curve
8: end for

```

Return: \mathbf{x}_{T+1}

5.3 A Note on the Linear Convergence Rate

Although our linear convergence rate depends on the number of facet inequalities m , it eliminates the dependence on the geometry of the domain that is needed in CG variants. For example, Jaggi and Lacoste-Julien [10] prove a linear rate of $\left(1 - \frac{\mu}{L} \left(\frac{\delta}{D}\right)^2\right)$ to get an ϵ -accurate solution for the away step FW algorithm, where δ is the pyramidal width of the domain. Now, consider the example in Figure 3 showing how the pyramidal width δ of a simple triangle domain changes as the angle θ changes. In particular, the pyramidal width will be arbitrarily small for small θ . However, note that the number of facets for this triangle domain is $m = 3$, and the number of breakpoints of the projections curve β is not dependent on the angle θ . Therefore, we smoothly interpolate between the $\left(1 - \frac{\mu}{L}\right)$ rate for PGD and the rates for CG variants (see Table 1 for a summary of these rates).

6 Shadow Conditional Gradient Method

Using our insights on descent directions, we propose using Frank-Wolfe steps earlier in the algorithm, and use shadow steps more frequently towards the end of the algorithm. Frank-Wolfe steps allow us to greedily skip a lot of facets that TRACE-OPT would go through since FW vertices form the end point of the projections curve (Theorem 4). Shadow steps operate as “optimal” away-steps (Lemma 8) thus reducing zig-zagging phenomenon [10] close to the optimal solution. As the algorithm progresses, one can expect Frank-Wolfe directions to become close to orthogonal to the negative gradient. However, in this case the norm of the shadow also starts diminishing (Lemma 7). Therefore, we choose FW direction in line 7 of Algorithm 4 whenever $\langle -\nabla f(\mathbf{x}_t), \mathbf{d}_t^{\text{FW}} \rangle \geq \langle -\nabla f(\mathbf{x}_t), \mathbf{d}_{\mathbf{x}_t}^{\Pi} / \|\mathbf{d}_{\mathbf{x}_t}^{\Pi}\| \rangle = \|\mathbf{d}_{\mathbf{x}_t}^{\Pi}\|$, and shadow directions otherwise. This is sufficient to give linear convergence.

Theorem 8. *Let $P \subseteq \mathbb{R}^n$ be a polytope with diameter D and suppose that $f : P \rightarrow \mathbb{R}$ is L -smooth and μ -strongly convex over P . Then, the primal gap $h(\mathbf{x}_t) := f(\mathbf{x}_t) - f(\mathbf{x}^*)$ of SHADOW-CG decreases geometrically:*

$$h(\mathbf{x}_{t+1}) \leq \left(1 - \frac{\mu}{LD^2}\right) h(\mathbf{x}_t),$$

with each iteration of the SHADOW-CG algorithm (assuming TRACE-OPT is a single step). Moreover, the number of shadow, in-face shadow and line-search oracle calls for an ϵ -accurate solution is $O\left((D^2 + \beta)\frac{L}{\mu} \log(\frac{1}{\epsilon})\right)$, where β is the number of breakpoints of the parametric projections curve that

the TRACE-OPT method visits.

Proof. In the algorithm, we either enter the TRACE-OPT procedure ($\mathbf{x}_{t+1} := \text{TRACE-OPT}(\mathbf{x}_t, \nabla f(\mathbf{x}_t))$), or we take a Frank-Wolfe step ($\mathbf{x}_{t+1} := \mathbf{x}_t + \gamma_t(\mathbf{v}_t - \mathbf{x}_t)$ for some $\gamma_t \in [0, 1]$). We split the proof of convergence into two cases depending on which case happens:

Case 1: *We enter the TRACE-OPT procedure.* Since $\text{TRACE-OPT}(\mathbf{x}_t, \nabla f(\mathbf{x}_t))$ traces the whole curve of $g(\lambda) = \Pi_P(\mathbf{x}_t - \lambda \nabla f(\mathbf{x}_t))$ with exact line-search, we know that at the point \mathbf{x}_{t+1} we have $f(\mathbf{x}_{t+1}) \leq f(g(\lambda))$ for all $\lambda > 0$. In particular, $f(\mathbf{x}_{t+1}) \leq f(g(1/L))$. Hence we get the same standard rate $(1 - \frac{\mu}{L})$ of decrease as PGD with fixed step size $1/L$ [33]. We include this result with a proof in Appendix D for completeness (Theorem 10).

Case 2: *We take a Frank-Wolfe step.* Let γ_t be the step size chosen by line-search for moving along the chosen FW direction $\mathbf{d}_t := \mathbf{v}_t - \mathbf{x}_t$, and let $\gamma_t^{\max} = 1$ be the maximum step-size that one can move along \mathbf{d}_t . Using the smoothness of f , we have $f(\mathbf{x}_{t+1}) \leq f(\mathbf{x}_t) + \gamma_t \langle \nabla f(\mathbf{x}_t), \mathbf{d}_t \rangle + \frac{L\gamma_t^2}{2} \|\mathbf{d}_t\|^2$. Define $\gamma_{\mathbf{d}_t} := \frac{\langle -\nabla f(\mathbf{x}_t), \mathbf{d}_t \rangle}{L\|\mathbf{d}_{\mathbf{x}_t}\|^2}$ to be the step-size minimizing the RHS of the previous inequality. It is important to note that $\gamma_{\mathbf{d}_t}$ is not the step-size used in the algorithm obtained from line-search. It is used to only lower bound the progress obtained from the line-search step, since, plugging in $\gamma_{\mathbf{d}_t}$ in the smoothness inequality yields:

$$h(\mathbf{x}_t) - h(\mathbf{x}_{t+1}) = f(\mathbf{x}_t) - f(\mathbf{x}_{t+1}) \geq \frac{\langle -\nabla f(\mathbf{x}_t), \mathbf{d}_t \rangle^2}{2L\|\mathbf{d}_t\|^2}. \quad (19)$$

We now split the proof depending on whether $\gamma_t < \gamma_t^{\max}$ or not:

(i) *First, suppose that $\gamma_t < \gamma_t^{\max}$.* We claim that we can use the step size from $\gamma_{\mathbf{d}_t}$ to lower bound the progress even if $\gamma_{\mathbf{d}_t}$ is not a feasible step size (i.e. when $\gamma_{\mathbf{d}_t} > 1$). To see this, note that the optimal solution of the line-search step is in the interior of the interval $[0, \gamma_t^{\max}]$. Define $\mathbf{x}_\gamma := \mathbf{x}_t + \gamma \mathbf{d}_t$. Then, because $f(\mathbf{x}_\gamma)$ is convex in γ , we know that $\min_{\gamma \in [0, \gamma_t^{\max}]} f(\mathbf{x}_\gamma) = \min_{\gamma \geq 0} f(\mathbf{x}_\gamma)$ and thus $\min_{\gamma \in [0, \gamma_t^{\max}]} f(\mathbf{x}_\gamma) = f(\mathbf{x}_{t+1}) \leq f(\mathbf{x}_\gamma)$ for all $\gamma \geq 0$. In particular, $f(\mathbf{x}_{t+1}) \leq f(\mathbf{x}_{\gamma_{\mathbf{d}_t}})$. Hence, we can use (19) to bound the progress per iteration as follows:

$$h(\mathbf{x}_t) - h(\mathbf{x}_{t+1}) \geq \frac{\langle -\nabla f(\mathbf{x}_t), \mathbf{d}_t^{\text{FW}} \rangle^2}{2L\|\mathbf{d}_t^{\text{FW}}\|^2} \quad (\text{using smoothness}) \quad (20)$$

$$\geq \frac{\left\langle -\nabla f(\mathbf{x}_t), \frac{\mathbf{d}_{\mathbf{x}_t}^{\text{II}}}{\|\mathbf{d}_{\mathbf{x}_t}^{\text{II}}\|} \right\rangle^2}{2LD^2} \quad (\text{choice of descent}) \quad (21)$$

$$\geq \frac{\mu}{LD^2} h(\mathbf{x}_t), \quad (22)$$

where (22) follows from applying Lemma 6 with $\mathbf{y} = \mathbf{x}^* - \mathbf{x}$ to obtain:

$$\left\langle \nabla f(\mathbf{x}_t), \frac{\mathbf{d}_{\mathbf{x}_t}^{\Pi}}{\|\mathbf{d}_{\mathbf{x}_t}^{\Pi}\|} \right\rangle^2 = \|\mathbf{d}_{\mathbf{x}_t}^{\Pi}\|^2 \geq \left\langle -\nabla f(\mathbf{x}_t), \frac{\mathbf{x}^* - \mathbf{x}_t}{\|\mathbf{x}^* - \mathbf{x}_t\|} \right\rangle^2 \geq 2\mu h(\mathbf{x}_t). \quad (23)$$

The last inequality in (23) follows from μ -strong convexity of the function* $f(\cdot)$. This shows the rate stated in the theorem.

(ii) *We have a boundary case: $\gamma_t = \gamma_t^{\max}$.* We further divide this case into two sub-cases:

- (a) First assume that $\gamma_{\mathbf{d}_t} \leq \gamma_t^{\max}$ so that the step size from smoothness is feasible. Then, using the same argument as above we also have a $(1 - \frac{\mu}{LD^2})$ -geometric rate of decrease.
- (b) Finally assume that $\gamma_{\mathbf{d}_t} > \gamma_t^{\max}$ and $\mathbf{d}_t = \mathbf{d}_t^{\text{FW}}$. Observe that $\gamma_{\mathbf{d}_t} = \frac{\langle -\nabla f(\mathbf{x}_t), \mathbf{d}_t^{\text{FW}} \rangle}{L\|\mathbf{d}_t^{\text{FW}}\|^2} > \gamma_t^{\max} = 1$ implies that $\langle -\nabla f(\mathbf{x}_t), \mathbf{d}_t^{\text{FW}} \rangle \geq L\|\mathbf{d}_t^{\text{FW}}\|_2^2$. Hence, using the fact that $\gamma_t = \gamma_t^{\max} = 1$ in the smoothness inequality given previously, we have:

$$h(\mathbf{x}_t) - h(\mathbf{x}_{t+1}) \geq \langle -\nabla f(\mathbf{x}_t), \mathbf{d}_t^{\text{FW}} \rangle - \frac{L}{2}\|\mathbf{d}_t^{\text{FW}}\|_2^2 \geq \frac{h(\mathbf{x}_t)}{2},$$

where the last inequality follows using the convexity of f as follows:

$$h(\mathbf{x}_t) \leq \langle -\nabla f(\mathbf{x}_t), \mathbf{x}^* - \mathbf{x}_t \rangle \leq \max_{\mathbf{v} \in P} \langle -\nabla f(\mathbf{x}_t), \mathbf{v} - \mathbf{x}_t \rangle. \quad (24)$$

Hence, we get a geometric rate of decrease of $1/2$.

The iteration complexity of the number of oracle calls stated in the theorem now follows using the above rate of decrease in the primal gap. \square

The theoretical bound on iteration complexity for a given fixed accuracy is better for SHADOW-WALK compared to SHADOW-CG. However, the computational complexity for SHADOW-CG is better since FW steps are cheaper to compute compared to shadow and we can avoid the potentially expensive computation via the TRACE-OPT-routine. Moreover, even if we do enter TRACE-OPT-routine, the addition of FW steps potentially reduces the number of iterations spent TRACE-OPT, since these steps greedily skip a lot of facets by wrapping maximally over the polytope. This is also observed in the experiments, as we discuss later.

A Practical Variant of Shadow-CG. In the SHADOW-CG algorithm, we had to compute the shadow $\mathbf{d}_{\mathbf{x}_t}^{\Pi}$ every iteration to determine whether we take a FW step or enter TRACE-OPT. With the aim of improving the computational complexity of the the algorithm, we now propose

Using the strong convexity inequality applied with $\mathbf{y} \leftarrow \mathbf{x}_t + \gamma(\mathbf{x}^ - \mathbf{x}_t)$ and $\mathbf{x} \leftarrow \mathbf{x}_t$ we obtain $f(\mathbf{x}_t + \gamma(\mathbf{x}^* - \mathbf{x}_t)) - f(\mathbf{x}_t) \geq \gamma \langle \nabla f(\mathbf{x}_t), \mathbf{x}^* - \mathbf{x}_t \rangle + \frac{\mu\gamma^2\|\mathbf{x}^* - \mathbf{x}_t\|^2}{2} \geq -\frac{\langle -\nabla f(\mathbf{x}_t), \mathbf{x}^* - \mathbf{x}_t \rangle^2}{2\mu\|\mathbf{x}^* - \mathbf{x}_t\|^2}$, where the second inequality is obtained by minimizing over γ . As the LHS is independent of γ , we can set $\gamma = 1$ to get $h(\mathbf{x}_t) = f(\mathbf{x}_t) - f(\mathbf{x}^*) \leq \frac{\langle -\nabla f(\mathbf{x}_t), \mathbf{x}^* - \mathbf{x}_t \rangle^2}{2\mu\|\mathbf{x}^* - \mathbf{x}_t\|^2}$.

Algorithm 5 Shadow CG with Gradient test (SHADOW-CG²)

Input: Polytope $P \subseteq \mathbb{R}^n$, function $f : P \rightarrow \mathbb{R}$, $\mathbf{x}_0 \in P$, tuning parameter $c \in (0, 1)$, and accuracy parameter ε .

... same as Algorithm 4, except changing lines 4-7 as follows...

1: Initialize $\alpha = 1$
4: **if** $C\|\nabla f(\mathbf{x}_t)\| \leq \langle -\nabla f(\mathbf{x}_t), \mathbf{d}_t^{\text{FW}} \rangle$
5: $\mathbf{d}_t := \mathbf{d}_t^{\text{FW}}$ and $\mathbf{x}_{t+1} := \mathbf{x}_t + \gamma_t \mathbf{d}_t$ ($\gamma_t \in [0, 1]$). ▷ use line-search
6: **else** $\mathbf{x}_{t+1} := \text{TRACE-OPT}(\mathbf{x}_t, \nabla f(\mathbf{x}_t))$. ▷ trace projections curve

Return: \mathbf{x}_{T+1}

another (cheap) way to determine whether we can take a FW step without computing the $\mathbf{d}_{\mathbf{x}_t}^{\Pi}$, while maintaining linear convergence. Recall from Lemma 6 that $\left\langle -\nabla f(\mathbf{x}_t), \frac{\mathbf{d}_{\mathbf{x}_t}^{\Pi}}{\|\mathbf{d}_{\mathbf{x}_t}^{\Pi}\|} \right\rangle = \|\mathbf{d}_{\mathbf{x}_t}^{\Pi}\|$. The left-hand side of this equality can be upper bounded by $\|\nabla f(\mathbf{x})\|$ using Cauchy-Schwartz, and thus we get $\|\nabla f(\mathbf{x}_t)\| \geq \|\mathbf{d}_{\mathbf{x}_t}^{\Pi}\|$. Therefore, $\|\mathbf{d}_{\mathbf{x}_t}^{\Pi}\|$ can be approximated by $c\|\nabla f(\mathbf{x}_t)\|$, where $c \in (0, 1)$ is a scalar.

We now propose our SHADOW-CG² algorithm, whose description is given in Algorithm 5. The algorithm is exactly the same as SHADOW-CG, but it now takes a FW step whenever $c\|-\nabla f(\mathbf{x}_t)\| \leq \langle -\nabla f(\mathbf{x}_t), \mathbf{d}_t^{\text{FW}} \rangle$. Note that the smaller c is, the more the algorithm prioritizes FW steps. Thus, the scalar c serves as a tuning parameter for the algorithm that is used to trade off the computational complexity of the algorithm with the descent progress achieved per iteration. This is demonstrated by the following result:

Theorem 9. *Let $P \subseteq \mathbb{R}^n$ be a polytope with diameter D and suppose that $f : P \rightarrow \mathbb{R}$ is L -smooth and μ -strongly convex over P . Then, the primal gap $h(\mathbf{x}_t) := f(\mathbf{x}_t) - f(\mathbf{x}^*)$ of SHADOW-CG² decreases geometrically:*

$$h(\mathbf{x}_{t+1}) \leq \left(1 - \frac{c\mu}{LD^2}\right) h(\mathbf{x}_t),$$

with each iteration of the SHADOW-CG² algorithm (assuming TRACE-OPT is a single step), where $c \in (0, 1)$ is the tuning parameter. Moreover, the number of shadow, in-face shadow and line-search oracle calls for an ϵ -accurate solution is $O\left(\left(\frac{D^2}{c} + \beta\right) \frac{L}{\mu} \log(\frac{1}{\epsilon})\right)$, where β is the number of breakpoints of the parametric projections curve that the TRACE-OPT method visits.

The same proof as that of Theorem 8 applies, after noting that $\|\nabla f(\mathbf{x})\| \geq \|\mathbf{d}_{\mathbf{x}_t}^{\Pi}\|$. We would like to remark the when the optimum \mathbf{x}^* is constrained, $\|\nabla f(\mathbf{x}^*)\|$ is lower bounded away from 0. Therefore, in the SHADOW-CG² algorithm it is preferable to choose the scalar c with small values to prioritize FW steps towards the end of the algorithm. In our computations, we did a grid-search over different values of c and found that $c = 0.1$ yielded excellent performance as we discuss next.

7 Computations

We implemented all algorithms in Python 3.5. We used **Gurobi** 9 [34] as a black box solver for some of the oracles assumed in the paper. All experiments were performed on a 16-core machine with

Intel Core i7-6600U 2.6-GHz CPUs and 256GB of main memory. This code and datasets used for our computations are available at <https://github.com/hassanmortagy/Walking-in-the-Shadow>. We are required to solve the following subproblems:

- (i) **Linear optimization:** Compute $\mathbf{v} = \arg \min_{\mathbf{x} \in P} \langle \mathbf{c}, \mathbf{x} \rangle$ for any $\mathbf{c} \in \mathbb{R}^n$. We elaborate on the implementation of the LO subproblems later on as it is dependent on the application.
- (ii) **Shadow computation:** Given any point $\mathbf{x} \in P$ and direction $\mathbf{w} \in \mathbb{R}^n$, compute $\mathbf{d}_x^\Pi(\mathbf{w})$. For the shadow oracle, we solve the problem $\mathbf{d}_x^\Pi(\mathbf{w}) = \arg \min_{\mathbf{d}} \{ \| -\nabla f(\mathbf{x}) - \mathbf{d} \|^2 : A_{I(\mathbf{x})}\mathbf{d} \leq 0 \}$ using `Gurobi`.^{†††}
- (iii) **Feasibility:** For any $\mathbf{x} \in P$ and direction $\mathbf{d} \in \mathbb{R}^n$, evaluate $\gamma^{\max} = \max\{\delta : \mathbf{x} + \delta\mathbf{d} \in P\} = \min_{j \in J(\mathbf{x}) : \langle \mathbf{a}_j, \mathbf{d} \rangle > 0} \frac{b_j - \langle \mathbf{a}_j, \mathbf{x} \rangle}{\langle \mathbf{a}_j, \mathbf{d} \rangle}$. This problem could be efficiently solved as we consider polytopes with a polynomial number of constraints. This is essentially the same as the simplex ratio.
- (iv) **Line-search:** Given any point $\mathbf{x} \in P$ and direction $\mathbf{d} \in \mathbb{R}^n$, solve the one-dimensional problem $\min_{\gamma \in [0, \gamma^{\max}]} f(\mathbf{x} + \gamma\mathbf{d})$. To solve that problem, we utilize a bracketing method^{‡‡‡} for line search (see, for example [27]).

Finally, to compute $\hat{\lambda}$ in step 5 of the TRACE-OPT algorithm, we utilize the procedure of solving a linear program outlined in Remark 3.

7.1 Video Co-localization

The first application we consider is the video co-localization problem from computer vision, where the goal is to track an object across different video frames. We used the YouTube-Objects dataset^{\$\$\$} and the problem formulation of Joulin et. al [5]. This consists of minimizing a quadratic function $f(\mathbf{x}) = \frac{1}{2}\mathbf{x}^T A\mathbf{x} + \mathbf{b}^T \mathbf{x}$, where $\mathbf{x} \in \mathbb{R}^{660}$, $A \in \mathbb{R}^{660 \times 660}$ and $\mathbf{b} \in \mathbb{R}^{660}$, over a flow polytope, the convex hull of paths in a network. Our linear minimization oracle over the flow polytope amounts to computing a shortest path in the corresponding directed acyclic graph. We now present the computational results.

We find that SHADOW-CG and SHADOW-CG² have a lower iteration count than other CG variants DICG, AFW and PFW (slightly higher than PGD) for this experiment. In particular, SHADOW-CG² takes slightly more iterations than SHADOW-CG, but takes significantly less wall-clock time (i.e., close to CG) without assuming oracle access to shadow, thus obtaining the best of both worlds. Moreover, without assuming oracle access, SHADOW-CG improves on the wall-clock time compared to PGD and SHADOW-WALK (close to CG). We also find that assuming access to shadow oracle, the SHADOW-CG algorithm outperforms the CG variants both in iteration count and

^{†††}This could also be computed approximately using the *matching pursuit* approach with FW of Locatello et. al [35], which extends FW to optimize convex function over cones (and not just polytopes). However, for our preliminary computations we chose Gurobi due its robustness and exact solutions.

^{‡‡‡}We specifically use golden-section search that iteratively reduces the interval locating the minimum.

^{\$\$\$}We obtained the data from <https://github.com/Simon-Lacoste-Julien/linearFW>.

wall-clock time. For completeness, we also compare these different algorithms with respect to the duality gap $\langle -\nabla f(\mathbf{x}_t), \mathbf{v}_t - \mathbf{x}_t \rangle$ (24) in Figure 5.

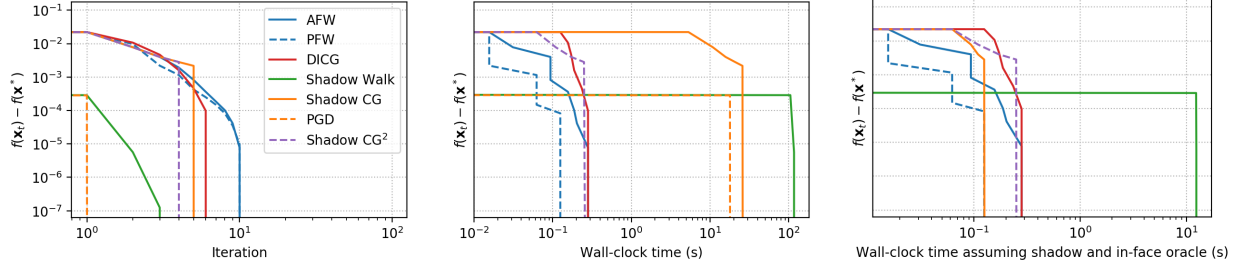


Figure 4: Optimality gap for the video co-localization problem: Away-step FW (AFW) [10], pairwise FW (PFW) [10], decomposition-invariant CG (DICG) [16], SHADOW-WALK (Algorithm 3), SHADOW-CG (Algorithm 4), and SHADOW-CG² (Algorithm 5). Left plot compares iteration count, middle and right plots compare wall-clock time with and without access to shadow oracle. We removed the PGD algorithm from the rightmost plot for a better comparison of other algorithms as it takes significantly more time due to the projection step.

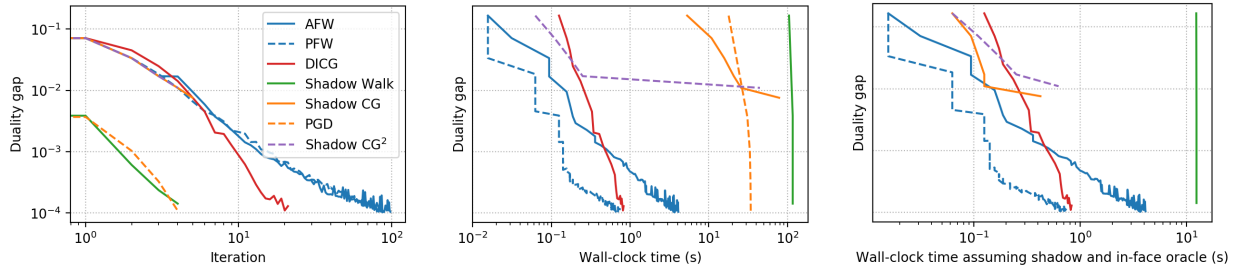


Figure 5: Duality gap for the video co-localization problem. Left plot compares iteration count, middle and right plots compare wall-clock time with and without access to shadow oracle. We removed PGD from the rightmost plot for a better comparison of other algorithms as it takes significantly more time due to the projection step and thus skews the plot.

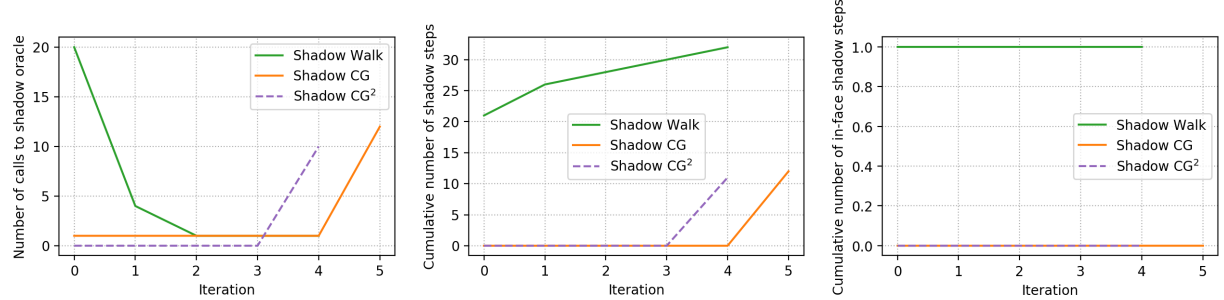


Figure 6: The left plot shows the number of shadow oracles calls made per iteration by SHADOW-WALK, SHADOW-CG, and SHADOW-CG². Note that in the plot we see that SHADOW-CG makes one shadow oracle call every iteration, whereas SHADOW-CG² does not. The middle plot compares the cumulative number of shadow steps taken. The right plot compares the cumulative number of in-face shadow steps taken.

7.2 Lasso Regression

The second application we consider is the Lasso regression problem, i.e., ℓ_1 -regularized least squares regression. This consists of minimizing a quadratic function $f(\mathbf{x}) = \|\mathbf{Ax} - \mathbf{b}\|$ over a scaled ℓ_1 -ball. We considered a random Gaussian matrix $\mathbf{A} \in \mathbb{R}^{50 \times 100}$ and a noisy measurement $\mathbf{b} = \mathbf{Ax}^*$ with \mathbf{x}^* being a sparse vector with 25 entries ± 1 , and some additive noise. Linear minimization over the ℓ_1 -ball, simply amounts to selecting the column of \mathbf{A} with best inner product with the residual vector $\mathbf{Ax} - \mathbf{b}$.

We present its computational results in Figure 7. In these experiments, we observe that SHADOW-WALK algorithm is superior in iteration count and outperforms all other CG variants. Moreover, SHADOW-CG has a significantly lower iteration count than AFW as expected. In addition, assuming access to a shadow oracle, both the SHADOW-WALK and SHADOW-CG algorithm have improvements over CG variants both in iteration count and wall-clock time.

We demonstrate computationally that the number of iterations spent in the TRACE-OPT procedure is a lot better than the worst-case bound we prove in Theorem 3 by looking at the number of oracles calls made by the SHADOW CG, SHADOW-CG², and SHADOW-WALK algorithms per iteration. Moreover, we also find that the addition of FW steps causes the SHADOW CG and SHADOW-CG² algorithms to take a significantly smaller number of shadow steps than SHADOW-WALK does. This behavior is demonstrated in Figures 6 and 9 corresponding to the two experiments, where the curve for the cumulative number of shadow steps taken by SHADOW-WALK is concave-like. This implies that the SHADOW-WALK algorithm spends a bigger number of iterations in the TRACE-OPT procedure in the beginning as it wants to wrap around the polytope. Note that both the SHADOW CG and SHADOW-WALK have the flexibility choosing FW steps, in which case the orange curve in the right plot of Figures 6 and 9 remains flat, and hence the step-wise structure of the curve.

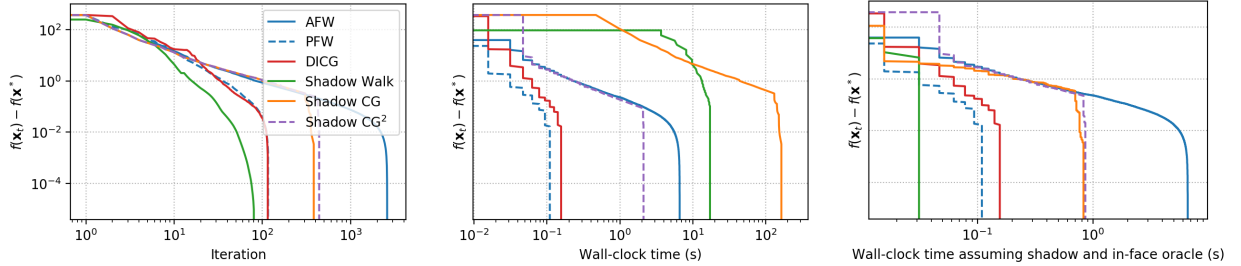


Figure 7: Optimality gaps for the Lasso regression problem. Left plot compares iteration count, middle and right plots compare wall-clock time with and without access to shadow oracle.

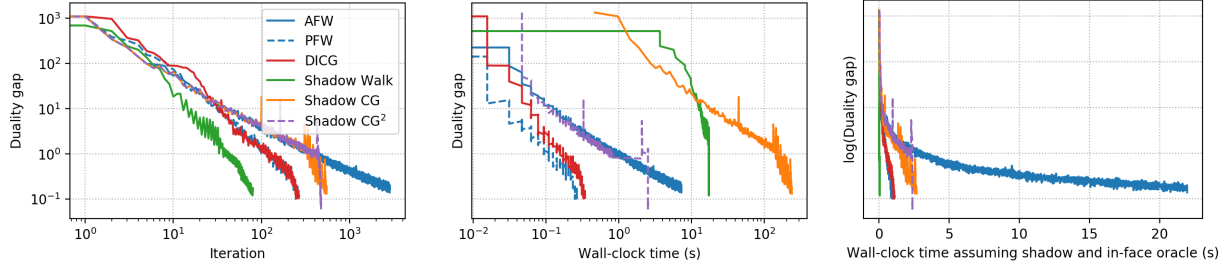


Figure 8: Duality gaps for the Lasso regression problem. Left plot compares iteration count, middle and right plots compare wall-clock time with and without access to shadow oracle

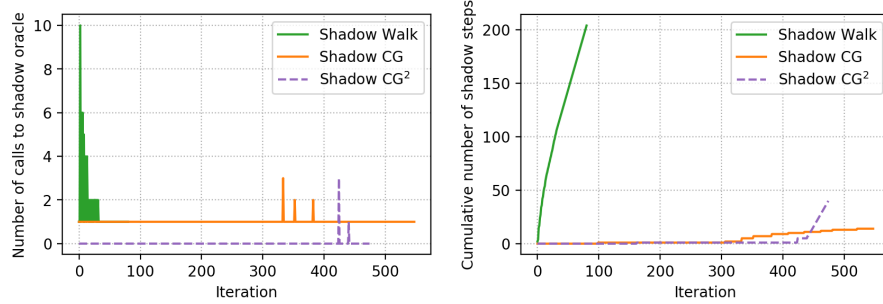


Figure 9: Left: Comparing the number of shadow oracles calls made per iteration by SHADOW-WALK, SHADOW-CG, and SHADOW-CG² in the Lasso regression instance. Right: Comparing the cumulative number of shadow steps taken. Here, we find that SHADOW-WALK, SHADOW CG and SHADOW-CG² algorithms do not take any in-face steps within TRACE-OPT. This is a common trend in the experiments where we observe that we rarely take in-face steps.

8 Acknowledgements

The research presented in this paper was partially supported by the NSF grant CRII-1850182, the Research Campus MODAL funded by the German Federal Ministry of Education and Research (grant number 05M14ZAM), and the Georgia Institute of Technology ARC TRIAD fellowship. We would also like to thank Damiano Zeffiro for pointing out a missing case in the statement of Theorem 2 in an earlier version of this paper, which is now corrected.

References

- [1] R. Freund, P. Grigas, and R. Mazumder, “An extended Frank–Wolfe method with “in-face” directions, and its application to low-rank matrix completion,” *SIAM Journal on Optimization*, vol. 27, no. 1, p. 319–346, 2015.
- [2] M. Jaggi, “Revisiting Frank-Wolfe: Projection-free sparse convex optimization,” in *Proceedings of the 30th international conference on machine learning*, 2013, pp. 427–435.

- [3] M. A. Bashiri and X. Zhang, “Decomposition-invariant conditional gradient for general polytopes with line search,” in *Proceedings of the 31st International Conference on Neural Information Processing Systems*, 2017, p. 2687–2697.
- [4] R. Lyons and Y. Peres, *Probability on trees and networks*. Cambridge University Press, New York, 2005.
- [5] A. Joulin, K. D. Tang, and F. Li, “Efficient image and video co-localization with frank-wolfe algorithm,” in *Computer Vision - ECCV 2014 - 13th European Conference*, 2014, pp. 253–268.
- [6] R. K. Ahuja, T. L. Magnanti, and J. B. Orlin, *Network Flows: Theory, Algorithms, and Applications*. Prentice-Hall, Inc., 1993.
- [7] S. Fujishige and S. Isotani, “A submodular function minimization algorithm based on the minimum-norm base,” *Pacific Journal of Optimization*, vol. 7, 2009.
- [8] A. S. Nemirovski and D. B. Yudin, “Problem complexity and method efficiency in optimization,” *Wiley-Interscience, New York*, 1983.
- [9] M. Frank and P. Wolfe, “An algorithm for quadratic programming,” *Naval Research Logistics Quarterly*, vol. 3, no. 1-2, pp. 95–110, 1956.
- [10] S. Lacoste-Julien and M. Jaggi, “On the global linear convergence of Frank-Wolfe optimization variants,” in *Advances in Neural Information Processing Systems (NIPS)*, 2015, pp. 496–504.
- [11] E. Levitin and B. Polyak, “Constrained minimization methods,” *USSR Computational Mathematics and Mathematical Physics*, vol. 6, p. 1–50, 1966.
- [12] M. D. Canon and C. Cullum, “A tight upper bound on the rate of convergence of Frank-Wolfe algorithm,” *SIAM Journal on Control*, vol. 6, no. 4, p. 509–516, 1968.
- [13] G. Lan, “The complexity of large-scale convex programming under a linear optimization oracle,” *arXiv preprint arXiv:1512.06142*, 2013.
- [14] J. GuéLat and P. Marcotte, “Some comments on wolfe’s ‘away step’,” *Mathematical Programming*, vol. 35, pp. 110–119, 1986.
- [15] D. Garber and E. Hazan, “A linearly convergent variant of the conditional gradient algorithm under strong convexity, with applications to online and stochastic optimization,” *SIAM Journal on Optimization*, vol. 26, no. 3, p. 1493–1528, 2016.
- [16] D. Garber and O. Meshi, “Linear-memory and decomposition-invariant linearly convergent conditional gradient algorithm for structured polytopes,” in *Proceedings of the 30th International Conference on Neural Information Processing Systems*, 2016, p. 1009–1017.
- [17] G. Braun, S. Pokutta, D. Tu, and S. Wright, “Blended conditional gradients: the unconditioning of conditional gradients,” *arXiv preprint arXiv:1805.07311*, 2018.
- [18] C. W. Combettes and S. Pokutta, “Boosting frank-wolfe by chasing gradients,” *arXiv preprint arXiv:2003.06369*, 2020.
- [19] G. Lan, S. Pokutta, Y. Zhou, and D. Zink, “Conditional accelerated lazy stochastic gradient descent,” in *International Conference on Machine Learning (ICML)*, 2017, pp. 1965–1974.

- [20] G. Lan and Y. Zhou, “Conditional gradient sliding for convex optimization,” *SIAM Journal on Optimization*, vol. 26, no. 2, pp. 1379—1409, 2016.
- [21] A. Beck and S. Shtern, “Linearly convergent away-step conditional gradient for non-strongly convex functions,” *Mathematical Programming*, vol. 164, pp. 1–27, 2017.
- [22] J. Pen  and D. Rodr guez, “Polytope conditioning and linear convergence of the frank-wolfe algorithm,” *arXiv preprint arXiv:1512.06142*, 2015.
- [23] F. Rinaldi and D. Zeffiro, “A unifying framework for the analysis of projection-free first-order methods under a sufficient slope condition,” *arXiv preprint arXiv:2008.09781*, 2020.
- [24] ——, “Avoiding bad steps in frank wolfe variants,” *arXiv preprint arXiv:2012.12737*, 2020.
- [25] M. Frank and P. Wolfe, “An algorithm for quadratic programming,” *Naval Research Logistics (NRL)*, vol. 3, no. 1-2, pp. 95–110, 1956.
- [26] J. C. Dunn, “Rates of convergence for conditional gradient algorithms near singular and nonsingular extremals,” *SIAM Journal on Control and Optimization*, vol. 17, no. 2, pp. 187–211, 1979.
- [27] D. P. Bertsekas, *Nonlinear programming*. Athena Scientific, 1997.
- [28] G. P. McCormick and R. A. Tapia, “The gradient projection method under mild differentiability conditions,” *SIAM Journal on Control*, vol. 10, no. 1, pp. 93–98, 1972.
- [29] C. D. Meyer, *Matrix analysis and applied linear algebra*. Siam, 2000, vol. 71.
- [30] J. J. Moreau, “D ecomposition orthogonale d’un espace hilbertien selon deux c ones mutuellement polaires,” *Comptes rendus hebdomadaires des s ances de l’Acad mie des sciences*, vol. 255, pp. 238–240, 1962.
- [31] D. Bertsekas, A. Nedic, and O. AE, *Convex Analysis and Optimization*. Athena Scientific, 2003.
- [32] W. Krichene, A. Bayen, and P. L. Bartlett, “Accelerated mirror descent in continuous and discrete time,” in *Advances in Neural Information Processing Systems 28*, 2015, pp. 2845–2853.
- [33] H. Karimi, J. Nutini, and M. Schmidt, “Linear convergence of gradient and proximal-gradient methods under the polyak-lojasiewicz condition,” in *European Conference on Machine Learning and Knowledge Discovery in Databases - Volume 9851*, ser. ECML PKDD 2016. Springer-Verlag, 2016, p. 795–811.
- [34] G. Optimization, “Gurobi optimizer reference manual version 7.5,” 2017, uRL: <https://www.gurobi.com/documentation/7.5/refman>.
- [35] F. Locatello, R. Khanna, M. Tschannen, and M. Jaggi, “A unified optimization view on generalized matching pursuit and frank-wolfe,” in *Artificial Intelligence and Statistics*. PMLR, 2017, pp. 860–868.
- [36] R. T. Rockafellar, *Convex analysis*. Princeton University Press, 1970.
- [37] T. H. Gronwall, “Note on the derivatives with respect to a parameter of the solutions of a system of differential equations,” *Annals of Mathematics*, pp. 292–296, 1919.

A The TRACE-OPT Algorithm

We now present our TRACE-OPT Algorithm, which chains together consecutive short descent steps and uses line-search until it minimizes the function f over the linear segments of projections curve. That way we are guaranteed progress that is at least as that of a single PGD step with fixed $1/L$ step size. One important property of TRACE-OPT is that it only requires one gradient oracle call. Also, if we know the smoothness constant L , then TRACE-OPT can be terminated early once we have traced the projections curve until we reach the PGD step with a fixed $1/L$ step size. The complete description of the algorithm is give below in Algorithm 6.

Algorithm 6 Tracing Projections Curve Optimally: TRACE-OPT(\mathbf{x}, \mathbf{w})

Input: Polytope $P \subseteq \mathbb{R}^n$, function $f : P \rightarrow \mathbb{R}$ and initialization $\mathbf{x} \in P$

```

1: Let  $\mathbf{x}_0 = \mathbf{x}$  and  $\gamma^{\text{total}} = 0$ .            $\triangleright$  fix starting point and initialize total step size
2: Compute  $\mathbf{d}_\mathbf{x}^\Pi := \lim_{\epsilon \downarrow 0} \frac{\Pi_P(\mathbf{x} - \epsilon \mathbf{w}) - \mathbf{x}}{\epsilon}$ .
3: while  $\mathbf{d}_\mathbf{x}^\Pi \neq \mathbf{0}$  do                                 $\triangleright$  check if we are at endpoint
4:   if  $\langle \mathbf{x}_0 - \gamma^{\text{total}} \mathbf{w} - \mathbf{x}, \mathbf{d}_\mathbf{x}^\Pi \rangle = 0$  then       $\triangleright$  determine if we take shadow step
5:     Compute  $\gamma^{\text{max}} = \max\{\delta \mid \mathbf{x} + \delta \mathbf{d}_\mathbf{x}^\Pi \in P\}$            $\triangleright$  line-search in shadow direction
6:      $\gamma^* \in \arg \min_{\gamma \in [0, \gamma^{\text{max}}]} f(\mathbf{x} + \gamma \mathbf{d}_\mathbf{x}^\Pi)$ .           $\triangleright$  check optimality of line-search
7:     Update  $\mathbf{x} = \mathbf{x} + \gamma^* \mathbf{d}_\mathbf{x}^\Pi$ .
8:   else
9:      $\hat{\mathbf{d}}_\mathbf{x}^\Pi, \gamma^{\text{max}} = \text{TRACE-IN-FACE}(\mathbf{x}_0, \mathbf{x}, \mathbf{w}, \gamma^{\text{total}})$ .           $\triangleright$  in-face step
10:    if  $\hat{\mathbf{d}}_\mathbf{x}^\Pi = \mathbf{0}$  then let  $\gamma^* = \gamma^{\text{max}}$ ,
11:      else  $\gamma^* \in \arg \min_{\gamma \in [0, \gamma^{\text{max}}]} f(\mathbf{x} + \gamma \hat{\mathbf{d}}_\mathbf{x}^\Pi)$ .           $\triangleright$  check optimality of line-search
12:      Update  $\mathbf{x} = \mathbf{x} + \gamma^* \hat{\mathbf{d}}_\mathbf{x}^\Pi$ .
13:    end if
14:    Update  $\gamma^{\text{total}} = \gamma^{\text{total}} + \gamma^*$ .           $\triangleright$  keep track of total step-size accrued
15:    if  $\gamma^* < \gamma^{\text{max}}$  then           $\triangleright$  we made sufficient descent progress
16:      break           $\triangleright$  suffices to also terminate when  $\gamma^{\text{total}} \geq 1/L$ 
17:    else
18:      Recompute  $\mathbf{d}_\mathbf{x}^\Pi := \lim_{\epsilon \downarrow 0} \frac{\Pi_P(\mathbf{x} - \epsilon \mathbf{w}) - \mathbf{x}}{\epsilon}$ 
19:    end if
20: end while

```

Return: \mathbf{x}

B Missing Proofs for Section 3

B.1 Missing Proofs for Section 3.1

B.1.1 Proof of Lemma 2

Lemma 2. Let $P \subseteq \mathbb{R}^n$ be a polytope. Let $\mathbf{x}_0 \in P$ and we are given $\nabla f(\mathbf{x}_0) \in \mathbb{R}^n$. Let $g(\lambda) = \Pi_P(\mathbf{x}_0 - \lambda \nabla f(\mathbf{x}_0))$ be the parametric projections curve. Then, if $N_P(g(\lambda)) = N_P(g(\lambda'))$ for some $\lambda < \lambda'$, then the curve between $g(\lambda)$ and $g(\lambda')$ is linear, i.e., $g(\delta\lambda + (1 - \delta)\lambda') = \delta g(\lambda) + (1 - \delta)g(\lambda')$, where $\delta \in [0, 1]$.

Proof. Fix $\lambda, \lambda' \geq 0$ arbitrarily such that $\lambda' > \lambda$. We will show that $\delta g(\lambda) + (1 - \delta)g(\lambda')$ satisfies the first-order optimality condition for $g(\delta\lambda + (1 - \delta)\lambda')$. For brevity, let I and J (resp. \tilde{I} and \tilde{J}) denote the index set of active and inactive constraints at $g(\lambda)$ (resp. $g(\lambda')$). Note that since

$N_P(g(\lambda')) = N_P(g(\lambda))$ we have $I = \tilde{I}$ and $J = \tilde{J}$. The first-order optimality of $g(\lambda)$ and $g(\lambda')$ yields

$$\mathbf{x}_0 - \lambda \nabla f(\mathbf{x}_0) - g(\lambda) = \boldsymbol{\mu}^\top \mathbf{A}_I \in N_P(g(\lambda)) \quad \text{for some } \boldsymbol{\mu} \in \mathbb{R}_+^{|I|} \quad (25)$$

$$\mathbf{x}_0 - \lambda' \nabla f(\mathbf{x}_0) - g(\lambda') = \tilde{\boldsymbol{\mu}}^\top \mathbf{A}_{\tilde{I}} = \tilde{\boldsymbol{\mu}}^\top \mathbf{A}_I \in N_P(g(\lambda)) \quad \text{for some } \tilde{\boldsymbol{\mu}} \in \mathbb{R}_+^{|I|}. \quad (26)$$

Thus, by aggregating equations (25) and (26) with weights δ and $(1 - \delta)$ respectively, we can conclude:

$$\mathbf{x}_0 - (\delta\lambda + (1 - \delta)\lambda') \nabla f(\mathbf{x}_0) - (\delta g(\lambda) + (1 - \delta)g(\lambda')) = (\delta\boldsymbol{\mu} + (1 - \delta)\tilde{\boldsymbol{\mu}})^\top \mathbf{A}_I \in N_P(g(\lambda)). \quad (27)$$

We now claim that

$$N_P(g(\lambda)) = N_P(\delta g(\lambda) + (1 - \delta)g(\lambda')). \quad (28)$$

Assuming (28) holds, we can equivalently write (27) as

$$\mathbf{x}_0 - (\delta\lambda + (1 - \delta)\lambda') \nabla f(\mathbf{x}_0) - (\delta g(\lambda) + (1 - \delta)g(\lambda')) \in N_P(\delta g(\lambda) + (1 - \delta)g(\lambda')),$$

so that $\delta g(\lambda) + (1 - \delta)g(\lambda')$ satisfies the optimality condition for $g(\delta\lambda + (1 - \delta)\lambda')$, as claimed.

We now prove the claim in (28). Since $I = \tilde{I}$ and $J = \tilde{J}$, we have

$$\begin{aligned} \mathbf{A}_I(\delta g(\lambda) + (1 - \delta)g(\lambda')) &= \delta \mathbf{A}_I g(\lambda) + (1 - \delta) \mathbf{A}_I g(\lambda') = \mathbf{b}_I \\ \mathbf{A}_J(\delta g(\lambda) + (1 - \delta)g(\lambda')) &= \delta \mathbf{A}_J g(\lambda) + (1 - \delta) \mathbf{A}_J g(\lambda') < \mathbf{b}_J \end{aligned}$$

This implies that $I = I(\delta g(\lambda) + (1 - \delta)g(\lambda'))$ and $J = J(\delta g(\lambda) + (1 - \delta)g(\lambda'))$, which proves (28) and concludes the proof. \square

B.1.2 Proof of Lemma 3

Lemma 3. *Let $P \subseteq \mathbb{R}^n$ be a polytope. Let $\mathbf{x}_0 \in P$ and $\nabla f(\mathbf{x}_0) \in \mathbb{R}^n$ be given. Further, let $g(\lambda) = \Pi_P(\mathbf{x}_0 - \lambda \nabla f(\mathbf{x}_0))$ denote the projections curve. Fix an arbitrary $\lambda > 0$. Then, $\lim_{\lambda' \downarrow \lambda} g(\lambda') = \lim_{\lambda' \uparrow \lambda} g(\lambda') = g(\lambda)$. Moreover, there exists $\delta' > 0$ and directions $\underline{\mathbf{d}}, \bar{\mathbf{d}} \in \mathbb{R}^n$ such that $g(\lambda - \epsilon) = g(\lambda) - \epsilon \underline{\mathbf{d}}$ and $g(\lambda + \epsilon) = g(\lambda) + \epsilon \bar{\mathbf{d}}$, for all $\epsilon \in (0, \delta']$.*

Proof. Assume that $\nabla f(\mathbf{x}_0) \neq \mathbf{0}$, since otherwise the result follows trivially. We now prove the result in the next two claims:

(a) *Continuity of the projections curve.* Fix an arbitrary $\lambda > 0$. We first show that $\lim_{\lambda' \downarrow \lambda} g(\lambda') = \lim_{\lambda' \uparrow \lambda} g(\lambda') = g(\lambda)$. Let $\epsilon > 0$ be arbitrary. Then, by non-expansiveness of the Euclidean projection operator over convex sets (see Section 2), we know that

$$\|g(\lambda) - g(\lambda + \epsilon)\| \leq \|(\mathbf{x}_0 - \lambda \nabla f(\mathbf{x}_0)) - (\mathbf{x}_0 - (\lambda + \epsilon) \nabla f(\mathbf{x}_0))\| = |\epsilon| \|\nabla f(\mathbf{x}_0)\|.$$

Thus, for any $\delta, \lambda' > 0$, whenever $|\lambda' - \lambda| < \delta$, we have $\|g(\lambda') - g(\lambda)\| \leq |\lambda' - \lambda| \|\nabla f(\mathbf{x}_0)\| < \delta \|\nabla f(\mathbf{x}_0)\|$. In particular, by choosing $\delta = \frac{\epsilon}{\|\nabla f(\mathbf{x}_0)\|}$, we have $\|g(\lambda') - g(\lambda)\| < \epsilon$. This implies that:

- For every $\epsilon > 0$, there exists $\delta > 0$ such that if $-\delta < \lambda' - \lambda < 0$, then $\|g(\lambda') - g(\lambda)\| < \epsilon$. Thus, we have $\lim_{\lambda' \uparrow \lambda} g(\lambda') = g(\lambda)$.
- Similarly, for every $\epsilon > 0$ there exists $\delta > 0$ such that if $0 < \lambda' - \lambda < \delta$, then $\|g(\lambda') - g(\lambda)\| < \epsilon$. Thus, we have $\lim_{\lambda' \downarrow \lambda} g(\lambda') = g(\lambda)$.

This establishes the continuity of the projections curve.

(b) *Piecewise linearity of the projections curve.* Fix an arbitrary $\lambda_0 > 0$ and define $\mathbf{y}_0 := g(\lambda_0)$. We now show that there exists a $\delta'_1 > 0$ and direction $\bar{\mathbf{d}} \in \mathbb{R}^n$ such that $g(\lambda_0 + \epsilon) = \mathbf{y}_0 + \epsilon \bar{\mathbf{d}}$, for all $\epsilon \in (0, \delta'_1]$. Suppose for a contradiction that the projections curve in the neighborhood of \mathbf{y}_0 is not linear, and let $\lambda_1 \in (\lambda_0, \infty)$ be any lambda such that the curve between \mathbf{y}_0 and $\mathbf{y}_1 := g(\lambda_1)$ is non-linear (there is no segment that is linear between \mathbf{y}_0 and \mathbf{y}_1). Now, consider the following points: $\lambda_{i+1} = \lambda_0 + (\lambda_1 - \lambda_0)/2^i$ for $i = 1, \dots, 2^m$ and define $\mathbf{y}_i := g(\lambda_i)$. Thus, $N_P(\mathbf{y}_i) \neq N_P(\mathbf{y}_j)$ for any $i, j = 0, \dots, 2^m + 1$ such that $i \neq j$, otherwise the curve would be linear between \mathbf{y}_i and \mathbf{y}_j contradicting our assumption (using Lemma 2). In other words, the normal cones at each of these points \mathbf{y}_i must be distinct, but this is more than the distinct normal cones in any polytope with m facet inequalities, which is a contradiction.

Using the exact similar argument, we know that there exists $\delta'_2 > 0$ and direction $\underline{\mathbf{d}} \in \mathbb{R}^n$ such that $g(\lambda - \epsilon') = g(\lambda) - \epsilon' \underline{\mathbf{d}}$ for all $\epsilon \in (0, \delta'_2]$. The result now follows by setting $\delta' := \min\{\delta'_1, \delta'_2\}$.

□

B.2 Missing Proofs in Section 3.3

B.2.1 Proof of Theorem 2

Theorem 2 (Tracing the projections curve). *Let $P \subseteq \mathbb{R}^n$ be a polytope. Let $\mathbf{x}_{i-1} \in P$ be the i th breakpoint in the projections curve $g(\lambda) = \Pi_P(\mathbf{x}_0 - \lambda \nabla f(\mathbf{x}_0))$, with $\mathbf{x}_{i-1} = \mathbf{x}_0$ for $i = 1$. Suppose we are given $\lambda_{i-1}^-, \lambda_{i-1}^+ \in \mathbb{R}$ so that they are respectively the minimum and the maximum step-sizes λ such that $g(\lambda) = \mathbf{x}_{i-1}$. If $\mathbf{d}_{\mathbf{x}_{i-1}}^{\Pi}(\nabla f(\mathbf{x}_0)) = \mathbf{0}$, then $\lim_{\lambda \rightarrow \infty} g(\lambda) = \mathbf{x}_{i-1}$ is the end point of $g(\lambda)$. Otherwise, $\mathbf{d}_{\mathbf{x}_{i-1}}^{\Pi}(\nabla f(\mathbf{x}_0)) \neq \mathbf{0}$, in which case we claim that:*

- (a) **Shadow steps:** *If $\langle \mathbf{x}_0 - \lambda_{i-1}^+ \nabla f(\mathbf{x}_0) - \mathbf{x}_{i-1}, \mathbf{d}_{\mathbf{x}_{i-1}}^{\Pi}(\nabla f(\mathbf{x}_0)) \rangle = 0$, then the projections curve moves maximally in the shadow direction, i.e., $\mathbf{x}_i := g(\lambda_i^-) = \mathbf{x}_{i-1} + (\lambda_i^- - \lambda_{i-1}^+) \mathbf{d}_{\mathbf{x}_{i-1}}^{\Pi}(\nabla f(\mathbf{x}_0))$ where $\lambda_i^- := \lambda_{i-1}^+ + \max\{\delta : \mathbf{x}_{i-1} + \delta \mathbf{d}_{\mathbf{x}_{i-1}}^{\Pi}(\nabla f(\mathbf{x}_0)) \in P\}$.*
- (b) **In-face steps:** *Otherwise, $\langle \mathbf{x}_0 - \lambda_{i-1}^+ \nabla f(\mathbf{x}_0) - \mathbf{x}_{i-1}, \mathbf{d}_{\mathbf{x}_{i-1}}^{\Pi}(\nabla f(\mathbf{x}_0)) \rangle \neq 0$. Let $\hat{\lambda}_{i-1} := \sup\{\lambda \mid N_P(g(\lambda')) = N_P(\mathbf{x}_{i-1}) \forall \lambda' \in [\lambda_{i-1}^-, \lambda]\}$. Then, $\hat{\mathbf{d}}_{\mathbf{x}_{i-1}}^{\Pi}(\nabla f(\mathbf{x}_0)) \neq \mathbf{d}_{\mathbf{x}_{i-1}}^{\Pi}(\nabla f(\mathbf{x}_0))$, $\lambda_{i-1}^+ < \hat{\lambda}_{i-1} < \infty$, and the next breakpoint in the curve occurs by walking in-face up to $\hat{\lambda}_{i-1}$, i.e., $\mathbf{x}_i := g(\hat{\lambda}_{i-1}) = \mathbf{x}_{i-1} + (\hat{\lambda}_{i-1} - \lambda_{i-1}^+) \hat{\mathbf{d}}_{\mathbf{x}_{i-1}}^{\Pi}(\nabla f(\mathbf{x}_0))$ and $\lambda_i^- := \hat{\lambda}_{i-1}$.*

We first show that if at breakpoint \mathbf{x}_{i-1} the shadow $\mathbf{d}_{\mathbf{x}_{i-1}}^{\Pi}(\nabla f(\mathbf{x}_0)) = \mathbf{0}$, then \mathbf{x}_{i-1} is the endpoint of the curve:

Lemma 9. *If $\mathbf{d}_{\mathbf{x}_{i-1}}^{\Pi}(\nabla f(\mathbf{x}_0)) = \mathbf{0}$, then $\lim_{\lambda \rightarrow \infty} g(\lambda) = \mathbf{x}_{i-1}$ is the end point of the projections curve $g(\lambda)$.*

Proof. Since $\mathbf{d}_{\mathbf{x}_{i-1}}^{\Pi}(\nabla f(\mathbf{x}_0)) = \mathbf{0}$, using Lemma 1 we have $-\nabla f(\mathbf{x}_0) \in N_P(\mathbf{x}_{i-1})$. Note that the first-order optimality condition of $g(\lambda_{i-1}^+) = \mathbf{x}_{i-1}$ is $\langle \mathbf{p}, \mathbf{z} - \mathbf{x}_{i-1} \rangle \leq 0$ for all $\mathbf{z} \in P$. Since $-\nabla f(\mathbf{x}_0) \in N_P(\mathbf{x}_{i-1})$ (i.e., $\langle -\nabla f(\mathbf{x}_0), \mathbf{z} - \mathbf{x}_{i-1} \rangle \leq 0 \forall \mathbf{z} \in P$) and $\lambda \geq \lambda_{i-1}^+$, we get $\langle \mathbf{x}_0 - \lambda \nabla f(\mathbf{x}_0) - \mathbf{x}_{i-1}, \mathbf{z} - \mathbf{x}_{i-1} \rangle \leq 0 \forall \mathbf{z} \in P$. Thus, \mathbf{x}_{i-1} satisfies the first-order optimality condition for $g(\lambda)$ when $\lambda \geq \lambda_{i-1}^+$. □

Proof of Theorem 2(a)-(b). Consider a breakpoint $\mathbf{x}_{i-1} := g(\lambda_{i-1}^+)$ and assume that $\mathbf{d}_{\mathbf{x}_{i-1}}^\Pi(\nabla f(\mathbf{x}_0)) \neq 0$ so that \mathbf{x}_{i-1} is not the endpoint of the projections curve. Since the projections curve is piecewise linear (Theorem 1), we know that $g(\lambda) = \mathbf{x}_{i-1} + (\lambda_i^- - \lambda_{i-1}^+) \mathbf{d}$ for $\lambda \in [\lambda_{i-1}^+, \lambda_i^-]$ and some direction $\mathbf{d} \in \mathbb{R}^n$. We will now show that either $\mathbf{d} = \mathbf{d}_{\mathbf{x}_{i-1}}^\Pi(\nabla f(\mathbf{x}_0))$ (in which case $\lambda_i^- = \lambda_{i-1}^+ + \max\{\delta : \mathbf{x}_{i-1} + \delta \mathbf{d}_{\mathbf{x}_{i-1}}^\Pi(\nabla f(\mathbf{x}_0)) \in P\}$) or $\mathbf{d} = \hat{\mathbf{d}}_{\mathbf{x}_{i-1}}^\Pi(\nabla f(\mathbf{x}_0))$ (in which case $\lambda_i^- = \hat{\lambda}_{i-1}$).

Fix $\epsilon \in (0, \lambda_i^- - \lambda_{i-1}^+)$. For brevity, let $I := I(\mathbf{x}_{i-1})$, $\tilde{I} := I(g(\lambda_{i+1}^+ + \epsilon))$, $\mathbf{d}_{\mathbf{x}_{i-1}}^\Pi := \mathbf{d}_{\mathbf{x}_{i-1}}^\Pi(\nabla f(\mathbf{x}_0))$, and $\hat{\mathbf{d}}_{\mathbf{x}_{i-1}}^\Pi := \hat{\mathbf{d}}_{\mathbf{x}_{i-1}}^\Pi(\nabla f(\mathbf{x}_0))$. Moreover, let $\mathbf{p}_{i-1} := \mathbf{x}_0 - \lambda_{i-1}^+ \nabla f(\mathbf{x}_0) - \mathbf{x}_{i-1}$ and $\mathbf{p}_\epsilon := \mathbf{x}_0 - (\lambda_{i-1}^+ + \epsilon) \nabla f(\mathbf{x}_0) - g(\lambda_{i+1}^+ + \epsilon)$ denote the normal vector of the projection at \mathbf{x}_{i-1} and $g(\lambda_{i+1}^+ + \epsilon)$ respectively. The first-order optimality of \mathbf{x}_{i-1} and $g(\lambda_{i+1}^+ + \epsilon)$ yields

$$\mathbf{p}_{i-1} = \boldsymbol{\alpha}_1^\top \mathbf{A}_I \in N_P(g(\lambda_{i+1}^+)) \quad \text{for some } \boldsymbol{\alpha}_1 \in \mathbb{R}_+^{|I|} \quad (29)$$

$$\mathbf{p}_\epsilon = \boldsymbol{\alpha}_2^\top \mathbf{A}_{\tilde{I}} \in N_P(g(\lambda_{i+1}^+ + \epsilon)) \quad \text{for some } \boldsymbol{\alpha}_2 \in \mathbb{R}_+^{|I|}. \quad (30)$$

Using the fact that $g(\lambda_{i+1}^+ + \epsilon) = \mathbf{x}_{i-1} + \epsilon \mathbf{d}$, and subtracting (29) from (30) we obtain:

$$\mathbf{p}_\epsilon - \mathbf{p}_{i-1} = \epsilon(-\nabla f(\mathbf{x}_0) - \mathbf{d}) = \boldsymbol{\alpha}_2^\top \mathbf{A}_{\tilde{I}} - \boldsymbol{\alpha}_1^\top \mathbf{A}_I. \quad (31)$$

Moreover, using the normal properties Theorem 1(i) we know that $N_P(g(\lambda_{i+1}^+ + \epsilon)) \subseteq N_P(\mathbf{x}_{i-1})$, and thus $\tilde{I} \subseteq I$ and $\mathbf{p}_\epsilon \in N_P(\mathbf{x}_{i-1})$. Therefore, letting $\tilde{\boldsymbol{\alpha}}_2 \in \mathbb{R}_+^{|I|}$ be such that $(\tilde{\boldsymbol{\alpha}}_2)_i = (\boldsymbol{\alpha}_2)_i$ for $i \in \tilde{I}$ and $(\tilde{\boldsymbol{\alpha}}_2)_i = 0$ for $i \in I \setminus \tilde{I}$, can write (31) as

$$(\mathbf{p}_\epsilon - \mathbf{p}_{i-1})/\epsilon = -\nabla f(\mathbf{x}_0) - \mathbf{d} = \boldsymbol{\alpha}^\top \mathbf{A}_I, \quad (32)$$

where $\boldsymbol{\alpha} = (\tilde{\boldsymbol{\alpha}}_2 - \boldsymbol{\alpha}_1)/\epsilon$. Furthermore, using the structure of orthogonal projections and the continuity of the projections curve, it follows that $\langle \mathbf{p}_\epsilon, \mathbf{d} \rangle = 0$ and $\langle \mathbf{p}_{i-1}, \mathbf{d} \rangle = 0^*$. Taking the inner product of both sides (33) with \mathbf{d} we have (31) as

$$0 = \langle \mathbf{d}, -\nabla f(\mathbf{x}_0) - \mathbf{d} \rangle = \langle \boldsymbol{\alpha}^\top \mathbf{A}_I, \mathbf{d} \rangle. \quad (33)$$

We now proceed by cases:

(a) *First suppose that $-\nabla f(\mathbf{x}_0) - \mathbf{d} \in N_P(\mathbf{x}_{i-1})$.* Thus, noting that $\mathbf{d} \in T_P(\mathbf{x}_{i-1})$ and using (33), we have that \mathbf{d} is the projection of $-\nabla f(\mathbf{x}_0)$ onto the tangent cone at \mathbf{x}_{i-1} , i.e., $\mathbf{d} = \mathbf{d}_{\mathbf{x}_{i-1}}^\Pi$, by Moreau's decomposition theorem [30] (see Section 3.3).

We now show the converse: if $\langle \mathbf{p}_{i-1}, \mathbf{d}_{\mathbf{x}_{i-1}}^\Pi \rangle = 0$, then $\mathbf{d} = \mathbf{d}_{\mathbf{x}_{i-1}}^\Pi$ (which further implies that $-\nabla f(\mathbf{x}_0) - \mathbf{d} \in N_P(\mathbf{x}_{i-1})$), and the next breakpoint $\mathbf{x}_i := g(\lambda_i^-) = \mathbf{x}_{i-1} + (\lambda_i^- - \lambda_{i-1}^+) \mathbf{d}_{\mathbf{x}_{i-1}}^\Pi(\nabla f(\mathbf{x}_0))$, where $\lambda_i^- = \lambda_{i-1}^+ + \max\{\delta : \mathbf{x}_{i-1} + \delta \mathbf{d}_{\mathbf{x}_{i-1}}^\Pi(\nabla f(\mathbf{x}_0)) \in P\}$. To do this, we show that $\mathbf{x}_{i-1} + (\lambda_i^- - \lambda_{i-1}^+) \mathbf{d}_{\mathbf{x}_{i-1}}^\Pi \in P$ satisfies first-order optimality for $g(\lambda_i^-)$. Indeed, for any $\mathbf{z} \in P$, we have

*To see this, note that first-order optimality at $g(\lambda_{i+1}^+ + \epsilon) = \mathbf{x}_{i-1} + \epsilon \mathbf{d}$ gives $\langle \mathbf{p}_\epsilon, \mathbf{z} - \mathbf{x}_{i-1} - \epsilon \mathbf{d} \rangle \leq 0 \forall \mathbf{z} \in P$. Considering $\mathbf{z} = \mathbf{x}_{i-1}$ in the previous inequality we have $\langle \mathbf{p}_\epsilon, \mathbf{d} \rangle \geq 0$. However, since $\mathbf{p}_\epsilon \in N_P(g(\lambda_{i+1}^+ + \epsilon))$ and $\mathbf{d} \in T_P(g(\lambda_{i+1}^+ + \epsilon))$, we have $\langle \mathbf{p}_\epsilon, \mathbf{d} \rangle \leq 0$ using the polar duality of $T_P(g(\lambda_{i+1}^+ + \epsilon))$ and $N_P(g(\lambda_{i+1}^+ + \epsilon))$. Thus, $\langle \mathbf{p}_\epsilon, \mathbf{d} \rangle = 0$.

$$\begin{aligned}
& \left\langle \mathbf{x}_0 - \lambda_i^- \nabla f(\mathbf{x}_0) - \mathbf{x}_{i-1} - (\lambda_i^- - \lambda_{i-1}^+) \mathbf{d}_{\mathbf{x}_{i-1}}^\Pi, \mathbf{z} - \mathbf{x}_{i-1} - (\lambda_i^- - \lambda_{i-1}^+) \mathbf{d}_{\mathbf{x}_{i-1}}^\Pi \right\rangle \\
&= (\lambda_i^- - \lambda_{i-1}^+) \underbrace{\left\langle \mathbf{p}_{i-1}, \mathbf{d}_{\mathbf{x}_{i-1}}^\Pi \right\rangle}_{\stackrel{(i)}{=} 0} - (\lambda_i^- - \lambda_{i-1}^+) \underbrace{\left\langle -\nabla f(\mathbf{x}_0) - \mathbf{d}_{\mathbf{x}_{i-1}}^\Pi, (\lambda_i^- - \lambda_{i-1}^+) \mathbf{d}_{\mathbf{x}_{i-1}}^\Pi \right\rangle}_{\stackrel{(ii)}{=} 0} \\
&\quad + \underbrace{\left\langle \mathbf{p}_{i-1}, \mathbf{z} - \mathbf{x}_{i-1} \right\rangle}_{\stackrel{(iii)}{\leq} 0} + (\lambda_i^- - \lambda_{i-1}^+) \underbrace{\left\langle -\nabla f(\mathbf{x}_0) - \mathbf{d}_{\mathbf{x}_{i-1}}^\Pi, \mathbf{z} - \mathbf{x}_{i-1} \right\rangle}_{\stackrel{(iv)}{\leq} 0} \leq 0,
\end{aligned}$$

where we used our assumption $\left\langle \mathbf{p}_{i-1}, \mathbf{d}_{\mathbf{x}_{i-1}}^\Pi \right\rangle = 0$ in (i), the definition of the shadow $\mathbf{d}_{\mathbf{x}_{i-1}}^\Pi := \Pi_{T_P(\mathbf{x}_{i-1})}(-\nabla f(\mathbf{x}_0))$ in (ii), the first-order optimality at \mathbf{x}_{i-1} in (iii), and the fact that $-\nabla f(\mathbf{x}_0) - \mathbf{d}_{\mathbf{x}_{i-1}}^\Pi \in N_P(\mathbf{x}_{i-1})$ (by Moreau's decomposition theorem) in (iv)[†].

To summarize, we have shown that $\mathbf{x}_i := g(\lambda_i^-) = \mathbf{x}_{i-1} + (\lambda_i^- - \lambda_{i-1}^+) \mathbf{d}_{\mathbf{x}_{i-1}}^\Pi (\nabla f(\mathbf{x}_0))$ (since λ_i^- is obtained by line-search for feasibility in P). In addition, we have shown that

$$-\nabla f(\mathbf{x}_0) - \mathbf{d} \in N_P(\mathbf{x}_{i-1}) \Leftrightarrow \mathbf{d} = \mathbf{d}_{\mathbf{x}_{i-1}}^\Pi \Leftrightarrow \left\langle \mathbf{p}_{i-1}, \mathbf{d}_{\mathbf{x}_{i-1}}^\Pi \right\rangle = 0. \quad (34)$$

This proves case (a) in the theorem statement.

(b) Now suppose $-\nabla f(\mathbf{x}_0) - \mathbf{d} \notin N_P(\mathbf{x}_{i-1})$. In other words, we have $\alpha_i < 0$ for some $i \in I$ and thus $-\nabla f(\mathbf{x}_0) - \mathbf{d}$ is in the rowspace of \mathbf{A}_I . Note that using (34) this implies that $\mathbf{d} \neq \mathbf{d}_{\mathbf{x}_{i-1}}^\Pi$. We will show that in this case $\mathbf{d} = \hat{\mathbf{d}}_{\mathbf{x}_{i-1}}^\Pi$ and the next breakpoint $\mathbf{x}_i := g(\hat{\lambda}_{i-1}) = \mathbf{x}_{i-1} + (\hat{\lambda}_{i-1} - \lambda_{i-1}^+) \hat{\mathbf{d}}_{\mathbf{x}_{i-1}}^\Pi$. To do that, we first show that \mathbf{d} satisfies the first order optimality condition for $\hat{\mathbf{d}}_{\mathbf{x}_{i-1}}^\Pi$, i.e., the unique projection of $-\nabla f(\mathbf{x}_0)$ onto $\text{Cone}(F - \mathbf{x}_{i-1})$, where F is the minimal face containing \mathbf{x}_{i-1} . Since $g(\lambda_{i+1}^+ + \epsilon) = \mathbf{x}_{i-1} + \epsilon \mathbf{d}$, by first-order optimality we have

$$\begin{aligned}
& \left\langle \mathbf{x}_0 - (\lambda_{i-1}^+ + \epsilon) \nabla f(\mathbf{x}_0) - \mathbf{x}_{i-1} - \epsilon \mathbf{d}, \mathbf{z} - \mathbf{x}_{i-1} - \epsilon \mathbf{d} \right\rangle = \epsilon \underbrace{\left\langle \mathbf{p}_{i-1}, \mathbf{d} \right\rangle}_{\stackrel{(i)}{=} 0} \\
& - \epsilon \underbrace{\left\langle -\nabla f(\mathbf{x}_0) - \mathbf{d}, \epsilon \mathbf{d} \right\rangle}_{\stackrel{(ii)}{=} 0} + \underbrace{\left\langle \mathbf{p}_{i-1}, \mathbf{z} - \mathbf{x}_{i-1} \right\rangle}_{\stackrel{(iii)}{\leq} 0} + \epsilon \left\langle -\nabla f(\mathbf{x}_0) - \mathbf{d}, \mathbf{z} - \mathbf{x}_{i-1} \right\rangle \leq 0 \quad \forall \mathbf{z} \in P,
\end{aligned} \quad (35)$$

where we used the structure of orthogonal projections in (i), equation (33) in (ii), and first-order optimality at \mathbf{x}_{i-1} in (iii). Since $-\nabla f(\mathbf{x}_0) - \mathbf{d} \notin N_P(\mathbf{x}_{i-1})$, there exists a vertex $\tilde{\mathbf{z}} \in P$ such that $\langle -\nabla f(\mathbf{x}_0) - \mathbf{d}, \tilde{\mathbf{z}} - \mathbf{x}_{i-1} \rangle > 0$. Furthermore, using (35) we know that for any such vertex first order optimality at \mathbf{x}_{i-1} holds strictly, i.e., $\langle \mathbf{p}_{i-1}, \tilde{\mathbf{z}} - \mathbf{x}_{i-1} \rangle < 0$. However, observe that the first first order optimality condition at $\mathbf{x}_{i-1} = g(\lambda_{i-1}^+)$ given by $\langle \mathbf{p}_{i-1}, \mathbf{z} - \mathbf{x}_{i-1} \rangle \leq 0$ is a defining inequality for the face F , i.e., it is verified by all $\mathbf{z} \in P$ and satisfied as equality by all $\mathbf{z} \in F$. Thus, $\tilde{\mathbf{z}} \notin F$, which further implies that $\langle -\nabla f(\mathbf{x}_0) - \mathbf{d}, \mathbf{z} - \mathbf{x}_{i-1} \rangle \leq 0$ for all $\mathbf{z} \in F$. This shows that $\mathbf{d} = \hat{\mathbf{d}}_{\mathbf{x}_{i-1}}^\Pi$ as claimed, since it satisfies the first order optimality condition for $\hat{\mathbf{d}}_{\mathbf{x}_{i-1}}^\Pi$ as the projection of $-\nabla f(\mathbf{x}_0)$ onto $\text{Cone}(F - \mathbf{x}_{i-1})$ given by $\left\langle -\nabla f(\mathbf{x}_0) - \hat{\mathbf{d}}_{\mathbf{x}_{i-1}}^\Pi, \mathbf{z} - \mathbf{x}_{i-1} \right\rangle \leq 0$

[†]To see this, note that the first order optimality of $\mathbf{d}_{\mathbf{x}_{i-1}}^\Pi := \Pi_{T_P(\mathbf{x}_{i-1})}(-\nabla f(\mathbf{x}_0))$ implies that $\langle -\nabla f(\mathbf{x}_0) - \mathbf{d}_{\mathbf{x}_{i-1}}^\Pi, \mathbf{y} - \mathbf{d}_{\mathbf{x}_{i-1}}^\Pi \rangle \leq 0, \forall \mathbf{y} \in T_P(\mathbf{x}_{i-1})$. Since $\mathbf{z} - \mathbf{x}_{i-1} \in T_P(\mathbf{x}_{i-1})$ for any $\mathbf{z} \in P$ and $\langle -\nabla f(\mathbf{x}_0) - \mathbf{d}_{\mathbf{x}_{i-1}}^\Pi, \mathbf{d}_{\mathbf{x}_{i-1}}^\Pi \rangle = 0$, we have $\langle -\nabla f(\mathbf{x}_0) - \mathbf{d}_{\mathbf{x}_{i-1}}^\Pi, \mathbf{z} - \mathbf{x}_{i-1} \rangle \leq 0 \forall \mathbf{z} \in P$, i.e., $-\nabla f(\mathbf{x}_0) - \mathbf{d}_{\mathbf{x}_{i-1}}^\Pi \in N_P(\mathbf{x}_{i-1})$.

$\forall \mathbf{z} \in F^\ddagger$.

Moreover, the next breakpoint $\mathbf{x}_i := g(\hat{\lambda}_{i-1}) = \mathbf{x}_{i-1} + (\hat{\lambda}_{i-1} - \lambda_{i-1}^+) \hat{\mathbf{d}}_{\mathbf{x}_{i-1}}^\Pi$ by the definition of $\hat{\lambda}_{i-1}$ and the fact that the projections curve leaves the minimal face after this point, and thus direction change in the projections curve must happen by Lemma 2. This proves case (b) in the theorem.

This completes the proof of Theorem 2. \square

C Missing Proofs for Section 4

C.1 Proof of Lemma 6

Lemma 6 (Steepest feasible descent of Shadow Steps). *Let P be a polytope defined as in (4) and let $\mathbf{x} \in P$ with gradient $\nabla f(\mathbf{x})$. Let \mathbf{y} be any feasible direction at \mathbf{x} , i.e., $\exists \gamma > 0$ s.t. $\mathbf{x} + \gamma \mathbf{y} \in P$. Then*

$$\left\langle -\nabla f(\mathbf{x}), \frac{\mathbf{d}_\mathbf{x}^\Pi}{\|\mathbf{d}_\mathbf{x}^\Pi\|} \right\rangle^2 = \|\mathbf{d}_\mathbf{x}^\Pi\|^2 \geq \left\langle \mathbf{d}_\mathbf{x}^\Pi, \frac{\mathbf{y}}{\|\mathbf{y}\|} \right\rangle^2 \geq \left\langle -\nabla f(\mathbf{x}), \frac{\mathbf{y}}{\|\mathbf{y}\|} \right\rangle^2. \quad (12)$$

Proof. We prove the result using first-order optimality of projections. First, observe that using Moreau's decomposition theorem we can uniquely decompose $-\nabla f(\mathbf{x}) = \mathbf{p} + \mathbf{d}_\mathbf{x}^\Pi$ such that $\langle \mathbf{d}_\mathbf{x}^\Pi, \mathbf{p} \rangle = 0$, where \mathbf{p} is the projection of $\nabla f(\mathbf{x})$ onto $N_P(\mathbf{x})$. Therefore, $\langle -\nabla f(\mathbf{x}), \mathbf{d}_\mathbf{x}^\Pi \rangle = \|\mathbf{d}_\mathbf{x}^\Pi\|^2$, which gives the first equality in (12).

We will now show that

$$\langle \mathbf{d}_\mathbf{x}^\Pi, \mathbf{y} \rangle \geq \langle -\nabla f(\mathbf{x}), \mathbf{y} \rangle. \quad (36)$$

To do that, we recall the first-order optimality condition for $g(\lambda) = \Pi_P(\mathbf{x} - \lambda \nabla f(\mathbf{x}))$ for $\lambda > 0$:

$$\langle g(\lambda) - \mathbf{x} + \lambda \nabla f(\mathbf{x}), \mathbf{z} - g(\lambda) \rangle \geq 0 \quad \forall \mathbf{z} \in P.$$

Using (8), we know that there exists some scalar λ^- such that $g(\lambda) = \mathbf{x} + \lambda \mathbf{d}_\mathbf{x}^\Pi$ for any $0 < \lambda < \lambda^-$. Hence, for any such $\lambda \in (0, \lambda^-)$, the first-order optimality condition becomes:

$$\langle \mathbf{x} + \lambda \mathbf{d}_\mathbf{x}^\Pi - \mathbf{x} + \lambda \nabla f(\mathbf{x}), \mathbf{z} - \mathbf{x} - \lambda \mathbf{d}_\mathbf{x}^\Pi \rangle = \lambda \langle \mathbf{d}_\mathbf{x}^\Pi + \nabla f(\mathbf{x}), \mathbf{z} - \mathbf{x} - \lambda \mathbf{d}_\mathbf{x}^\Pi \rangle \geq 0, \quad (37)$$

for all $\mathbf{z} \in P$. Note that the above equation holds for any $\mathbf{z} \in P$ and $\lambda \in (0, \lambda^-)$.

Since, $\mathbf{x} + \gamma \mathbf{y} \in P$, it follows that $\mathbf{x} + \bar{\lambda} \mathbf{y}$ is also in P , where $\bar{\lambda} = \min\{\lambda^-/2, \gamma\}$. Thus, since $\bar{\lambda} \in (0, \lambda^-)$ and $\mathbf{x} + \bar{\lambda} \mathbf{y} \in P$, we can plug in $\bar{\lambda}$ for λ and $\mathbf{x} + \bar{\lambda} \mathbf{y}$ for \mathbf{z} in (37) to obtain $\bar{\lambda}^2 \langle \mathbf{d}_\mathbf{x}^\Pi + \nabla f(\mathbf{x}), \mathbf{y} - \mathbf{d}_\mathbf{x}^\Pi \rangle \geq 0$. Thus, using the fact that $\langle -\nabla f(\mathbf{x}), \mathbf{d}_\mathbf{x}^\Pi \rangle = \|\mathbf{d}_\mathbf{x}^\Pi\|^2$, this implies

$$\langle \mathbf{d}_\mathbf{x}^\Pi, \mathbf{y} \rangle \geq \|\mathbf{d}_\mathbf{x}^\Pi\|^2 + \langle -\nabla f(\mathbf{x}), \mathbf{y} - \mathbf{d}_\mathbf{x}^\Pi \rangle = \langle -\nabla f(\mathbf{x}), \mathbf{y} \rangle$$

as claimed in (36).

[‡]The first order optimality condition for $\hat{\mathbf{d}}_{\mathbf{x}_{i-1}}^\Pi$ is $\langle -\nabla f(\mathbf{x}_0) - \hat{\mathbf{d}}_{\mathbf{x}_{i-1}}^\Pi, \mathbf{y} - \hat{\mathbf{d}}_{\mathbf{x}_{i-1}}^\Pi \rangle \leq 0$ for any feasible direction $\mathbf{y} \in \text{Cone}(F - \mathbf{x}_{i-1})$. Since $\langle -\nabla f(\mathbf{x}_0) - \hat{\mathbf{d}}_{\mathbf{x}_{i-1}}^\Pi, \hat{\mathbf{d}}_{\mathbf{x}_{i-1}}^\Pi \rangle = 0$ by definition of $\hat{\mathbf{d}}_{\mathbf{x}_{i-1}}^\Pi$ and any $\mathbf{y} \in \text{Cone}(F - \mathbf{x}_{i-1})$ can be written as $\alpha(\mathbf{z} - \mathbf{x}_{i-1})$ for some $\mathbf{z} \in F$ and $\alpha \geq 0$, this first order optimality condition reduces to $\langle -\nabla f(\mathbf{x}_0) - \hat{\mathbf{d}}_{\mathbf{x}_{i-1}}^\Pi, \mathbf{z} - \mathbf{x}_{i-1} \rangle \leq 0 \quad \forall \mathbf{z} \in F$. Since $\langle \mathbf{d}, -\nabla f(\mathbf{x}_0) - \mathbf{d} \rangle = 0$ by (33) and $\langle -\nabla f(\mathbf{x}_0) - \mathbf{d}, \mathbf{z} - \mathbf{x}_{i-1} \rangle \leq 0 \quad \forall \mathbf{z} \in F$, we have that \mathbf{d} satisfies first-order optimality for $\hat{\mathbf{d}}_{\mathbf{x}_{i-1}}^\Pi$.

We can now complete the proof using (36) as follows

$$\left\langle -\nabla f(\mathbf{x}), \frac{\mathbf{d}_x^\Pi}{\|\mathbf{d}_x^\Pi\|} \right\rangle^2 = \|\mathbf{d}_x^\Pi\|^2 \geq \left\langle \mathbf{d}_x^\Pi, \frac{\mathbf{y}}{\|\mathbf{y}\|} \right\rangle^2 \geq \left\langle -\nabla f(\mathbf{x}), \frac{\mathbf{y}}{\|\mathbf{y}\|} \right\rangle^2,$$

where we used Cauchy-Schwartz in the first inequality and (36) in the second inequality. \square

C.2 Proof of Lemma 7

Lemma 7 (Primal gap estimate). *Let P be a polytope defined as in (4) and fix $\mathbf{x} \in P$. Then, $\|\mathbf{d}_x^\Pi\| = 0$ if and only if $\mathbf{x} = \mathbf{x}^*$, where $\mathbf{x}^* = \arg \min_{\mathbf{x} \in P} f(\mathbf{x})$.*

Proof. First assume that $\|\mathbf{d}_x^\Pi\| = 0$ so that $\mathbf{d}_x^\Pi = \mathbf{0}$. Using (8), we know that $\mathbf{d}_x^\Pi = \frac{g(\epsilon) - \mathbf{x}}{\epsilon}$ for $\epsilon > 0$ sufficiently small. Hence, the assumption that $\mathbf{d}_x^\Pi = \mathbf{0}$ implies that $g(\epsilon) = \mathbf{x}$. Using the first-order optimality of $g(\epsilon)$ we have $\langle \mathbf{x} - \epsilon \nabla f(\mathbf{x}) - g(\epsilon), \mathbf{z} - g(\epsilon) \rangle \leq 0 \quad \forall \mathbf{z} \in P$. However, since $g(\epsilon) = \mathbf{x}$, this becomes $\langle -\epsilon \nabla f(\mathbf{x}), \mathbf{z} - \mathbf{x} \rangle \leq 0 \quad \forall \mathbf{z} \in P$. This is equivalent to saying $-\nabla f(\mathbf{x}) \in N_P(\mathbf{x})$, so that $\mathbf{x} = \mathbf{x}^*$.

Conversely suppose that $\mathbf{x} = \mathbf{x}^*$. Then, it follows that $-\nabla f(\mathbf{x}) \in N_P(\mathbf{x})$. Using Lemma 1, this implies that $g(\lambda) = \mathbf{x}$ for all $\lambda > 0$. Since from (8) we know that $\mathbf{d}_x^\Pi = \frac{g(\epsilon) - \mathbf{x}}{\epsilon}$ for $\epsilon > 0$ sufficiently small, it follows that $\mathbf{d}_x^\Pi = \mathbf{0}$. Thus, $\|\mathbf{d}_x^\Pi\| = 0$ as claimed. \square

C.3 Connecting Shadow-steps to Away-steps

Lemma 8 (Away steps). *Let P be a polytope defined as in (4) and fix $\mathbf{x} \in P$. Let $F = \{\mathbf{z} \in P : \mathbf{A}_{I(\mathbf{x})}\mathbf{z} = \mathbf{b}_{I(\mathbf{x})}\}$ be the minimal face containing \mathbf{x} . Further, choose $\delta_{\max} = \max\{\delta : \mathbf{x} - \delta \mathbf{d}_x^\Pi \in P\}$ and consider the away point $\mathbf{a}_x = \mathbf{x} - \delta_{\max} \mathbf{d}_x^\Pi$ obtained by moving maximally along the the direction of the negative shadow. Then, \mathbf{a}_x lies in F and the corresponding away-direction is simply $\mathbf{x} - \mathbf{a}_x = \delta_{\max} \mathbf{d}_x^\Pi$.*

We first recall this result from Bashiri and Zhang [3]:

Lemma 10 (Best away vertex, [3]). *Let P be a polytope defined as in (4) and fix $\mathbf{x} \in P$. Let $F = \{\mathbf{z} \in P : \mathbf{A}_{I(\mathbf{x})}\mathbf{z} = \mathbf{b}_{I(\mathbf{x})}\}$ be the minimal face containing \mathbf{x} and define $A := \{\mathbf{v} \in \text{vert}(P) : \mathbf{v} \in F\}$ to be the set of vertices in F . Also, let*

$$\mathcal{S}(\mathbf{x}) := \{S : S \subseteq \text{vert}(P) \mid \mathbf{x} \text{ is a proper convex combination of all the elements in } S\}$$

be the set of all possible active sets for \mathbf{x} . Then,

$$\max_{\mathbf{v} \in A} \langle \nabla f(\mathbf{x}), \mathbf{v} \rangle = \max_{S \in \mathcal{S}(\mathbf{x})} \max_{\mathbf{v} \in S} \langle \nabla f(\mathbf{x}), \mathbf{v} \rangle.$$

Proof. For the first direction, we claim that any $S \in \mathcal{S}(\mathbf{x})$ must be contained in $A = \text{vert}(F)$. Let $S \in \mathcal{S}(\mathbf{x})$. Then, we can write $\mathbf{x} = \sum_{\mathbf{v} \in S} \alpha_{\mathbf{v}} \mathbf{v}$, where $\alpha_{\mathbf{v}} \in (0, 1)$ and $\sum_{\mathbf{v} \in S} \alpha_{\mathbf{v}} = 1$. Fix $\mathbf{y} \in S$ and let $\mathbf{z} := \frac{1}{1 - \alpha_{\mathbf{y}}} \sum_{\mathbf{v} \in S \setminus \{\mathbf{y}\}} \alpha_{\mathbf{v}} \mathbf{v} \in P$. Then, $\mathbf{x} = \alpha_{\mathbf{y}} \mathbf{y} + (1 - \alpha_{\mathbf{y}}) \mathbf{z}$. Now, if $\langle \mathbf{a}_i, \mathbf{x} \rangle = b_i$, then the fact that $\langle \mathbf{a}_i, \mathbf{z} \rangle \leq b_i$ implies that $\langle \mathbf{a}_i, \mathbf{y} \rangle = b_i$, so that $\mathbf{y} \in A$.

Conversely, we claim that any $\mathbf{v} \in A$ lies in some $S \in \mathcal{S}(\mathbf{x})$. Let $\mathbf{v} \in A$. Consider $\mathbf{z}_\alpha = \frac{1}{1 - \alpha} (\mathbf{x} - \alpha \mathbf{v})$ for $\alpha \in (0, 1)$. First, if $\langle \mathbf{a}_i, \mathbf{x} \rangle = b_i$ (i.e. $i \in I(\mathbf{x})$), since we have $\langle \mathbf{a}_i, \mathbf{v} \rangle = b_i$ by choice of \mathbf{v} , it follows that $\langle \mathbf{a}_i, \mathbf{z}_\alpha \rangle = b_i$. Otherwise, if $\langle \mathbf{a}_i, \mathbf{x} \rangle < b_i$ (i.e. $i \in J(\mathbf{x})$) then $\lim_{\alpha \downarrow 0} \langle \mathbf{a}_i, \mathbf{z}_\alpha \rangle = \langle \mathbf{a}_i, \mathbf{x} \rangle < b_i$. Thus, since we have a finite number of constraints, we can ensure that $\langle \mathbf{a}_i, \mathbf{z}_{\alpha^*} \rangle \leq b_i$ for all $i \in J(\mathbf{x})$, where α^* is sufficiently small. Thus, we have shown we can write $\mathbf{x} = (1 - \alpha^*) \mathbf{z}_{\alpha^*} + \alpha^* \mathbf{v}$, where $\mathbf{z}_{\alpha^*} \in P$. Therefore, there exists some active $S \in \mathcal{S}(\mathbf{x})$ containing \mathbf{v} . \square

Proof of Lemma 8. First, if $\delta_{\max} = 0$, then $\mathbf{a}_t = \mathbf{x}_t$, and the result holds trivially. Now assume that $\delta_{\max} > 0$. By definition of \mathbf{d}_x^Π , we know that $\mathbf{A}_{I(x)}\mathbf{d}_x^\Pi \leq \mathbf{0}$. Hence, since $-\mathbf{d}_x^\Pi$ is also feasible, it follows that we must have $\mathbf{A}_{I(x)}\mathbf{d}_x^\Pi = \mathbf{0}$. This then implies that $\mathbf{A}_{I(x)}\mathbf{a}_x = \mathbf{A}_{I(x)}(\mathbf{x} - \delta_{\max}\mathbf{d}_x^\Pi) = \mathbf{A}_{I(x)}\mathbf{x} = \mathbf{b}_{I(x)}$. Thus, we have $\mathbf{a}_x \in F$. Moreover, in the proof of the previous lemma (Lemma 10), we show that the vertices of F in fact form all possible away steps. The result then follows. \square

D Convergence of Projected Gradient Descent

We will invoke the following theorem in the global linear convergence proof of Theorem 7 and Theorem 8:

Theorem 10 (Theorem 5 in [33]). *Consider the problem $\min_{x \in \mathcal{X}} f(\mathbf{x})$, where $\mathcal{X} \subseteq \mathbb{R}^n$ is a convex and compact domain, and $f : \mathcal{X} \rightarrow \mathbb{R}$ is L -smooth and μ -strongly convex over \mathcal{X} . Further, consider the projected gradient descent (PGD) algorithm with a step-size of $1/L$: $\mathbf{x}_{t+1} := \Pi_{\mathcal{X}}(\mathbf{x}_t - \nabla f(\mathbf{x}_t)/L)$. Then the primal gap $h(\mathbf{x}_t) := f(\mathbf{x}_t) - f(\mathbf{x}^*)$ of the PGD algorithm decreases geometrically:*

$$h(\mathbf{x}_{t+1}) \leq \left(1 - \frac{\mu}{L}\right) h(\mathbf{x}_t), \quad (38)$$

with each iteration of the PGD algorithm.

We present a proof of this result for completeness. First, we need the following technical lemma for the proof:

Lemma 11 (Lemma 1 in [33]). *Let $\mathcal{X} \subseteq \mathbb{R}^n$ be a convex and compact domain and suppose that $f : \mathcal{X} \rightarrow \mathbb{R}$ is L -smooth and μ -strongly convex over \mathcal{X} . For any $\mathbf{x} \in \mathcal{X}$ and $c \in \mathbb{R}$, define*

$$D(\mathbf{x}, c) := -2c \min_{\mathbf{y} \in \mathcal{X}} \left\{ \langle \nabla f(\mathbf{x}), \mathbf{y} - \mathbf{x} \rangle + \frac{c}{2} \|\mathbf{y} - \mathbf{x}\|^2 \right\}.$$

Then, we have $D(\mathbf{x}, L) \geq D(\mathbf{x}, \mu)$ for all $\mathbf{x} \in \mathcal{X}$.

Proof. Fix any $\mathbf{x} \in \mathcal{X}$. Therefore, by completing the square we have

$$\begin{aligned} D(\mathbf{x}, c) &= -\min_{\mathbf{y} \in \mathcal{X}} \left\{ 2c \langle \nabla f(\mathbf{x}), \mathbf{y} - \mathbf{x} \rangle + c^2 \|\mathbf{y} - \mathbf{x}\|^2 \right\} \\ &= \min_{\mathbf{y} \in \mathcal{X}} \left\{ \|\nabla f(\mathbf{x})\|^2 - \|\nabla f(\mathbf{x})\|^2 - 2c \langle \nabla f(\mathbf{x}), \mathbf{y} - \mathbf{x} \rangle - c^2 \|\mathbf{y} - \mathbf{x}\|^2 \right\} \\ &= \|\nabla f(\mathbf{x})\|^2 - \min_{\mathbf{y} \in \mathcal{X}} \|c(\mathbf{y} - \mathbf{x}) + \nabla f(\mathbf{x})\|^2 \\ &= \|\nabla f(\mathbf{x})\|^2 - \min_{\bar{\mathbf{y}} \in c(\mathcal{X} - \mathbf{x})} \|\bar{\mathbf{y}} + \nabla f(\mathbf{x})\|^2, \end{aligned}$$

where in the last equality we used the change of variables $\bar{\mathbf{y}} = c(\mathbf{y} - \mathbf{x})$.

We now claim that, since by definition $\mu \leq L$, we have $\mu(\mathcal{X} - \mathbf{x}) \subseteq L(\mathcal{X} - \mathbf{x})$. Let $\mathbf{z} \in \mu(\mathcal{X} - \mathbf{x})$ and we will show that $\mathbf{z} \in L(\mathcal{X} - \mathbf{x})$. Since $\mathbf{z} \in \mu(\mathcal{X} - \mathbf{x})$, we could write $\mathbf{z} = \mu(\mathbf{y} - \mathbf{x}) = L(\frac{\mu}{L}(\mathbf{y} - \mathbf{x}))$ for some $\mathbf{y} \in \mathcal{X}$. To prove the claim we now show that $\frac{\mu}{L}(\mathbf{y} - \mathbf{x}) \in \mathcal{X} - \mathbf{x}$. Since $\mathbf{y} - \mathbf{x} \in \mathcal{X} - \mathbf{x}$ and $\mathbf{0} = \mathbf{x} - \mathbf{x} \in \mathcal{X} - \mathbf{x}$, it follows that $\frac{\mu}{L}(\mathbf{y} - \mathbf{x}) = \frac{\mu}{L}(\mathbf{y} - \mathbf{x}) + (1 - \frac{\mu}{L})\mathbf{0} \in \mathcal{X} - \mathbf{x}$ by the convexity of $\mathcal{X} - \mathbf{x}$ and the fact that $\mu \leq L$. Thus, we have $\mathbf{z} \in L(\mathcal{X} - \mathbf{x})$ and the claim follows.

Now using this claim we have

$$\begin{aligned}
D(\mathbf{x}, L) &= \|\nabla f(\mathbf{x})\|^2 - \min_{\bar{\mathbf{y}} \in L(\mathcal{X} - \mathbf{x})} \|\bar{\mathbf{y}} + \nabla f(\mathbf{x})\|^2 \\
&\geq \|\nabla f(\mathbf{x})\|^2 - \min_{\bar{\mathbf{y}} \in \mu(\mathcal{X} - \mathbf{x})} \|\bar{\mathbf{y}} + \nabla f(\mathbf{x})\|^2 \quad (\text{using } \mu(\mathcal{X} - \mathbf{x}) \subseteq L(\mathcal{X} - \mathbf{x})) \\
&= D(\mathbf{x}, \mu)
\end{aligned}$$

as desired. \square

Proof of Theorem 10. Let $g(\lambda) = \Pi_P(\mathbf{x} - \lambda \nabla f(\mathbf{x}))$ be the curve parameterized by the step-size λ . Recall that by the proximal definition of the projection (see e.g., [27]) we have

$$g(1/L) = \Pi_{\mathcal{X}}(\mathbf{x}_t - \nabla f(\mathbf{x}_t)/L) = \arg \min_{\mathbf{y} \in \mathcal{X}} \left\{ \langle \nabla f(\mathbf{x}_t), \mathbf{y} - \mathbf{x}_t \rangle + \frac{L}{2} \|\mathbf{y} - \mathbf{x}_t\|^2 \right\}. \quad (39)$$

We can now show the $(1 - \frac{\mu}{L})$ rate of decrease as follows:

$$h(\mathbf{x}_t) - h(\mathbf{x}_{t+1}) = f(\mathbf{x}_t) - f(\mathbf{x}_{t+1}) \quad (40)$$

$$= f(\mathbf{x}_t) - f(g(1/L)) \quad (41)$$

$$\geq - \left(\langle \nabla f(\mathbf{x}_t), g(1/L) - \mathbf{x}_t \rangle + \frac{L}{2} \|g(1/L) - \mathbf{x}_t\|^2 \right) \quad (42)$$

$$= - \min_{\mathbf{y} \in \mathcal{X}} \left\{ \langle \nabla f(\mathbf{x}_t), \mathbf{y} - \mathbf{x}_t \rangle + \frac{L}{2} \|\mathbf{y} - \mathbf{x}_t\|^2 \right\} \quad (43)$$

$$= \frac{1}{2L} \left(-2L \min_{\mathbf{y} \in \mathcal{X}} \left\{ \langle \nabla f(\mathbf{x}_t), \mathbf{y} - \mathbf{x}_t \rangle + \frac{L}{2} \|\mathbf{y} - \mathbf{x}_t\|^2 \right\} \right) \quad (44)$$

$$\geq \frac{\mu}{L} \left(- \min_{\mathbf{y} \in \mathcal{X}} \left\{ \langle \nabla f(\mathbf{x}_t), \mathbf{y} - \mathbf{x}_t \rangle + \frac{\mu}{2} \|\mathbf{y} - \mathbf{x}_t\|^2 \right\} \right) \quad (45)$$

$$= \frac{\mu}{L} \left(\max_{\mathbf{y} \in \mathcal{X}} \left\{ \langle -\nabla f(\mathbf{x}_t), \mathbf{y} - \mathbf{x}_t \rangle - \frac{\mu}{2} \|\mathbf{y} - \mathbf{x}_t\|^2 \right\} \right) \quad (46)$$

$$\geq \frac{\mu}{L} \left(\langle -\nabla f(\mathbf{x}_t), \mathbf{x}^* - \mathbf{x}_t \rangle - \frac{\mu}{2} \|\mathbf{x}^* - \mathbf{x}_t\|^2 \right) \quad (47)$$

$$\geq \frac{\mu}{L} h(\mathbf{x}_t), \quad (48)$$

where (42) follows from the smoothness inequality given in Section 2 applied with $\mathbf{y} \leftarrow g(1/L)$ and $\mathbf{x} \leftarrow \mathbf{x}_t$, (43) follows from the definition of $g(1/L)$ given in (39), (45) follows from Lemma 11, (47) follows from the fact that $\mathbf{x}^* \in \mathcal{X}$, and finally (48) follows from the strong convexity inequality given in Section 2 applied with $\mathbf{y} \leftarrow \mathbf{x}^*$ and $\mathbf{x} \leftarrow \mathbf{x}_t$. \square

E Missing Proofs for Section 5

E.1 Proof of Theorem 5

Theorem 5. *Let $\phi : \mathcal{D} \rightarrow \mathbb{R}$ be a mirror map that is strongly convex and differentiable, and assume that the directional derivative $\mathbf{d}_{X(t)}^\phi$ exists for all $t \geq 0$. Then, the dynamics for mirror descent (17) are equivalent to the shadow dynamics $\dot{X}(t) = \mathbf{d}_{X(t)}^\phi$ with the same initial conditions $X(0) = \mathbf{x}_0 \in P$.*

Proof. Consider the dynamics given in (17). Using the chain rule we know that

$$\dot{X}(t) = \frac{d}{dt} \nabla \phi^*(Z(t)) = \left\langle \nabla^2 \phi^*(Z(t)), \dot{Z}(t) \right\rangle = \left\langle \nabla^2 \phi^*(Z(t)), -\nabla f(X(t)) \right\rangle.$$

By definition, the directional derivative of $\nabla \phi^*$ with respect to the direction $-\nabla f(X(t))$ is given by (see for example [27])

$$\nabla_{-\nabla f(X(t))}^2 \phi(Z(t)) := \lim_{\epsilon \downarrow 0} \frac{\nabla \phi^*(Z(t) - \epsilon \nabla f(X(t))) - \nabla \phi^*(Z(t))}{\epsilon} = \left\langle \nabla^2 \phi^*(Z(t)), -\nabla f(X(t)) \right\rangle$$

Hence, using this fact we have

$$\begin{aligned} \dot{X}(t) &= \left\langle \nabla^2 \phi^*(Z(t)), -\nabla f(X(t)) \right\rangle \\ &= \lim_{\epsilon \downarrow 0} \frac{\nabla \phi^*(Z(t) - \epsilon \nabla f(X(t))) - \nabla \phi^*(Z(t))}{\epsilon} \\ &= \lim_{\epsilon \downarrow 0} \frac{\nabla \phi^*(Z(t) - \epsilon \nabla f(X(t))) - X(t)}{\epsilon} \quad (\text{using ODE definition in (17)}) \end{aligned}$$

Since ϕ is differentiable on the image of $\nabla \phi^*$, it is known that $\nabla \phi = (\nabla \phi^*)^{-1}$ (in particular, from the duality of ϕ and ϕ^* we know that $\mathbf{x} = \nabla \phi^*(\tilde{\mathbf{x}})$ if and only if $\tilde{\mathbf{x}} = \nabla \phi(\mathbf{x})$; see Theorem 23.5 in [36]). Moreover, by definition of the mirror descent ODE given in (17), we have $X(t) = \nabla \phi^*(Z(t))$. Using these facts we get $Z(t) = (\nabla \phi^*)^{-1}(X(t)) = \nabla \phi(X(t))$. Thus,

$$\dot{X}(t) = \lim_{\epsilon \downarrow 0} \frac{\nabla \phi^*(\nabla \phi(X(t)) - \epsilon \nabla f(X(t))) - X(t)}{\epsilon} = \mathbf{d}_{X(t)}^\phi$$

which coincides with dynamics for moving in the shadow of the gradient given in (18). \square

E.2 Proof of Theorem 6

Theorem 6. *Let $P \subseteq \mathbb{R}^n$ be a polytope and suppose that $f : P \rightarrow \mathbb{R}$ is differentiable and μ -strongly convex over P . Consider the shadow dynamics $\dot{X}(t) = \mathbf{d}_{X(t)}^\Pi$ with initial conditions $X(0) = \mathbf{x}_0 \in P$. Then for each $t \geq 0$, we have $X(t) \in P$. Moreover, the primal gap $h(X(t)) := f(X(t)) - f(\mathbf{x}^*)$ associated with the shadow dynamics decreases as: $h(X(t)) \leq e^{-2\mu t} h(\mathbf{x}_0)$.*

Proof. First, the fact that $X(t) \in P$ for all $t \geq 0$ is guaranteed by the equivalence between the dynamics of PGD (17) and shadow dynamics asserted in Theorem 6, which by construction satisfy $X(t) \in P$ for all $t \geq 0$. Now the proof for the convergence rate uses a Lyapunov argument, where we let $h(X(t))$ be our Lyapunov potential function. Using the chain rule we have

$$\frac{dh(X(t))}{dt} = \left\langle \nabla f(X(t)), \dot{X}(t) \right\rangle \tag{49}$$

$$= \left\langle \nabla f(X(t)), \mathbf{d}_{X(t)}^\Pi \right\rangle \tag{50}$$

$$= -\|\mathbf{d}_{X(t)}^\Pi\|^2 \tag{51}$$

$$\leq -2\mu h(X(t)), \tag{52}$$

where we used the fact that $\dot{X}(t) = \mathbf{d}_{X(t)}^\Pi$ in (50), the fact that $\left\langle -\nabla f(X(t)), \mathbf{d}_{X(t)}^\Pi \right\rangle = \|\mathbf{d}_{X(t)}^\Pi\|^2$ in (51), and finally the primal gap estimate (23) in (52).

Integrating both sides of the above inequality we have (using Grönwall's inequality [37])

$$\int_0^t \frac{dh(X(t))}{h(X(t))} \leq \int_0^t -\mu dt \implies \ln \left(\frac{h(X(t))}{h(\mathbf{x}_0)} \right) \leq -2\mu t,$$

which further implies $h(X(t)) \leq e^{-2\mu t} h(\mathbf{x}_0)$ as claimed. \square

E.3 Proof of Theorem 7

Theorem 7. *Let $P \subseteq \mathbb{R}^n$ be a polytope and suppose that $f : P \rightarrow \mathbb{R}$ is L -smooth and μ -strongly convex over P . Then the primal gap $h(\mathbf{x}_t) := f(\mathbf{x}_t) - f(\mathbf{x}^*)$ of the SHADOW WALK algorithm decreases geometrically:*

$$h(\mathbf{x}_{t+1}) \leq \left(1 - \frac{\mu}{L}\right) h(\mathbf{x}_t)$$

with each iteration of the SHADOW WALK algorithm (assuming TRACE-OPT is a single step). Moreover, the number of oracle calls to shadow, in-face shadow and line-search oracles to obtain an ϵ -accurate solution is $O\left(\beta \frac{L}{\mu} \log\left(\frac{1}{\epsilon}\right)\right)$, where β is the maximum number of breakpoints of the parametric projections curve that the TRACE-OPT method visits.

Proof. Since $\mathbf{x}_{t+1} := \text{TRACE}(\mathbf{x}_t, \nabla f(\mathbf{x}_t))$ and $\text{TRACE}(\mathbf{x}_t, \nabla f(\mathbf{x}_t))$ traces the whole curve of $g(\lambda) = \Pi_P(\mathbf{x}_t - \lambda \nabla f(\mathbf{x}_t))$ with exact line-search, it follows that $f(\mathbf{x}_{t+1}) \leq f(g(\lambda))$ for all $\lambda > 0$. In particular, $f(\mathbf{x}_{t+1}) \leq f(g(1/L))$, and we are thus guaranteed to make at least as much progress per iteration as that of projected gradient descent (PGD) step with a fixed-step size of $1/L$. Thus, using Theorem 10 about the convergence rate of PGD, we have $h(\mathbf{x}_{t+1}) \leq \left(1 - \frac{\mu}{L}\right) h(\mathbf{x}_t)$ as claimed. Moreover, the iteration complexity of the number of oracle calls stated in the theorem, now follows using the above rate of decrease in the primal gap. \square